INTERNATIONAL COMMISSION ON LARGE DAMS
Committee on Computational Aspects of Analysis and Design of Dams

10th Benchmark Workshop on Numerical Analysis of Dams
September 16-18, 2009 – Paris, FRANCE

Theme B

ANALYSIS OF A CONCRETE FACE ROCKFILL DAM INCLUDING CONCRETE FACE LOADING AND DEFORMATION

Formulator : Camilo Marulanda, INGETEC S.A.

C. Marulanda, Ingetec S.A.,
Cra 6 No. 30a-30 Bogotá, Colombia
marulanda@ingetec.com.co

Patrice Anthiniac, Coyne et Bellier

P.Anthiniac, Coyne et Bellier
9, allée des Barbanniers
92632 GENNEVILLIERS Cedex

The information package for the preparation of contributions to Theme B consists of :

- the present description — ThemeB 2009.doc
- the cross section drawing — ThemeB.dwg
- the input date Excel file — ThB_data.xls
- the template file for results — ThB_ResXXXX.xls

1. INTRODUCTION

The construction of Concrete Faced Rockfill Dams (CFRD) has increased in the last decades. This enthusiasm for CFRDs has its origin in both its inherent stability characteristics and its construction and schedule features. Also its foundation requirements and treatments that are less strict and more straightforward to carry out, particularly when compared to gravity or arch dams have made this type of dam a very attractive solution. As a consequence, the CFRD is currently a very common type of dam with several projects recently finished or under construction with heights above 180 m. The design and development of CFRD dams, have been based primarily on precedent and empiricism, however, recent incidents have shown that the extrapolation of precedents with the current procedures can have serious consequences. Recent events have shown the need to improve the current design approaches and evolve beyond empiricism which should include the development of analytical methodologies to analyze the behavior of this type of dams.

The settlements from CFRD dams are mainly the result of compaction of the fill and foundation under loads from the weight of rockfill and reservoir pressure and are a function of rock type, gradation and compaction conditions. A large portion of the total settlement of the rockfill occurs during construction. The post-construction settlements result from a gradual readjustment of the rockfill structure. The original rockfill dams were composed of rockfill dumped loosely in position with an impervious face. Large settlements were a feature of these dumped rockfill dams. It was also thought earlier that the fill should be composed of individual rocks of large uniform size to give rock to rock contact. As a consequence high deformations occurred in some of the early CFRD's creating considerable leakage problems. Excessive slab movements were generally attributed to low compaction of the dumped rockfill. In modern CFRDs, well graded rockfills placed in layers of 1m or less are used and are well compacted to obtain a less compressible and stiffer fill. However, as higher and higher dams are built, the deformations of these very high dams will increase considerably and could be similar in magnitude to the deformations measured in the low height, dumped rockfill, old generation CFRDs. Therefore, with deformations of similar magnitudes, it should be anticipated similar leakage problems if no additional measures are taken.

Numerical Analyses are now a common tool to predict dam behavior, including the behavior of the concrete face. However the physical mechanisms involved in the interaction of the different structural components of a CFRD dam is a very complex problem to model. This theme aims at identifying the key physical mechanisms that should be included in a numerical analysis to adequately predict the behavior of a CFRD. This will be performed by trying to reproduce in a three dimensional model the cracking pattern observed on the upstream face of a high CFRD.

The problem consists in predicting the development of deformations and stresses on the concrete face during construction and reservoir impoundment The concrete face, since it is a very slender element, behaves as a shell and its displacements are control by the deformation of the rockfill. The developments of stresses in the slabs are essentially caused by the deformation of the rockfill due to its own weight and the hydrostatic load of the reservoir. In addition, stresses due to concrete curing and temperature gradients will develop in the concrete face. The design of a concrete face should consider all the mechanisms that contribute to the development of stresses in the face. These mechanisms include the development of friction between the rockfill and the concrete face, the three dimensional deformation of the concrete face during construction and reservoir impounding. Nevertheless, the difficulty in obtaining analytical solutions that include all of these mechanisms and the absence of computational tools that allowed the calculations of the combined effect of the

mechanisms acting on the slabs, contributed to the development of design procedures that were based primarily on precedent and empiricism. A sign of this tendency is the determination of the concrete slab thickness, which is essentially based on precedent.

The proposed exercise is inspired from the recent incidents of cracks in the concrete face have been observed in high CFRD dams including Barra Grande (186 m high,665 m crest length, concrete face area 108,000m², rockfill volume 11.8 million m³ made of highly compressible basalt), Campos Novos (202 m high, crest length 590 m, concrete face area 105,000 m², rockfill volume 12.9 million m³ made of highly compressible basalt) both in Brazil and Mohale dam in Lesotho (145 m high, crest length 600m, concrete face area 73,400 m², rockfill volume 7.5 million m³). The general characteristics of the recent incidents, where cracking has occurred, have been described in Sobrinho et al. [1], Pinto [2], and Johannesson [3]. Figure 1 illustrates the extent of these incidents.

Figure 1: Extent of concrete face failure at (a) Campos Novos (b) Barra Grande and (c) Mohale

The case history that was selected as the benchmark example for theme B of the 10th ICOLD Workshop on Numerical Analysis of Dams was the Mohale dam in Lesotho. This dam is 145 m high, with a crest length of 600 m and a total fill volume of approximately 7.5 million m³, making it the highest dam of this type in Africa (reference Hydropower 1997). The dam was constructed of basalt rockfill. Figure 2 presents the location of the project and a general view of the dam. When the reservoir level reached its maximum elevation, significant dam movements occurred; which in turn increased the compressive stresses within the center portion of the concrete face, resulting in shear failure of the slab. Assessment of the instrumentation data indicated that the initial slab cracking took place between slabs 17 and 18 at the crest level due to high horizontal stresses [3]. After this incident seepage increased considerably, peaking at around 600 l/s. Figure 4 and Figure 5 show the slab spalling seen from the dam crest.

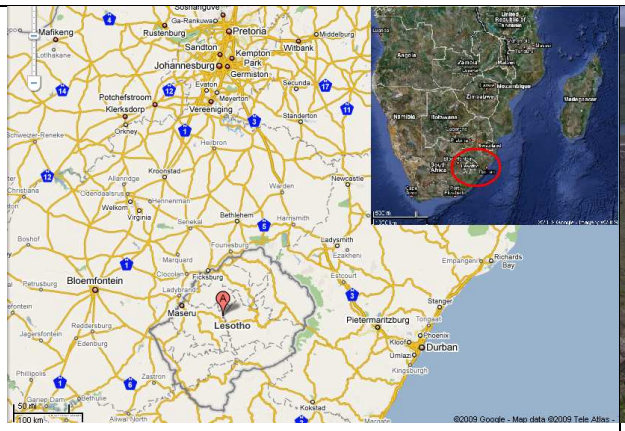

Figure 2: Map of Lesotho indicating the location of the project

Figure 3: Mohale dam seen from downstream on Dec 24, 2004 [1]

Figure 4: Crack seen from above between slabs 17 and 18 (Ref [3])

Figure 5: Slabs 17 and 18 after removing sheared concrete (Ref [3])

The objective for the participants of this theme is to reproduce on a numerical model the cracking pattern observed on the concrete face of Mohale Dam (Figure 23). The following minimum requirements shall be incorporated in their numerical model:

The participants to this theme should incorporate in the analysis the following minimum requirements in their numerical model:

- Three dimensional model using the simplified topography provided to the participants of this workshop.

- Incorporation of the concrete face into the numerical model.

1 *http://en.wikipedia.org/w/index.php?title=Mohale_dam&oldid=240432327 (last visited Mar. 28, 2009).*

- Use of the dam zoning and the construction sequence presented in this document.

2. INPUT DATA

All detailed information on input data is provided in the **ThB_Data.xls** file.

2.1. Dam Geometry

The cross section of the Mohale dam with its corresponding zones and crest details including the parapet wall is presented in Figure 6. Figure 7 presents the plan view of the dam (The topography of the dam site will be provided to all participants as a .dwg file). The upstream and downstream slopes are 1V:1.40H. The crest is 600 meter wide and its elevation is at 2084 m.

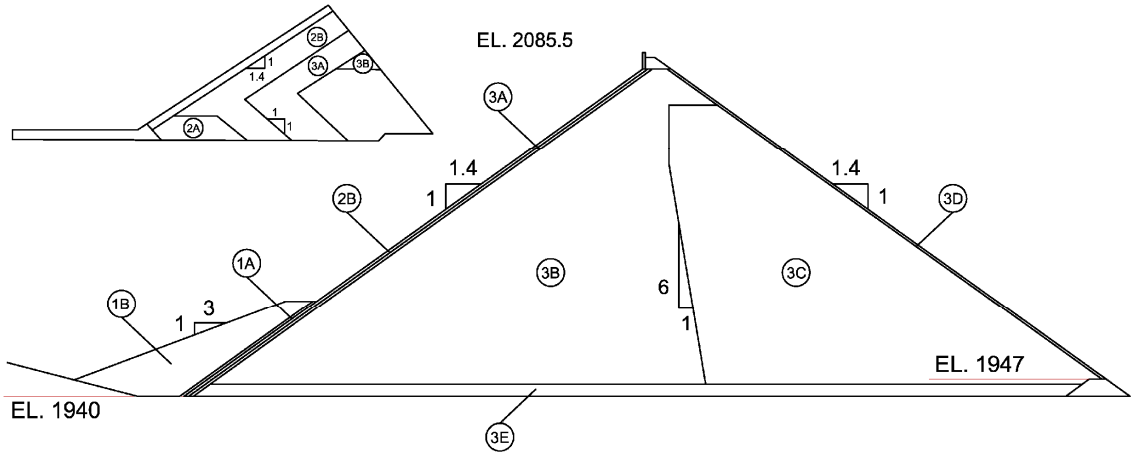

(a)

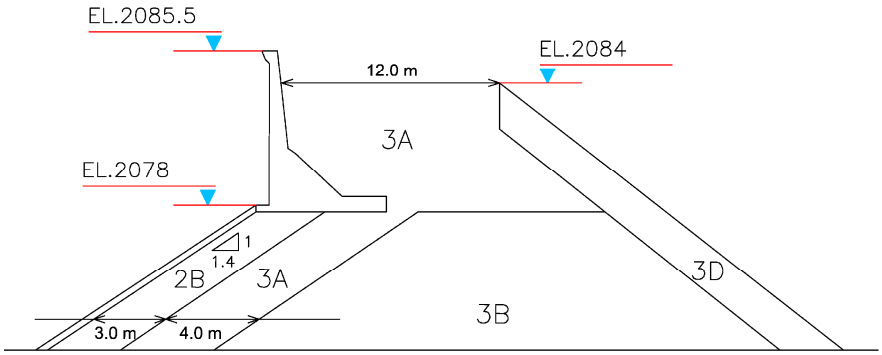

(b)

Figure 6: (a) Dam zoning and (b) Parapet wall. (Ref [3])

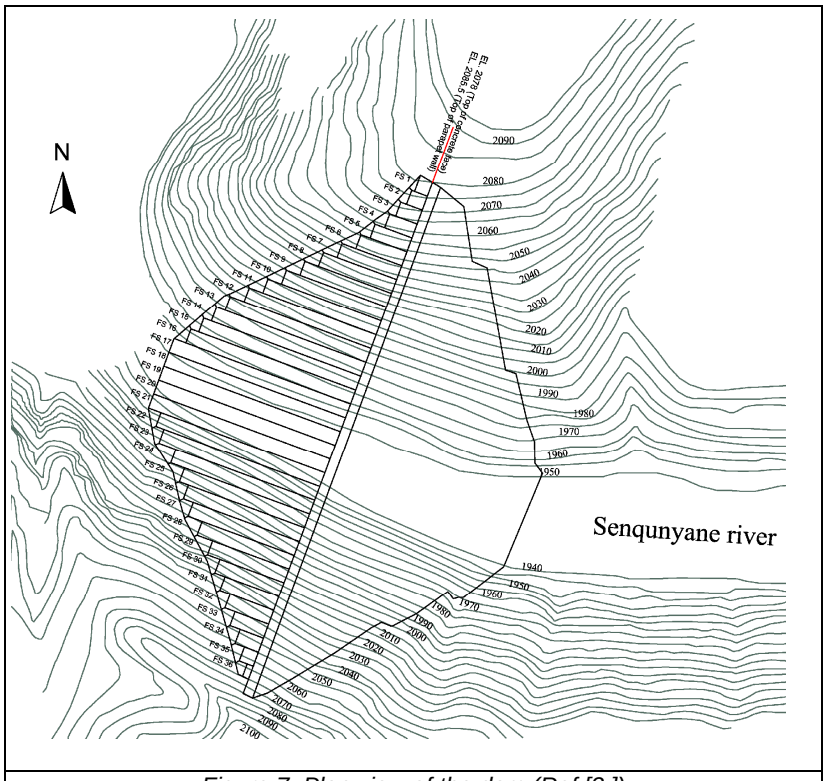

Figure 7: Plan view of the dam (Ref [3])

The thickness of the concrete face was determined as a function of the hydrostatic pressure, following the classical equation e=0.30 + 0.003H; where e is the slab thickness and H is the hydrostatic head. Reinforcement was 0.4% in the vertical direction while horizontal reinforcement amounted to 0.35% [3].

2.2. Construction sequence

Based on available construction data, the simplified construction sequence shown in Figure 8 to Figure 10 was developed and includes the most relevant construction stages. Figure 11 illustrates the reservoir level versus time. Table 1 presents the lift thicknesses used for the different zones of the dam.

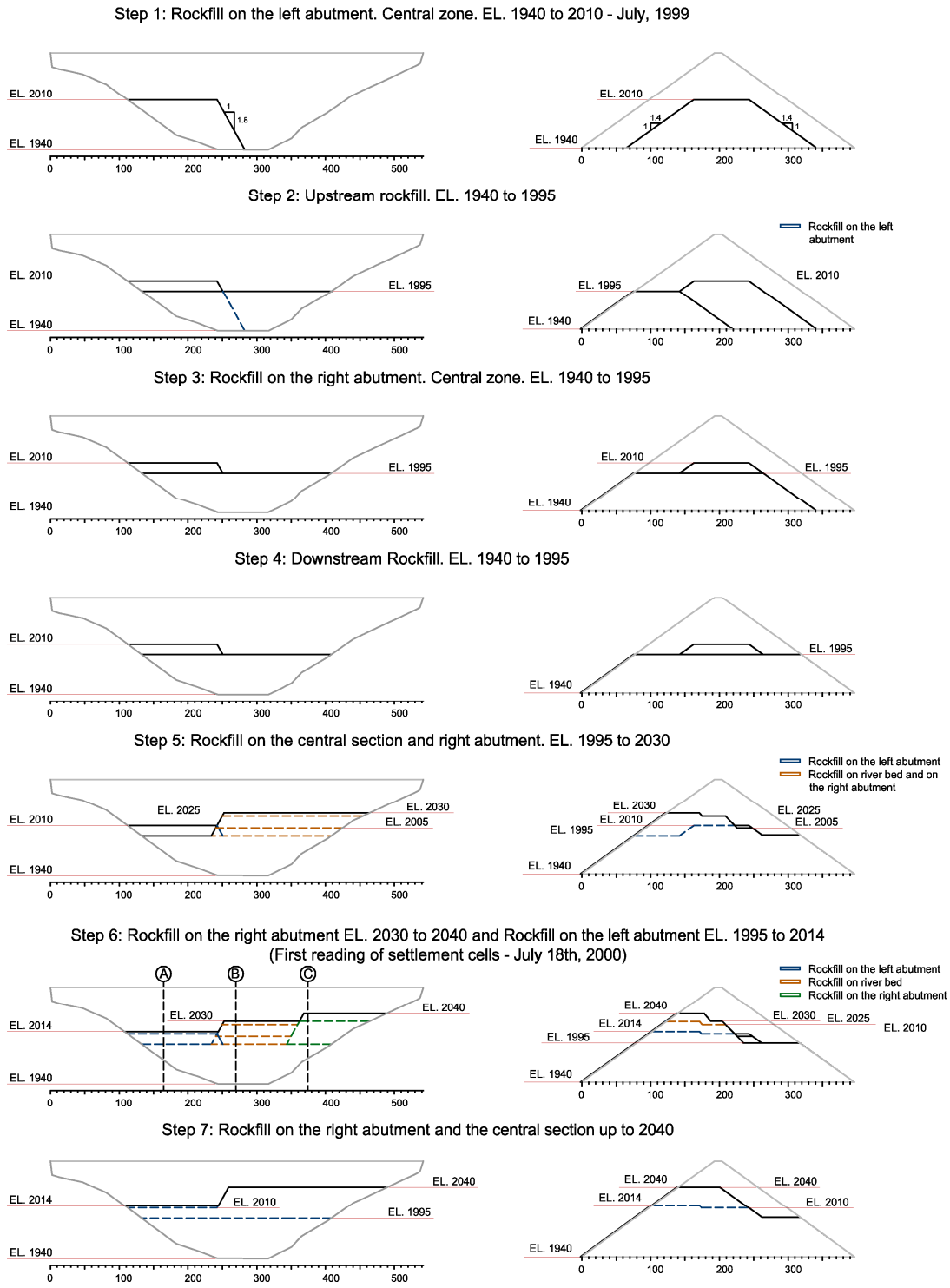

Figure 8: Construction sequence. Steps 1 to 7

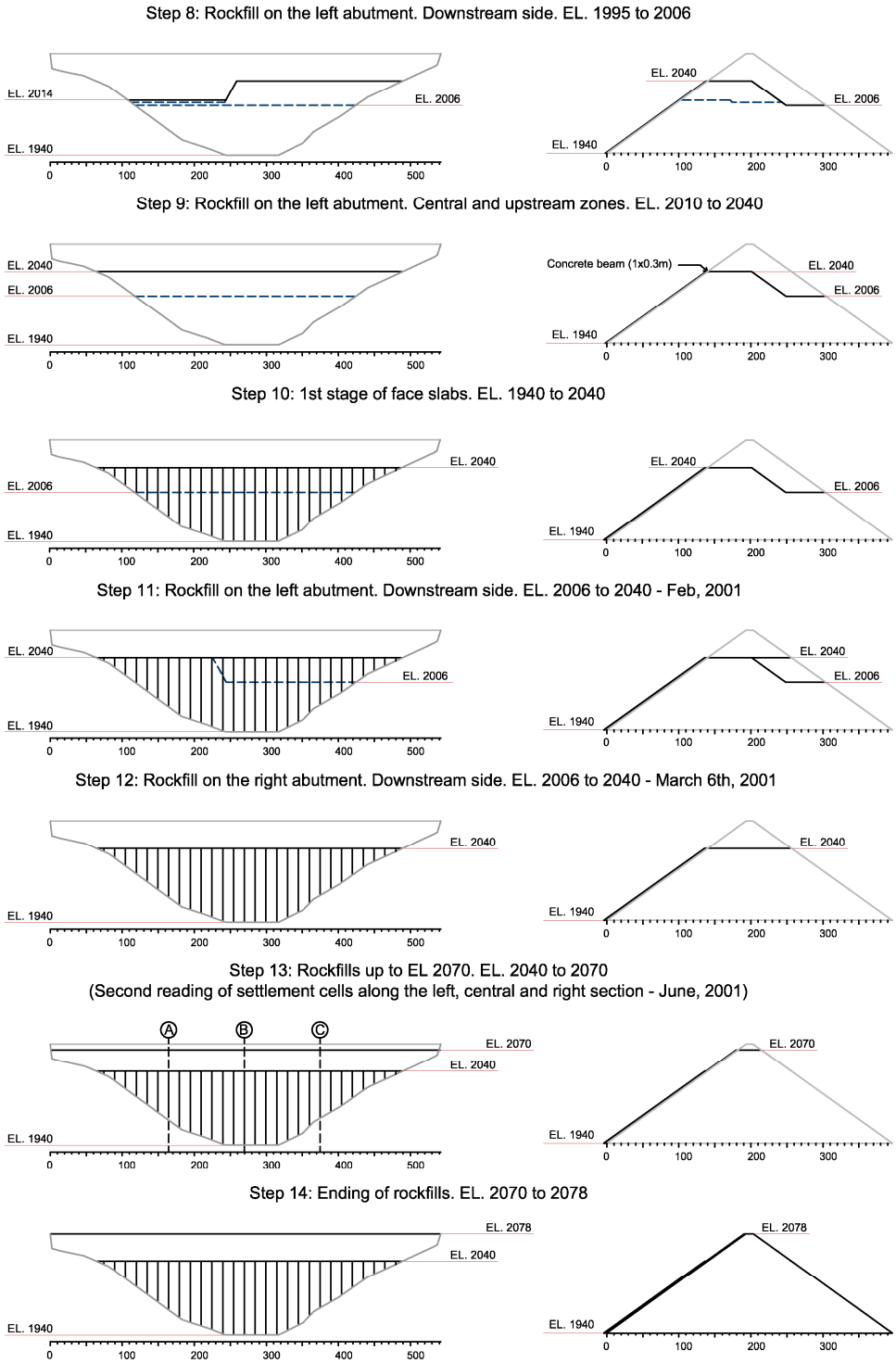

Figure 9: Construction sequence. Steps 8 to 14

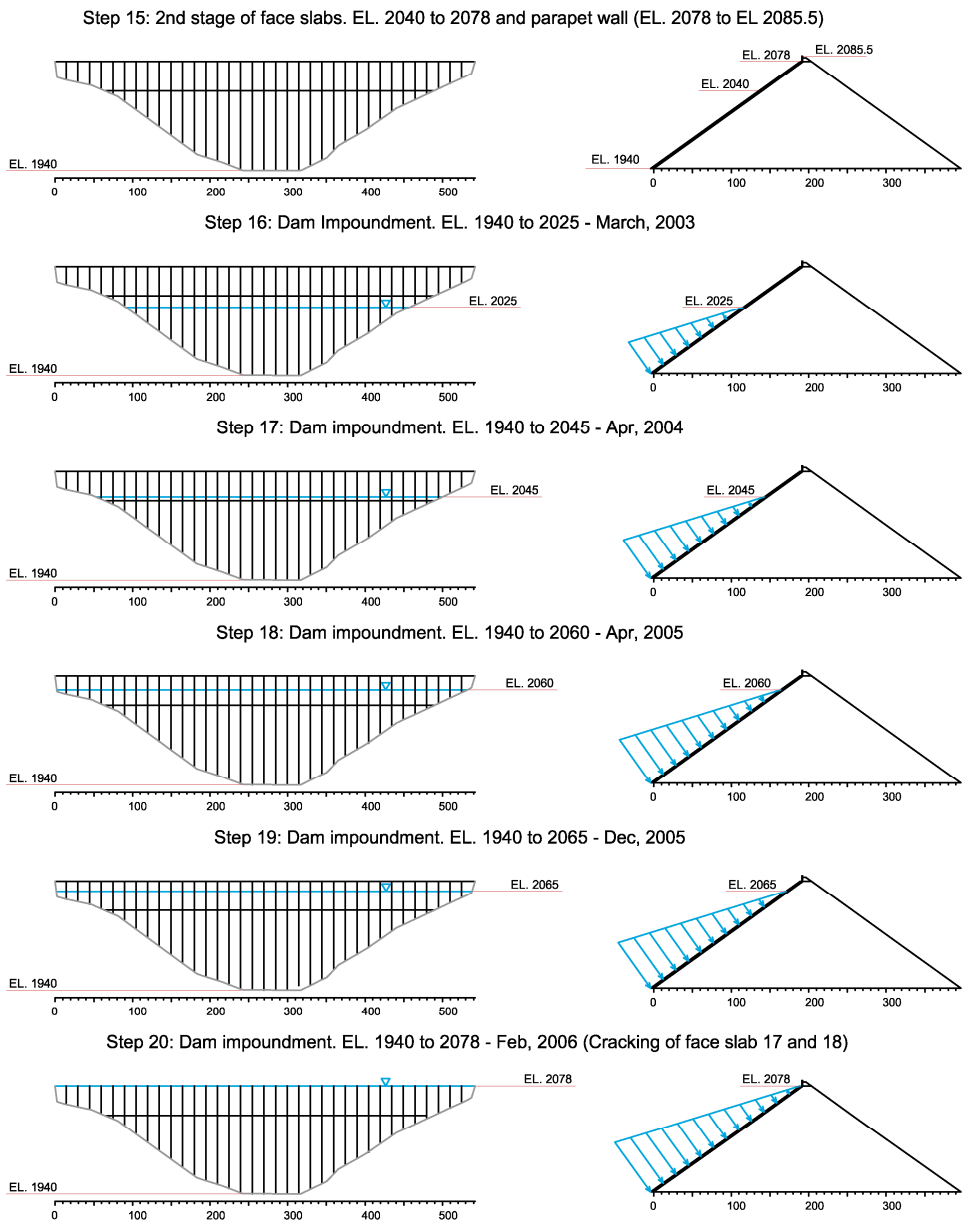

Figure 10: Construction sequence. Steps 15 to 20

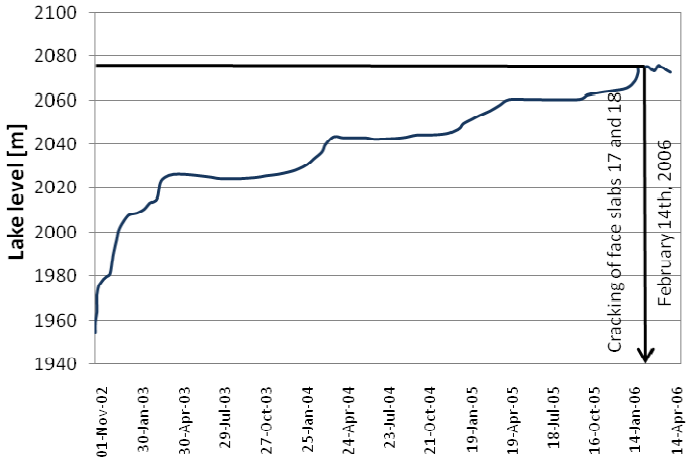

Figure 11: Reservoir levels (Ref [3])

Table 1: Placement requirements (Ref [8])

Zone	Description	Lift height [m]
1A	Impervious fill	0.3
1B	Random fill	0.6
1C	Impervious fill	0.3
2A	Fine filter	0.4
2B	Durable crushed doleritic basalt	0.4
3A	Selected small quarry run rock	0.4
3B	Quarry run rockfill	1.0
3C	Quarry run rockfill	2.0
3D	Selected durable rock	NA
3E	Quarry run doleritic basalt	1.0/2.0

Figure 12 shows a concrete beam constructed at elevation 2040 for carrying paving equipment. During the initial reservoir impoundment several horizontal cracks appeared in the concrete face around this elevation as shown in Figure 13. It is believed that these cracks are related to the local stiffening due to presence of the concrete beam [3]. No further information is available regarding this issue, however it is considered that this information might be relevant to the participants.

Figure 12: Concrete Beam at EL. 2040 (Ref [3])

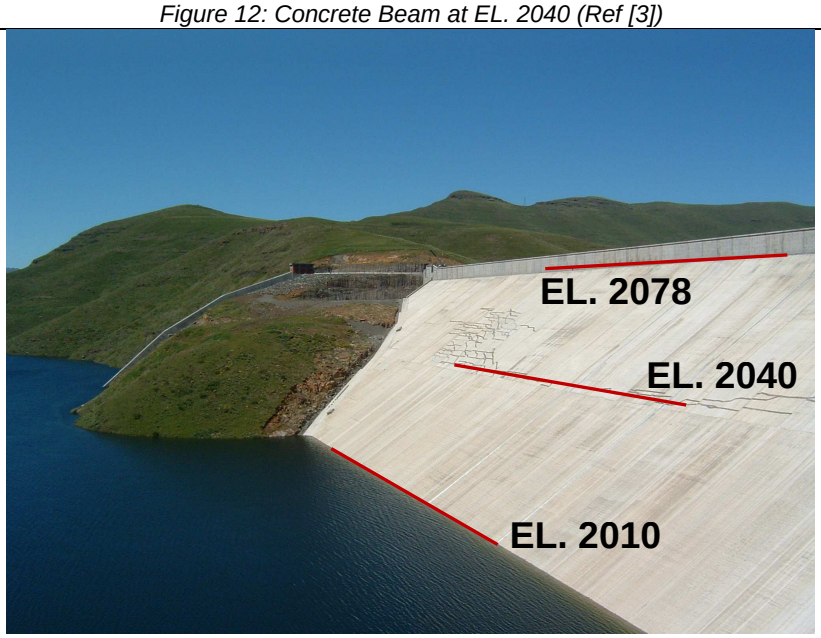

Figure 13: Horizontal cracking of face slab at EL. 2040 when reservoir reached EL. 2010 - (Aprox. Jan, 2003). (Ref [3])

2.3. Material Characterization

The description of the main zones of the Mohale dam is included in Table 2. The gradation curves for these main zones are listed in Table 3 and Table 4. The index properties obtained during construction for the different zones are presented in Table 5. Based on published data, the basalt rockfill used in Mohale was strong, however, very angular with high void ratio. After initial compaction, the fill creates an interlocking, with an apparent modulus in the range of 100 MPa, however once the load on top increases, grain breakage occurs, which may start at a low confinement of only 0.2 MPa (see Figure 14).

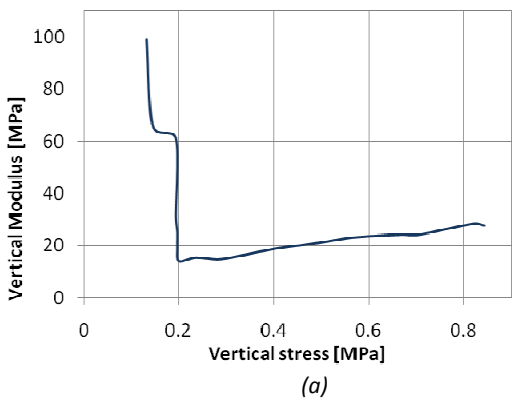

Figure 14: Settlement/load data and moduli for (a) poorly and (b) well graded basalt in Mohale dam (Ref [3])

Face concrete was conventional C25, with 30% fly ash and w/c ratio of 0.45-0.47 [4]. The compressive strength for the concrete measured during construction was higher than 28 MPa, however based on the strain measurements discussed later failure of the face occurred at lower stress values. The compressive strength of the curb measured after 12 hours was 0.9 MPa.

Table 2: Definition of Mohale dam zones (Ref [5])

Zone	Description
1	Stone powered from crushing plant or fly ash, covered by overburden
2	Fine filter (at perimeter joint), doleritic basalt
3	Crushed doleretic basalt
4	Selected small quarry run rock
5 and 6A	Quarry run rockfill
6B	Erosion protection consisting of doleritic basalt as riprap

Table 3: General Gradation requirements for rockfill (Ref [8])

Zone	Description	Gradation
1A	Impervious fill	Min 30% passing #200 sieve
1B	Random fill	Semi impervious earthfill
1C	Impervious fill	Max 30% passing #200 sieve
2A	Fine filter	D15=0.3 to 0.7 mm
2B	Durable crushed doleritic basalt	Max. particle size 76 mm
3A	Selected small quarry run rock	Max. particle size 300 mm
3B	Quarry run rockfill	<200: max 10%, <25mm: max 50%
3C	Quarry run rockfill	<200: max 10%, <25mm: max 50%
3D	Selected durable rock	60%>0.6m
3E	Quarry run doleritic basalt	<200: max 5%, <25mm: max 40%

Table 4: Gradation requirements for zones 5A, 5B and 6A (Ref [5])

Sieve size [mm]	Zone 5A	Zone 5B	Zone 6A
25 mm	< 30%	< 30%	< 30%
0.0075 mm	< 10%	< 10%	< 10%

Table 5: Summary of index properties of fill materials (Ref [6])

Material type	γ [Kgf/m³]	γ_s [Kgf/m³]	e [-]	n (%)
2A	2493	3000	0.20	16.7
2B	2459	3000	0.22	18.0
3A	2350	3000	0.28	21.9
3B	2230	2800	0.26	20.6
3C	2182	2800	0.28	21.9
3E	2274	3000	0.32	24.2

2.4. Instrumentation data

2.4.1 Settlement Readings

Figure 15 presents the location of different settlement cells across the sections indicated in Step 6 and 13 in Figure 8. The readings taken at those cells at two different stages of construction are presented in Table 6. The modulus of the rockfill calculated as indicated in the ICOLD bulletin of concrete face rockfill dams with the settlement data are also included in Table 6.

The settlements due reservoir impounding up to EL. 2075 are presented in Figure 16.

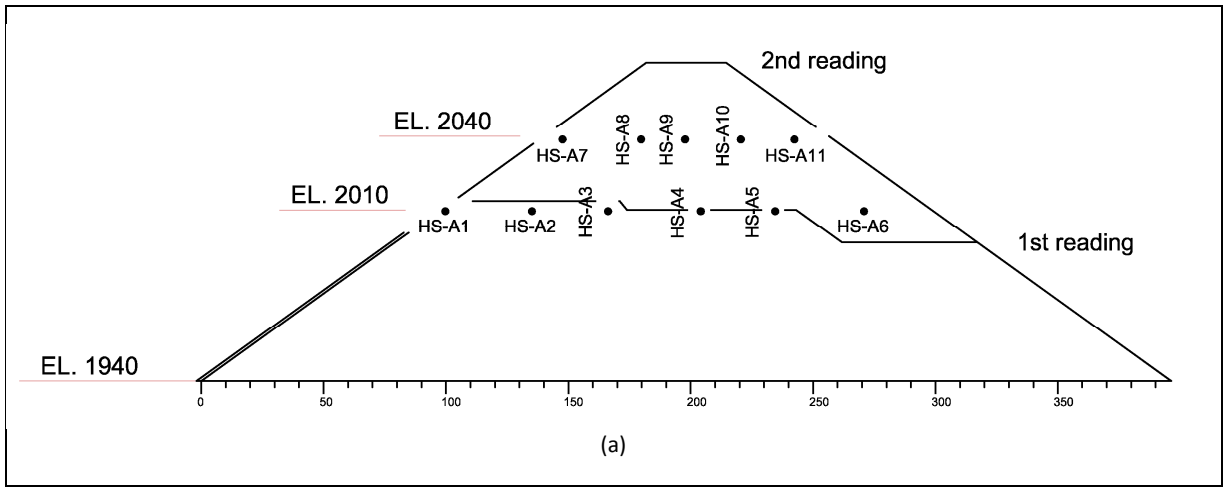

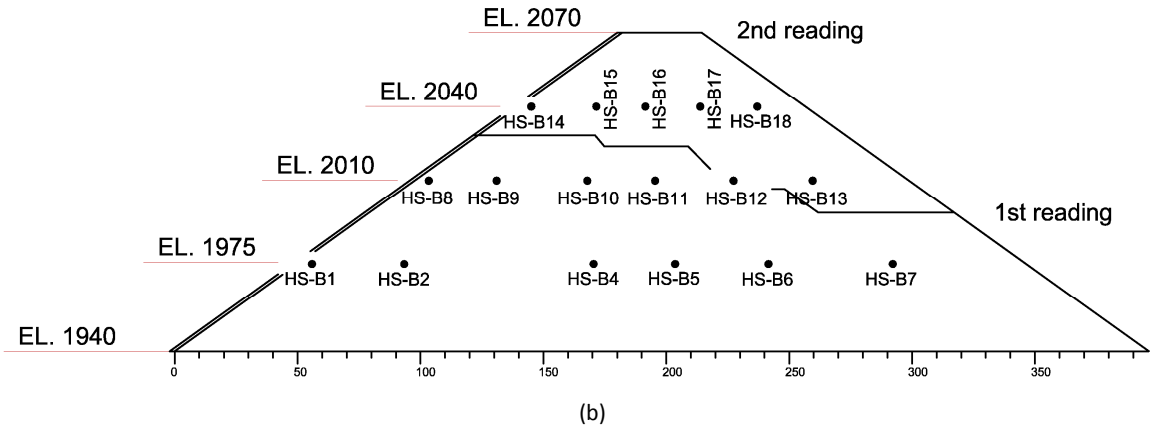

(b)

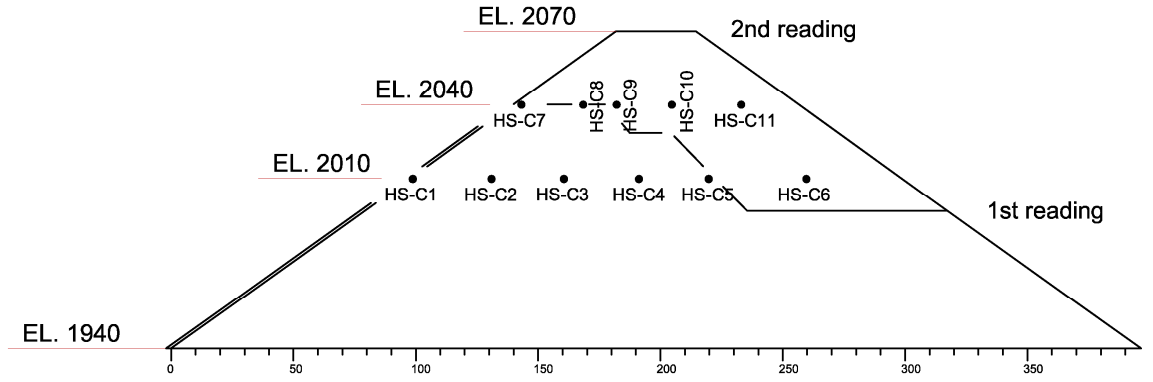

(c)

Figure 15: Location of settlement cells. (a) Left abutment, (b) Central section, (c) Right abutment.

(Ref [6], Ref [7])

Table 6: Summary of settlement readings after construction stage 5 (Ref [6])

Cell no.	1st reading		2nd reading	
	S [m]	Ev [MPa]	S [m]	Ev [MPa]
HS-A1	0.09	34.7	0.41	-
HS-A2	0.02	133.7	0.64	65.71
HS-A3	0.01	168.9	0.81	95.86
HS-A4	-	-	1.35	70.47
HS-A5	-	-	1.49	48.52
HS-A6	-	-	1.34	23.86
HS-A7	-	-	1.26	8.13
HS-A8	-	-	1.12	41.77
HS-A9	-	-	1.47	33.43
HS-A10	-	-	1.53	27.59
HS-A11	-	-	1.20	14.70
HS-B1	0.44	14.0	0.68	4.63
HS-B2	0.71	41.5	1.44	16.87
HS-B4	1.09	35.7	1.83	36.84
HS-B5	1.32	28.4	2.28	32.47
HS-B6	0.93	26.8	2.06	28.52
HS-B7	0.64	28.2	1.93	15.99

Cell no.	1st reading		2nd reading	
	S [m]	Ev [MPa]	S [m]	Ev [MPa]
HS-B8	0.45	20.6	0.83	8.16
HS-B9	0.50	54.6	1.27	29.39
HS-B10	0.55	45.6	2.27	34.73
HS-B11	0.52	40.3	2.35	40.35
HS-B12	-	-	2.68	29.74
HS-B13	-	-	2.24	19.62
HS-B14	-	-	0.59	16.40
HS-B15	-	-	1.64	31.14
HS-B16	-	-	2.16	31.17
HS-B17	-	-	1.7	39.89
HS-B18	-	-	1.58	20.18
HS-C1	0.32	17.6	0.59	-
HS-C2	0.47	64.7	1.02	34.74
HS-C3	0.80	37.5	1.72	40.93
HS-C4	0.81	22.8	2.15	44.10
HS-C5	-	-	2.15	41.10
HS-C6	-	-	1.93	22.93
HS-C7	-	-	0.55	8.18
HS-C8	-	-	1.08	42.71
HS-C9	-	-	1.69	39.94
HS-C10	-	-	1.23	55.06
HS-C11	-	-	1.28	29.76

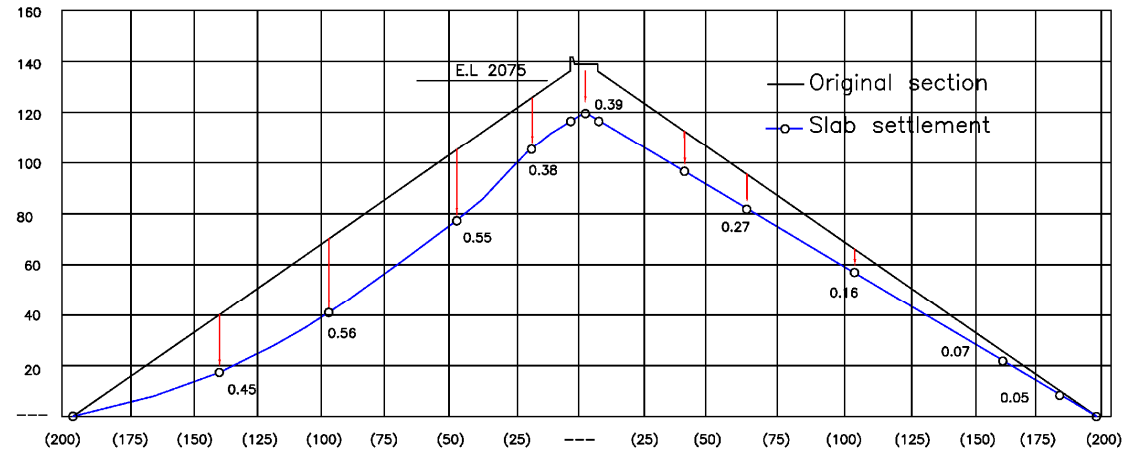

Figure 16: Surface settlements for lake level at EL 2075 (Ref [3])

Figure 17 to Figure 19 present deformation contours due only to maximum reservoir loading for downstream and cross valley deformation, and settlement values, respectively.

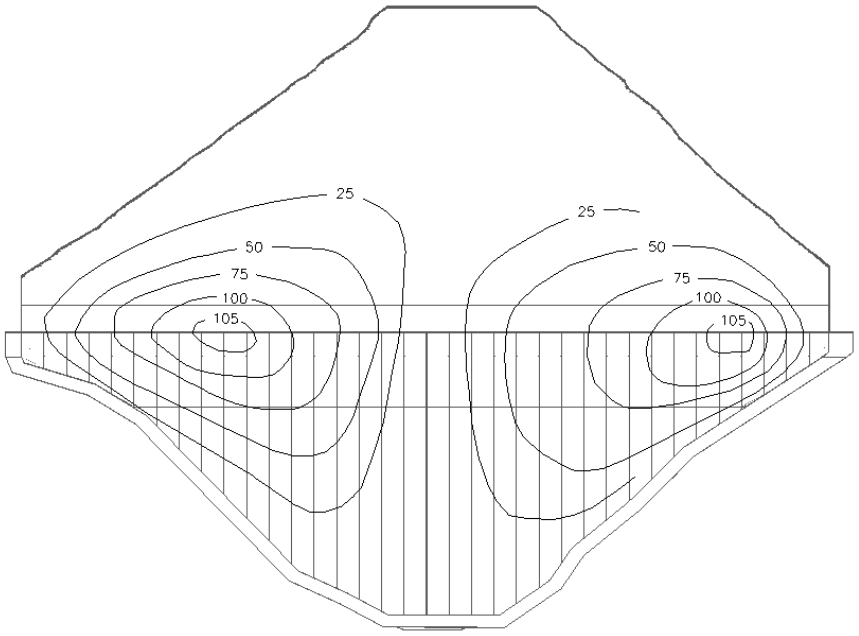

Figure 17: Cross valley movements for full reservoir loading (Ref [3])

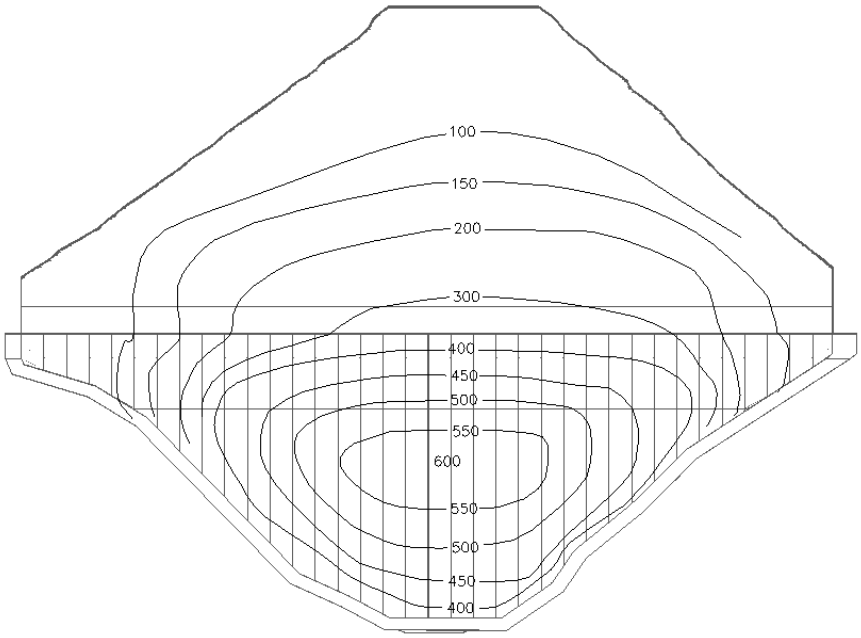

Figure 18: Settlements full reservoir loading (Ref [3])

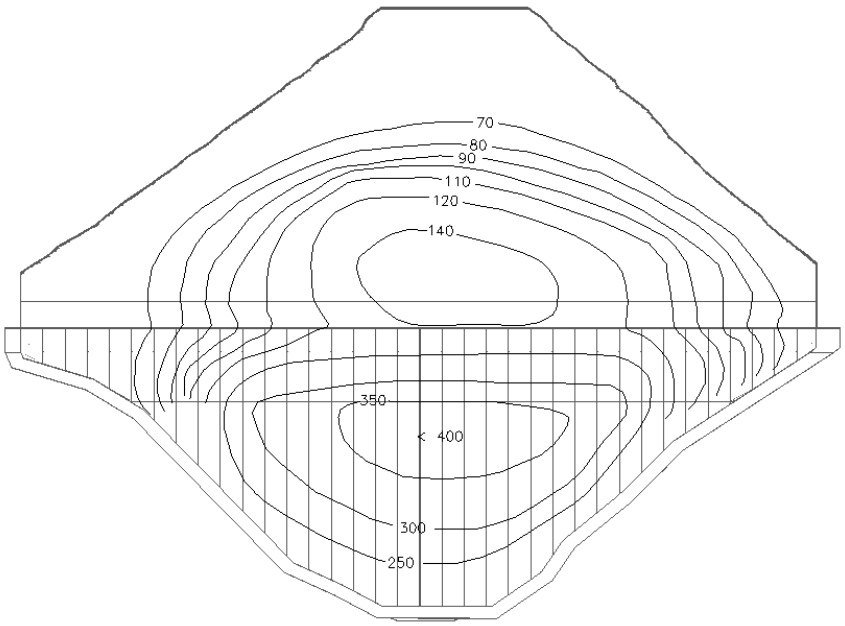

Figure 19: Downstream deformation for full reservoir loading (Ref [3])

Settlement readings against reservoir level of five different settlement cells installed at elevation 2040 are presented in Figure 20.

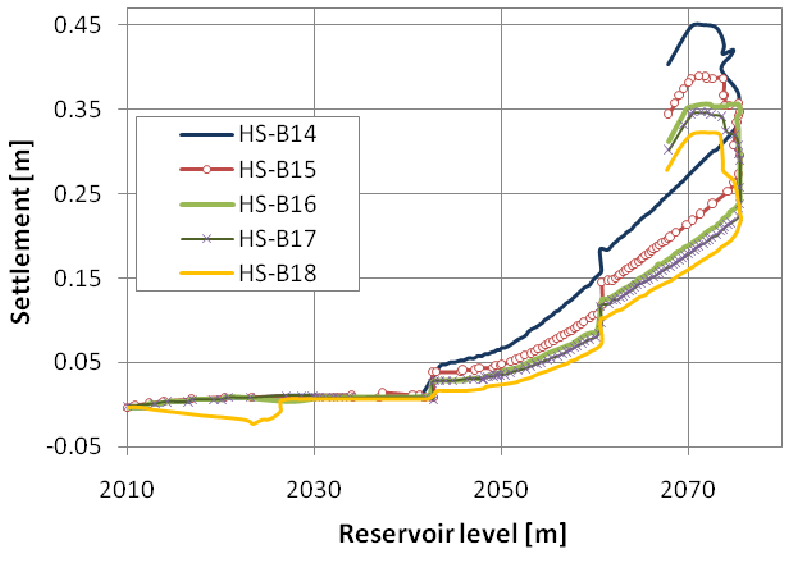

Figure 20: Cell settlement w.r.t. reservoir levels (Ref [3])

2.4.2 Load Cells

As part of the instrumentation system installed in the Mohale dam, load cells were installed at different elevations. Figure 21 presents the location of these cells across Section B (see Figure 8). The measurements of five different load cells are presented in Figure 22.

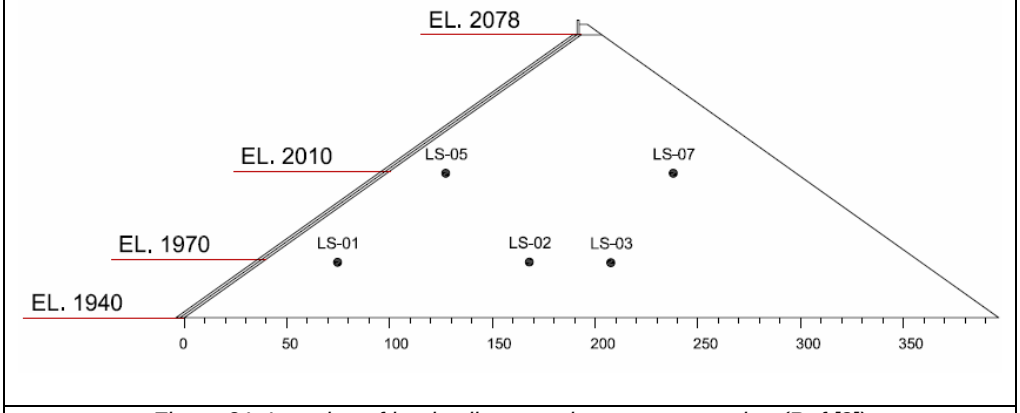

Figure 21: Location of load cells at maximum cross section (Ref [3])

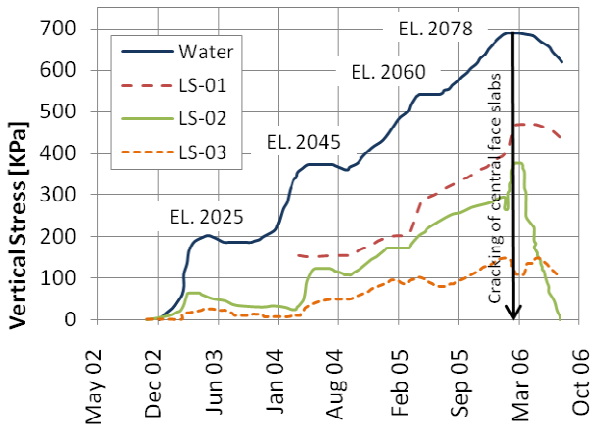

(a)

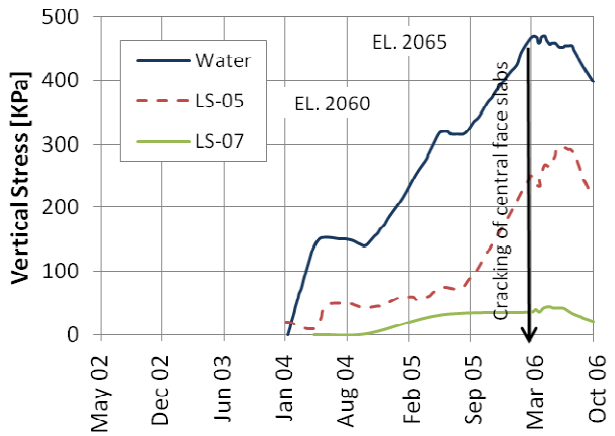

(b)

Figure 22: Load measured and reservoir load above cells vs time (Ref [3])

2.4.1 Strain Gauges

In slabs 18 and 21, a total of eight strain gauges were installed within the concrete (Identified as SG1 to SG8 in Figure 23). Figure 24 to Figure 26 present the strain measurements on each instrument. The strain cells provided excellent data, showing where and when the slab failure occurred. Spalling at the joint between slabs 17 and 18 occured at a strain of 600 – 620µm, corresponding to a compressive stress of around 20 MPa. Subsequently, vertical strain at depth increased slowly until failure occurred at slab 21 on February 14 at strain of approximately 650 µm (see Figure 26), corresponding to compression of around 24 MPa. Figure 27 presents the horizontal and vertical stresses calculated for slab 21 at the time of slab failure and after stress release. The stresss is calculated by the following equation, using a Poisson ratio of 0.25 as presented by Johannesson [3].

$$\sigma_v = \frac{E}{1-\nu^2} * (\varepsilon_v + \nu * \varepsilon_h) \quad ; \quad \sigma_h = \frac{E}{1-\nu^2} * (\varepsilon_h + \nu * \varepsilon_v)$$

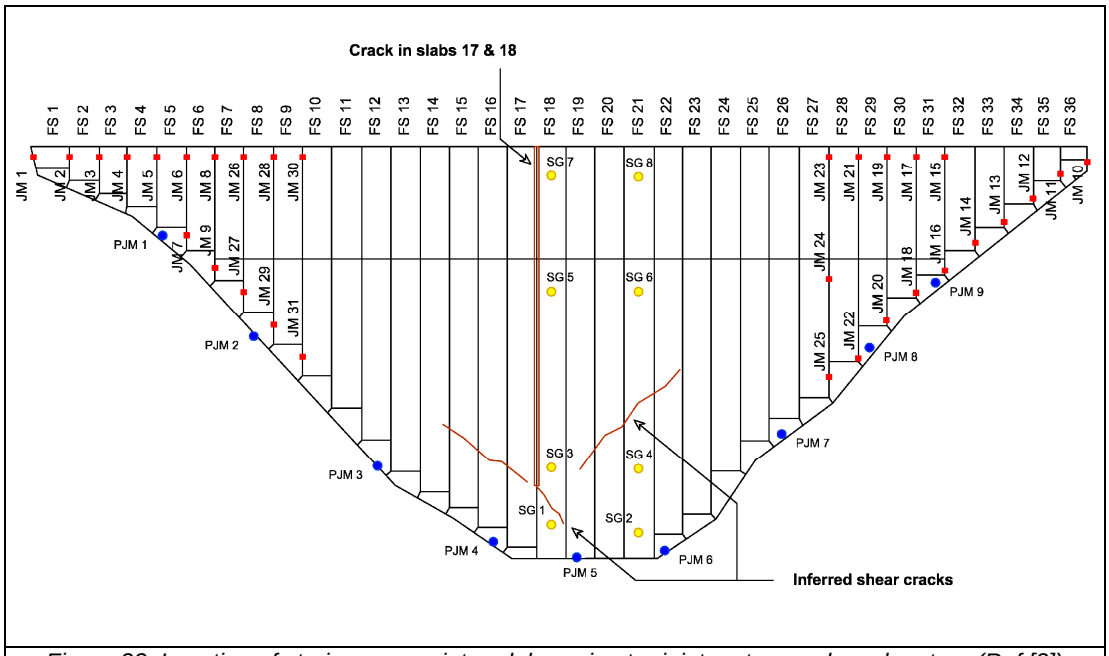

Figure 23: Location of strain gauges, inter-slab, perimeter joint meters and crack patern (Ref [3])

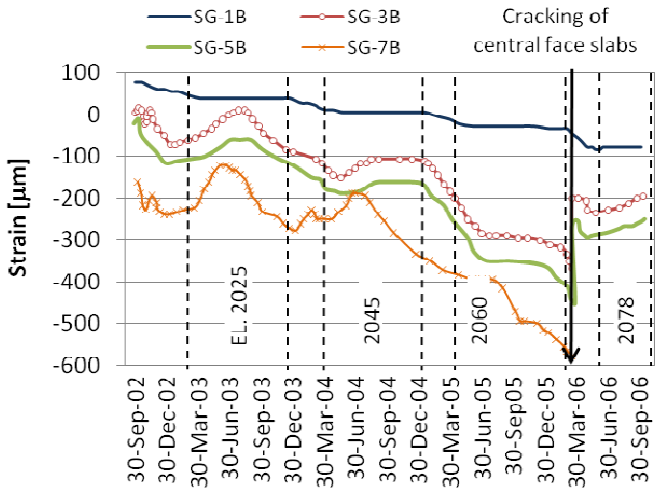

Figure 24: Horizontal strain in slab 18 (Ref [3])

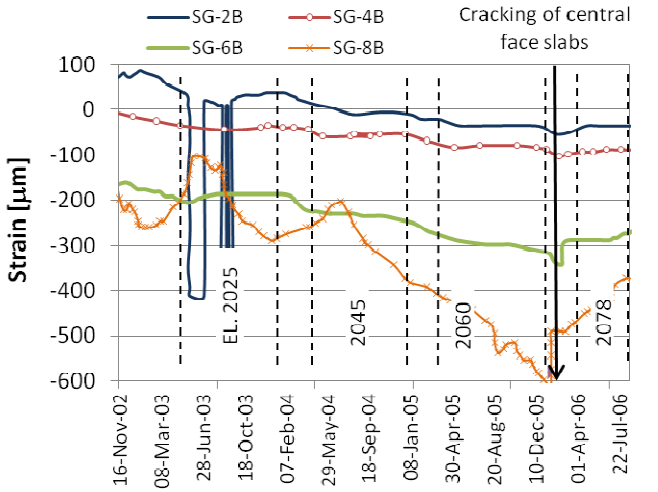

Figure 25: Horizontal strain in slab 21 (Ref [3])

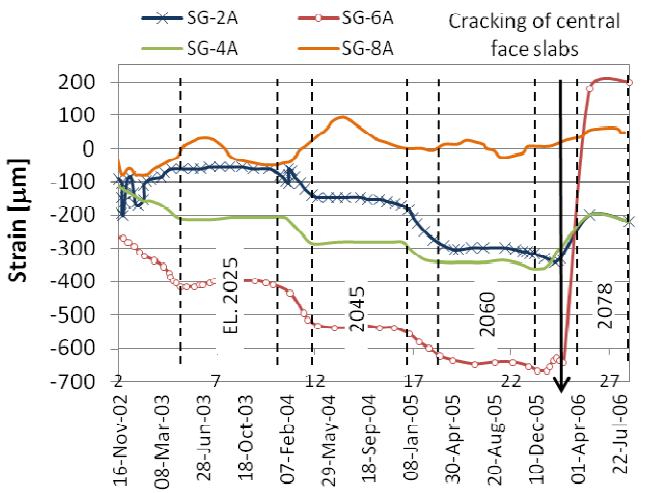

Figure 26: Vertical strain in slab 21 (Ref [3])

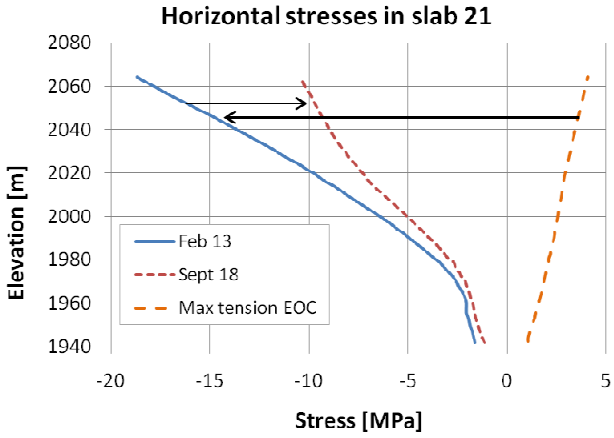

(a)

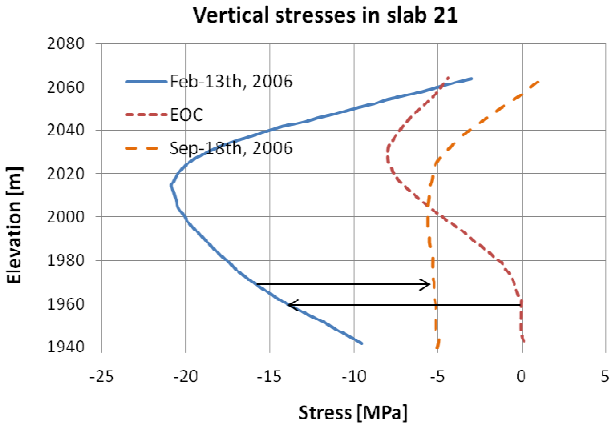

(b)

Figure 27: (a) Horizontal and (b) vertical stress for slab 21 at the end of construction, at time of cracking and for full reservoir (Ref [3])

2.4.1 Joint Readings

Readings of total joint meter movements (JM) and Perimeter joint movements (PJM) for full reservoir load are summarized in Table 7 and Table 8, respectively. The location of these instruments is indicated in Figure 23.

Table 7: Summary of inter-slab joint openings (Ref [3])

JM top	1	2	3	4	5	6	8	26	28	30
Opening [mm]	1	2	12	21	26	21	8	3	2	3

JM bottom	7	9	27	29	31	22	20	19	18	16	14	13	12	11	10
Opening [mm]	24.6	42.7	42.7	13.2	9.5	3.4	4.3	19.6	30.9	18.9	27.7	21	20.1	21.6	2.4

Table 8: Summary of perimeter joint openings at EL. 2078 (Ref [3])

PJM	X [mm]	Y [mm]	Z [mm]
9	30.7	22.8	-3.6
8	32.0	31.1	-4.0

PJM	X [mm]	Y [mm]	Z [mm]
7	19.2	9.4	4.2
6	6.6	5.2	2.4
4	-7.4	17.3	4.2
3	-10.0	23.2	7.0
2	-15.6	16.6	-12.9
1	-1.4	4.6	0.0

Figure 28 presents two sets of readings at the inter-slab joints at EL. 2040. The first were taken when all main dam components reached EL. 2040 (approximately Step 10 in Figure 9), the second when the rockfills are at EL. 2070 Step 13 in Figure 9). As shown, cracks were observed at mid-height between face slabs 23 to 27.

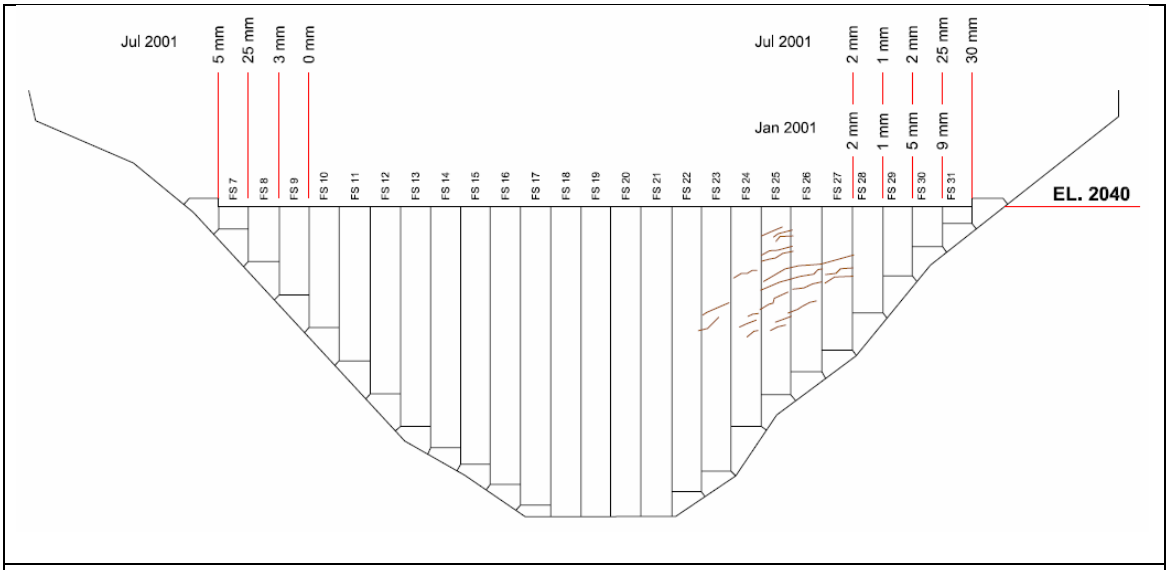

Figure 28: Opening of inter-slab joints on Jan 2001 (Aprox. Step 10) and July 2001 (Aprox. Step 13) and observed cracks in face slabs at EL. 2040 (Ref [7])

2.4.2 Face deformation

Figure 29 illustrates face deflection at the end of construction for slabs 21 and 27.

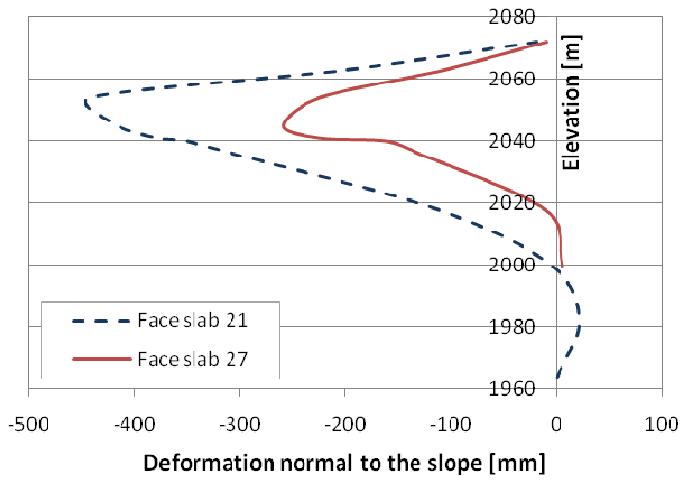

Figure 29: Deformation of face slabs 21 and 27 at the end of construction (Ref [7])

The displacements observed across the concrete face at EL. 2040 (First stage of face slabs) when the rockfill reaches EL. 2070 (Step 13 in Figure 9) are plotted in Figure 30. Worth noting is the existing gap between the curb and the face slabs, reaching almost 2 cm in the middle point.

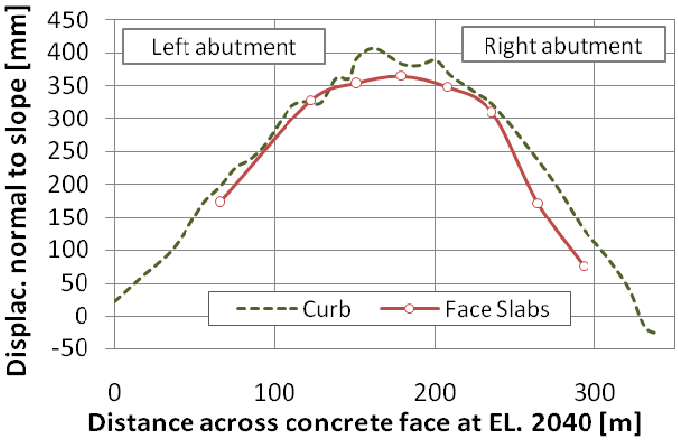

Figure 30: Displacements normal to slope for curb and face slabs at EL. 2040 – Step 13 (Ref [7])

Readings of the displacements at crest level are presented in Figure 31 to Figure 33. Figure 31 presents relative displacements across the dam axis from left to right abutment for two impounding levels; 2060 and 2078, respectively. Figure 32 shows the displacements normal to the dam axis. These displacements are mostly downstream, though the available readings for the lowest impounding level (EL. 2060) suggest that the dam crest moves slightly upstream in the central part. Finally, Figure 33 indicates settlements for three impounding levels. It should be noted that displacements drastically increase in the three components when the reservoir level reached EL. 2078.

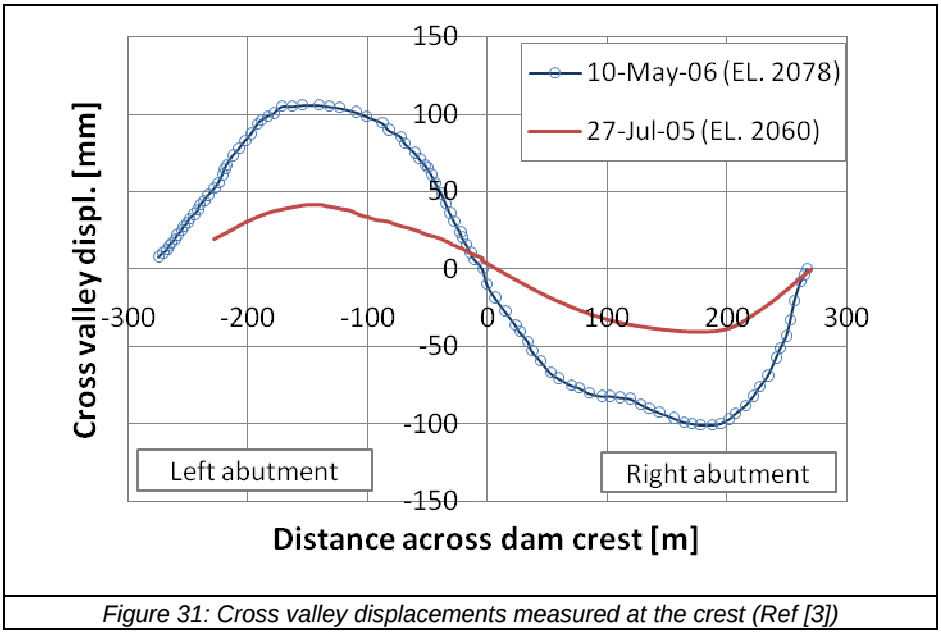

Figure 31: Cross valley displacements measured at the crest (Ref [3])

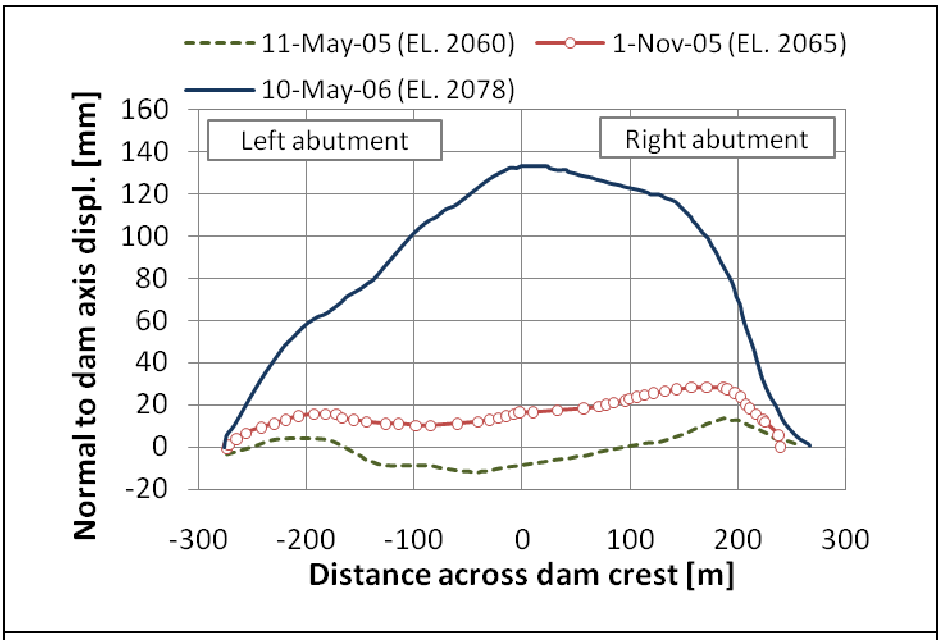

Figure 32: Displacements normal to dam axis measured at the crest (Ref [3])

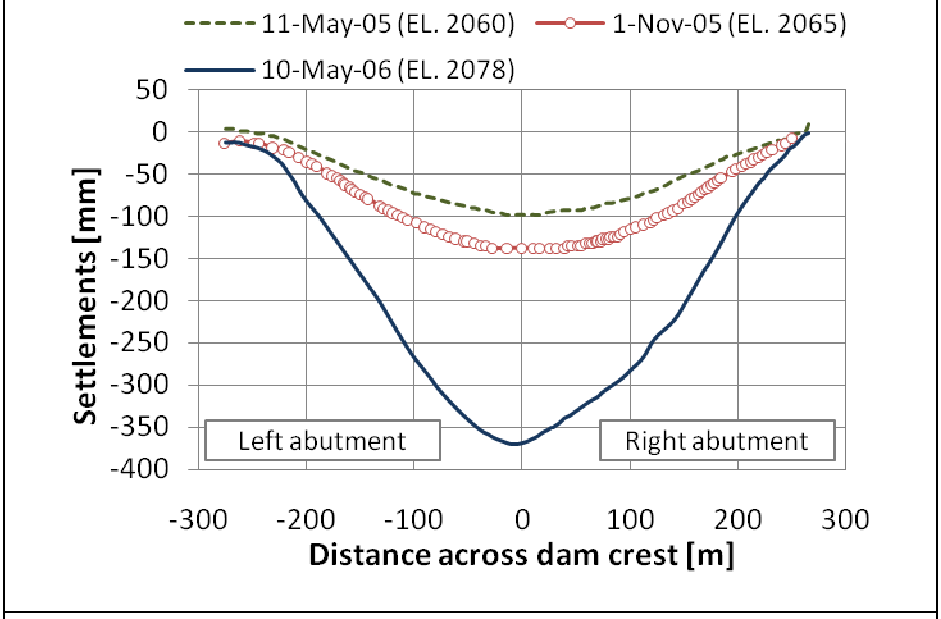

Figure 33: Settlements across dam crest (Ref [3])

Finally, Figure 34 shows the location of cracks observed in the curb. At this particular stage, the concrete face reached EL. 2040 whilst the rockfill was at EL. 2070 (See Step 13 in Figure 9). The amount of opening for almost all observed cracks was less than 15 mm, however a 120 mm wide opening was observed in the vertical crack between slabs 28 and 29.

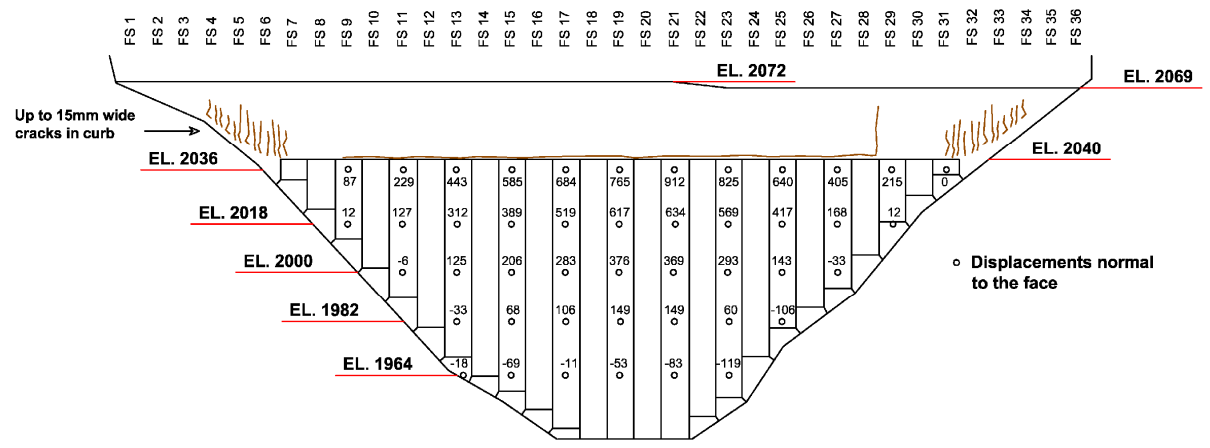

Figure 34: Crack pattern observed in curb and values of displacements normal to the face at various locations – Step 13 (Ref [7])

3. REQUESTED RESULTS

All Participants are kindly requested to provide a paper with 15 pages maximum, in which all assumptions are clearly exposed (especially as regards initial and boundary conditions). For comparison purposes, the participants must also give their key results under a prescribed format, in a EXCEL file derived from the **ThB_ResXXXX.xls** provided, where they will replace XXXX by an acronym of their organisation.

3.1. Fill Settlements

Settlement contours for three longitudinal sections and one cross section along the dam crest shall be presented. The results shall be presented at the end of construction and after reservoir impoundment The location of each section is indicated in step 6 in Figure 8.

3.2. Stresses within the Dam

The calculated prinicial and vertical stresses obtained from the analysis on 5 points within the fill shall be presented. The location of each point is illustrated in Figure 21. The results shall be presented at the end of construction and after impoundment.

3.3. Strains and stresses within the Concrete Face

The calculated vertical, horizontal and principal stresses and strains within the concrete face obtained form the analysis at eight different locations must be reported. The location of each point is illustrated in Figure 23. The participants should also present a contour plot of the calculated stresses and strain in the entire concrete face. The results shall be presented at the end of construction and after impountment. Participants shall also present the crack pattern derived from their analyses.

3.4. Face deflection

Face deflection along three face slabs shall be reported. The location of each section is also illustrated in Figure 8 (section A, B and C). The results shall be presented at the end of construction and after impoundment.

3.5. Joint openings

The estimated joing openings of 40 points distributed within the perimetral joint and the vertical joints shall be presented. The location of each point is shown in Figure 23. The results shall be presented at the end of construction and after impountment.

4. References

[1] SOBRINHO J.A., XAVIER L.V., ALBERTONI C., CORREA C., FERNANDES R. (2007) – "Performance and concrete repair at Campos Novos" Hydropower and dams. Issue two.

[2] PINTO N.L.S., (2007) – "A Challenge of very high CFRD dams: Very high concrete face compressive stresses" 5th Int. Conf. on Dam Eng., Lisbon, Portugal

[3] Johanneson P. (2007). Lessons learned from the cracking of Mohale CFRD slab. International WaterPower and Dams Construction, August, 2007

[4] Johanneson P. (2007). Slab performance on a few CFRDS and suggested improvements in slab design. Workshop on High Dam Know-how, May 22-24, 2007, Yichang, China.

[5] Johannenson P. (2007). Modified zoning and compaction requirements for future high CFRDs. Workshop on High Dam Know-how, May 22-24, 2007, Yichang, China.

[6] W. Riemer. Personal communication. Construction schedule, settlement readings and pictures during construction.

[7] W. Riemer. Personal communication. Construction sequence, settlement readings and deformation of face slabs during construction.

[8] Gratwick C., Johannenson P., Tohlang S., Tente T., Monapathi, N. (2000). Mohale Dam, Lesotho. Proceedings of the International symposium on Concrete Faced Rockfill Dams. 19-22 September 2000. Beijing, China.

[9] W. Riemer. Personal communication. Summary of main construction steps.

[10] Johannesson, Gratwick, Badenhorst and Nthako (1997). The design of the Mohale Dam", 8th Annual South African Institution of Civil Engineers Congress.

[11] Johannesson, P., (1997). Leshoto, Mohale Dam; Hydropower and Dams, Issue Four.

[12] Johannesson, P., Gratwick, C., Nthako, S. (1997). Mohale CFRD, Design Considerations; 3rd International Hydropower Conference, Trondheim, Norway.

A CFRD CASE USING 3D MODELLING.

10th Benchmark Workshop on Numerical Analysis of Dams

September 16-18, 2009 – Paris, France

C. Nieto[1], J-C. Philippe[1], M. Werst[1], P. Anthiniac[1].

[1]TRACTEBEL ENGINEERING - COYNE ET BELLIER, 9 allée des Barbanniers, 92632 Gennevilliers Cedex, France.

ABSTRACT: A numerical study of Mohale CFRD in Lesotho is performed using 3D FEM modeling and a non linear elasto plastic constitutive law. The modeling includes the assessment of stress and strains at the concrete face. Comparisons between in-situ measurements and numerical results show relevant differences. Because the results of this study are not being still accomplished, our contribution concerns a critical analysis of the methods.

Key Words: Concrete Face Rockfill Dam, Non-linear numerical analysis, Upstream face deflections, Rockfill settlements.

1 INTRODUCTION

The dam's construction current practice makes the Concrete Faced Rockfill Dams (CFRD) one of the most popular type. This popularity is due to their relative construction simplicity, low cost of raw materials, general stability and short term construction. The construction techniques have evolved from a rockfill material dumped before the 60's to a set of construction guidelines including compaction nowadays. However the current practice is still empirical and this approach has shown its restrictions. Therefore the use of numerical method is intended to give some highlights about the complex behavior of this kind of structure and the interaction of its components. In this context the theme B of the 10th Benchmark Workshop on Numerical Analysis of Dams presents an opportunity to compare different techniques of analysis of a well documented case study [1].

The case study refers to Mohale Dam [2] where cracks observations were reported during impoundment. These problems have been experienced in other cases, i.e. Campos Novos and Barra Grande [3] in Brazil and Tianshenqiao-1 in Chine [4]. The consequences among others are the increase in leakage flow, inter slabs joint opening as well as perimetral joint or slabs overlapping. The causes are still discussed. In one hand, the non linear behavior of granular materials combined with, on the other hand, the soil structure interaction (embankment – concrete slabs).
The size of the structures involved, as well as their interactions make the numerical modeling of Mohale dam a three dimensional multi-scale problem.

The results presented afterwards correspond to the set of two finite element models. The first model intends to represent the embankment behavior. Only the rockfill materials are considered. The displacement field at the upstream face is recovered and applied as load condition to the second model representing the concrete face. In this strategy two different FE codes were used: for the former model, a geomechanic specialized FE software named GEFDyn and for the latter the ANSYS software. This strategy assumes that the reservoir hydrostatic pressure is perfectly transferred to the upstream face of the embankment body.. However this relationship is not assumed in the second model, where interface elements are used to simulate the settlements transfer by friction existing between the embankment and the concrete face. The principal details of each model are described afterwards.

2 MOHALE'S PROJECT GENERAL DESCRIPTION

The 145 m high Mohale Dam is located in central Lesotho and is part of the Lesotho Highlands Water Project. The upstream / downstream slopes are 1.4h-1v and the crest length reaches 600 m. The dam was constructed of basalt rockfill on a basalt foundation. The construction stage took place between early 1998 [5] and 2000 [2]. The materials zoning is shown in figure 1 and their description in tables 1 to 3. More specific design details are found in reference [5].

Table 1. Definition of Mohale Dam Zones [1]

Zone	Description
1	Stone powered from crushing plant or fly ash, covered by overburden
2	Fine filter (at perimeter joint), doleritic basalt
3	Crushed doleretic basalt
4	Selected small quarry run rock
5 and 6A	Quarry run rockfill
6B	Erosion protection consisting of doleritic basalt as riprap

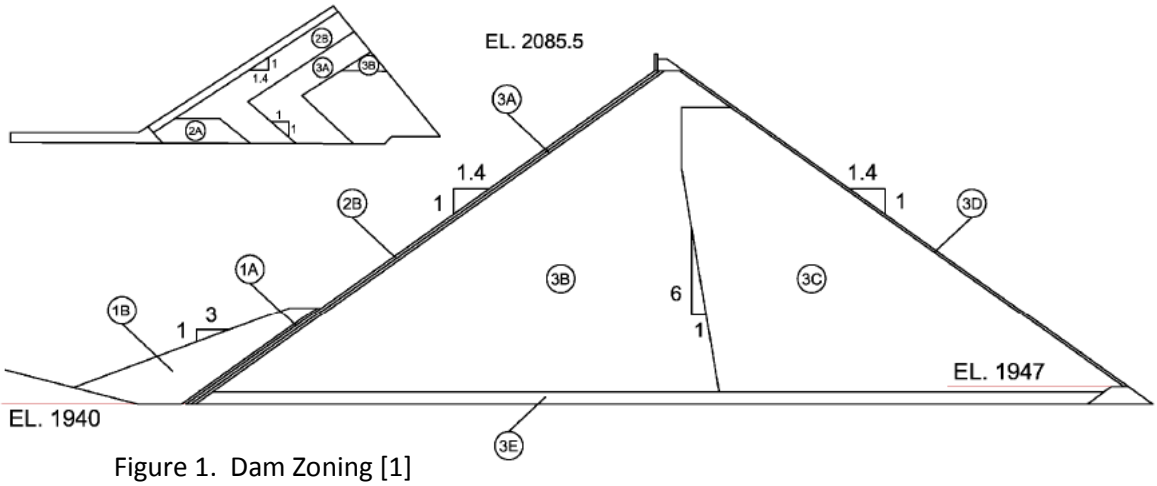

Figure 1. Dam Zoning [1]

Table 2. General Description, lift height and gradation for zones in Mohale Dam [1]

Zone	Description	Lift height [m]	Gradation
1A	Impervious fill	0.3	Min 30% passing #200 sieve
1B	Random fill	0.6	
1C	Impervious fill	0.3	Max 30% passing #200 sieve
2A	Fine filter	0.4	D15=0.3 to 0.7 mm
2B	Durable crushed doleritic basalt	0.4	Max. particle size 76 mm
3A	Selected small quarry run rock	0.4	Max. particle size 300 mm
3B	Quarry run rockfill	1.0	<200: max 10%, <25mm: max 50%
3C	Quarry run rockfill	2.0	<200: max 10%, <25mm: max 50%
3D	Selected durable rock	NA	60%>0.6m
3E	Quarry run doleritic basalt	1.0/2.0	<200: max 5%, <25mm: max40%

Table 3. Summary of index properties of fill materials [1]

Material type	γ [Kgf/m³]	γ_s [Kgf/m³]	e [-]	n (%)
2A	2493	3000	0.20	16.7
2B	2459	3000	0.22	18.0
3A	2350	3000	0.28	21.9
3B	2230	2800	0.26	20.6
3C	2182	2800	0.28	21.9
3E	2274	3000	0.32	24.2

3 MODEL DESCRIPTION

As mentioned before the strategy adopted was to analyse the problem by means of two models. The first model was intended to simulate the behaviour of the rockfill embankment during construction and impoundment. Then the displacement field at the upstream face was recovered and applied as an external load to the second model representing the upstream concrete face. The former model was developed using GEFDyn, a finite element code developed by Coyne-et-Bellier and other partners[1], specialised in geotechnical structures with non linear behaviour. The model representing the concrete face was analysed using ANSYS FE Code.

3.1 EMBANKMENT MODEL

By analysing the geometrical data provided in theme B some questions were formulated. By tracing the cross-valley profile at crest location, this profile was found to not match with the rest of profiles given all along the theme B [1]. In theme B the profiles showed the left abutment rising up from elevation1940 while contours level plan gave an elevation of 1950. Therefore, in reason of the lack of more information, the level contours at left abutment were reduced by 10m (See Annexe 1).

The modelling hypothesis for the embankment model can be summarized as:

- Both abutments and foundation are considered as infinitely rigid; therefore they are not included in the model.
- There is no consideration of relative movements at the interface between the embankment and the abutments or foundation. This leads to null displacements imposed at boundary nodes at the foundation contact.
- The material zoning is simplified; finally just three set of parameters are used to represent the materials.
- The construction scheme is simplified and reduced to three main stages all characterised by a lift height of 5 meters. The first stage follows the upstream-downstream profile given for section B at the state of First Reading as shown in figure 2a. However a homogeneous lift in the cross-valley direction has been adopted. The second stage (figure 2b) follows the u/s-d/s

1 *EDF, BRGM & ECP-LMSSMat Laboratory*

profile of B section until the stage of concrete slabs construction. Finally the construction is achieved by completing the section.

A constitutive non-associated elasto-plastic model is proposed within the framework of isotropic hardening plasticity using effective stress and characteristic state concept. In this model, four mechanics are defined: three plane strains mechanisms associated to three perpendicular planes for the deviatoric behaviour, and a mechanism for the isotropic behaviour. The four mechanisms are coupled. A cinematic condition is introduced in the deviatoric mechanisms to allow the creation of volumetric plastic strains under deviatoric loading.

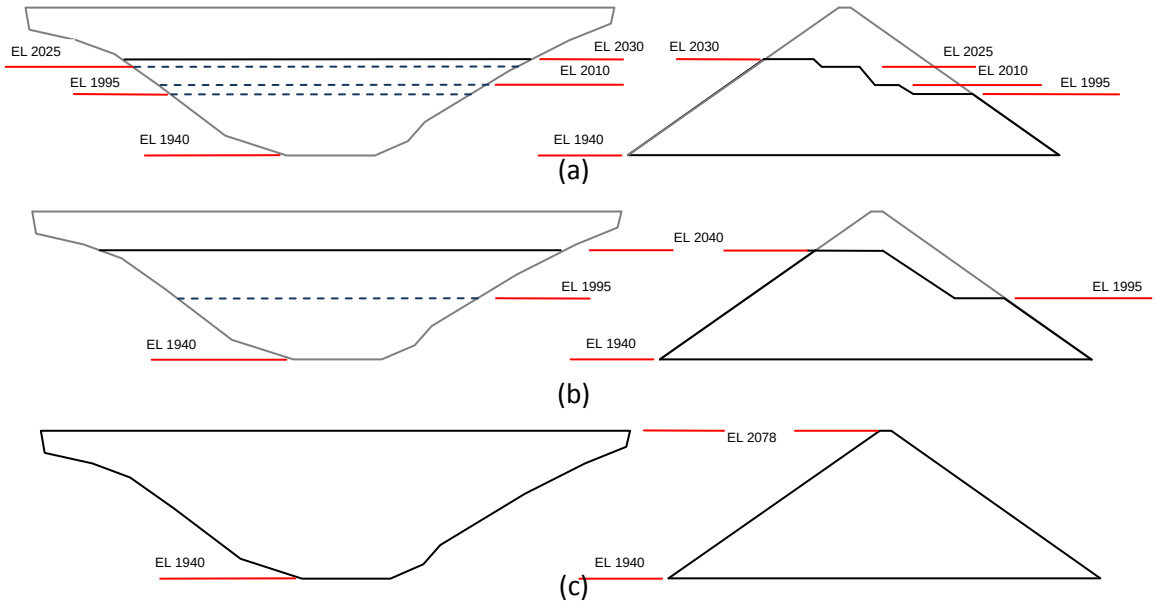

Figure 2. Simplified construction scheme. (a) First stage construction. (b) Second stage construction. (c) Final profile construction.

Parameters estimation for Rock fill Materials

Due to the lack of laboratory or field data concerning the mechanical characteristics of the rockfill materials, a numerical back analysis has been carried out in order to estimate the parameters needed for the numerical simulations. Initially a 3D finite element model was built with data issued from previous experience in Coyne et Bellier. However this 3D model was found to be fairly expensive in computation time. Then, a comparison between the simulation results of a 2D model and the initial 3D model was done. The agreements between the two models were found to be very acceptable for the "B section", this aspect let us to continue the back analysis over the 2D model.
The scope of the back analysis was to found a set of parameters matching the settlement readings given for the benchmark. In order to compare the different models an unbiased error estimator was defined (equation 1).

$$[1] \quad ES = \frac{\sum_{i=1}^{n} \left(T_m^i - T_c^i \right)^2}{\sum_{i=1}^{n} \left(T_m^i \right)^2}$$

Where T_m corresponds to the measured settlement at a point *i* and T_c corresponds to the calculated settlement at the same point. For each set of parameters the error estimator was calculated at first and second reading stages and also for the settlements of the face after impoundment.
The zoning of parameters is shown in figure 3, and the values retained from the back-analysis process are given in table 4.
The simulation results for first and second reading stages are plotted in figure 4.

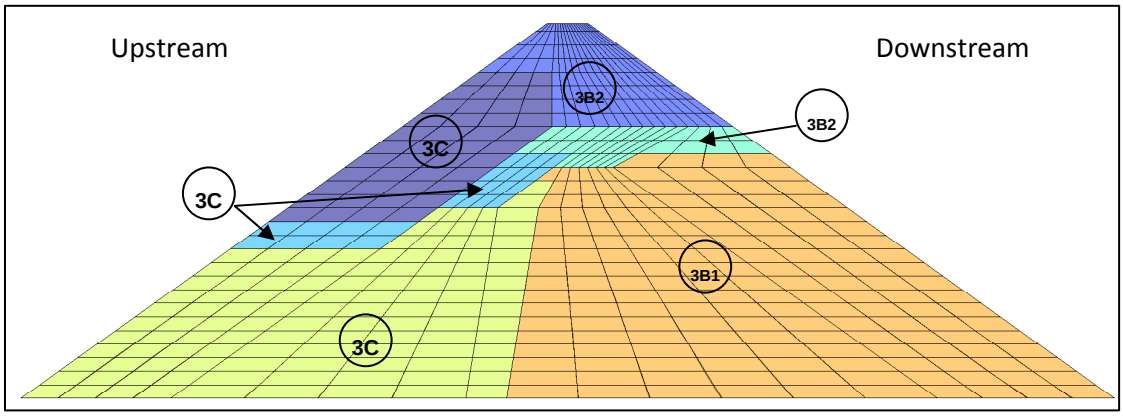

Figure 3. Materials zoning at maximal section.

Table 4: Model Parameters

Elasticity			
Material	3B1	3B2	3C
K_{ref} [MPa]*	30,1	21,8	17,1
G_{ref} [MPa]*	19,3	12	11,1
n*	0,2	0,2	0,3
p_{ref} [MPa]	1	1	1
Critical State and Plasticity			
ϕ_{pp}[°]**	38	38	38
β	17	17	17
d	2.5	2.5	2.5
b	0,2	0,2	0,2
p_{co}[MPa]	1,5	1,5	1,5
Flow Rule and Isotropic Hardening			
ψ[°]	35	35	35
α_ψ	1	1	1
a_m	1,8e-2	1,8e-2	1,8e-2
a_{cyc}	2e-4	2e-4	2e-4
C	1e-4	1e-4	1e-4
c_{cyc}	5e-5	5e-5	5e-5
M	1	1	1
Threshold Domains			
r^{ela}	1e-2	1e-2	1e-2
r^{hys}	5e-2	5e-2	5e-2
r^{mob}	0,9	0,9	0,9
r^{ela}_{iso}	1e-4	1e-4	1e-4

* $K = K_{ref}\left(\frac{p}{p_{ref}}\right)^n$

** Friction angle at critical estate.

3.2 CONCRETE FACE MODEL

The modelling of the concrete face was made as described below.

The concrete face model is constituted by three layers:

- a downstream "transition" layer aiming to use different meshes for the upstream face of the 3D model and for the concrete face itself. This transition is modelled by shell elements having a very high stiffness;
- a sliding interface, governed by a Coulomb friction law. This interface is modelled by node-to-node contact elements;
- the concrete face itself modelled by shell elements with a constant thickness of 50 cm (minimum thickness of the concrete face is 30 cm and maximum 70 cm [1]).

The field of displacements of the upstream face of the 3D rockfill embankment model is applied to the downstream face of the "transition" layer.

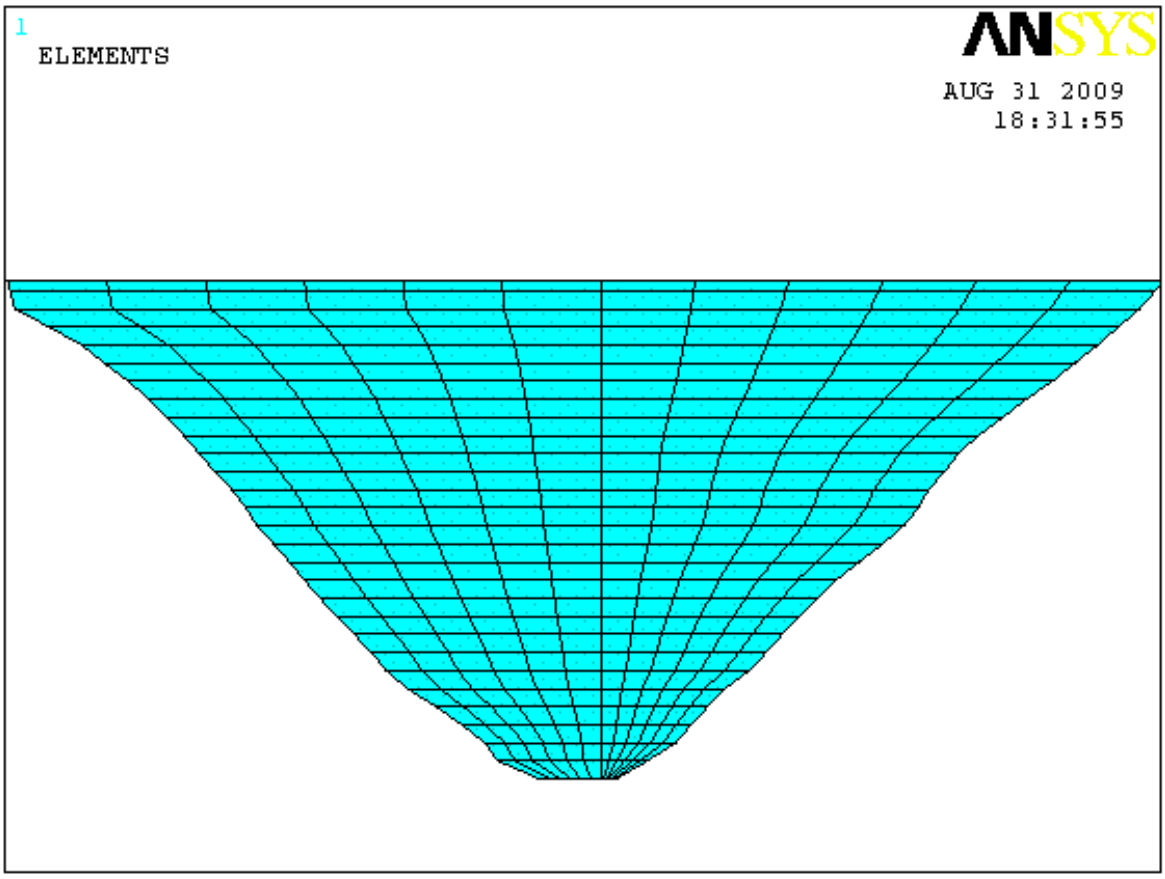

Figure 4: Mesh of the concrete face

Elements used

The contact element used for the interface is described on the picture below:

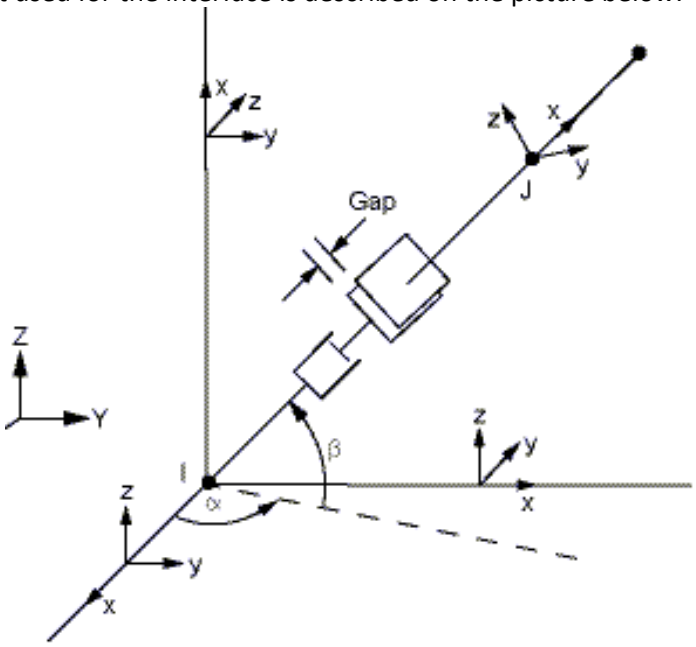

Figure 5: Contact node to node

This element represents contact and sliding between any two nodes of any types of elements. The element is governed by a Coulomb friction law.

In order to have an understanding behaviour of the interface, the extremely stiff plate is placed upstream to the concrete face. The interface should be always restrained in that way.

With this assumption, the normal stress through the interface is not the same than applying the water pressure. The normal stress is the results of the equilibrium between the stiffness of the concrete face and the stiffness of the interface (which transmit the settlements of the rockfill).

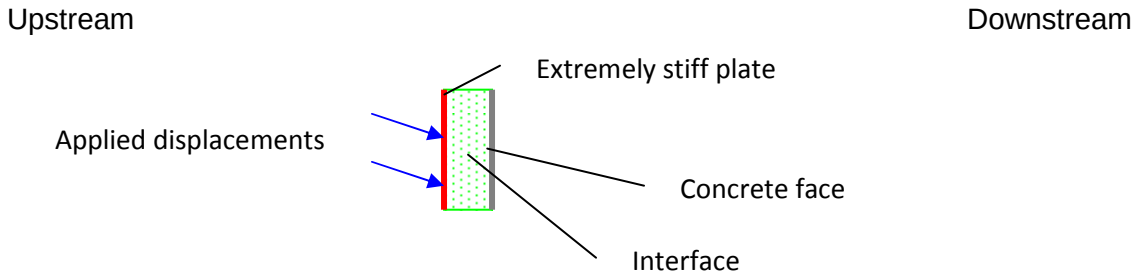

Figure 6: Sketch of the concrete face computation

To represent the concrete face, a 4 node finite strain shell elements is used. This ANSYS element is suitable for analyzing thin to moderately thick shell structures. It is also well suited for linear, large rotation, and/or large strain nonlinear applications (to go further).

Materials properties

Concrete face:

For reasons of convergence, the concrete face is calculated with an elastic law.

E = 10 GPa (concrete long term Young Modulus – f_{c28} = 25 MPa)
v = 0.2

Interface:

The coefficient of friction is taken approximately in 2/3 of the internal coefficient of friction of the rockfill. f = 0.5.

The tangential and normal stiffness equal 12.5e6 MN/m, in order to transmit the displacements without too many strains.

Load cases

The extremely stiff plate has for load the displacements imposed by the settlement of the rock fill at different stages:

- the end of construction (before 2nd stage of face slabs - displacements applied below EL. 2040),
- the impoundment at the elevation of 2025,2045,2060
- the end of impoundment at EL. 2078.

The concrete face has for load the displacements transmit by the interface.

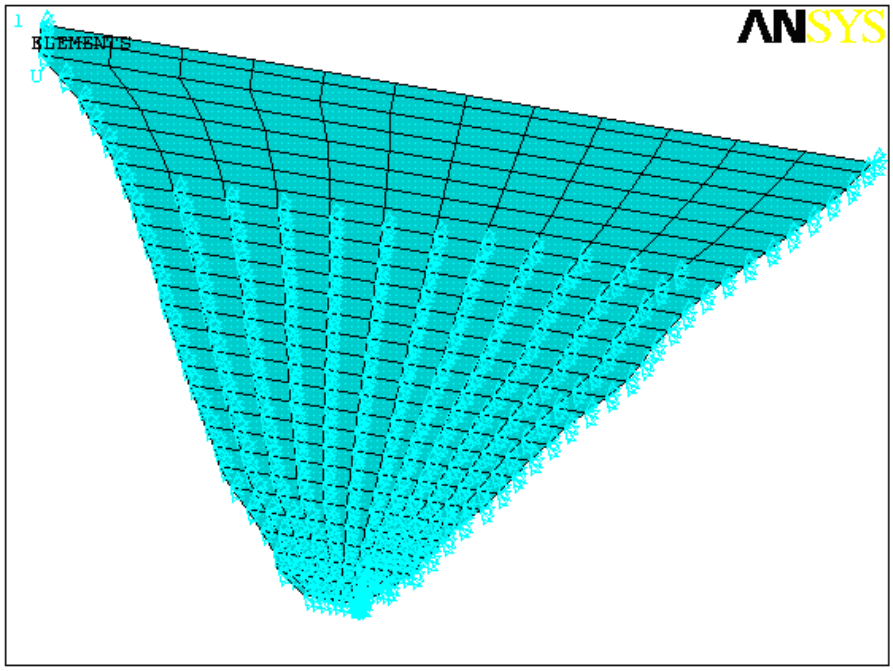

Figure 7: Displacement loads on the nodes of the extremely stiff plate

4 RESULTS

Simulations Results – Rock fill behaviour

The results requested in the workshop in terms of settlements are shown in figures in appendix A.

During construction stage the settlements magnitude seems to match with the field data especially at section B for all the settlement cells. Figure A5 shows that the assessed settlements are lower than the measured, in a part it is explained because the back analysis took also into account the impoundment stage where a stiffer behavior is observed. The Young modulus obtained from the back-analysis corresponding to zones 3B1, 3B2 and 3C are around 47.8, 34.6 and 27.1 MPa respectively. These moduli are in the rage of the moduli inferred from the data obtained at the end of construction (see [2]). The difference between the measured and the calculated settlements are more important in section A. A reason for that is that apparently this zone seems to have a lower modulus according to field data in reference [2]. Sections B and C have similar moduli and in consequence the results of the construction settlements assessment are better.

For impoundment stage the calculated settlements have two different tendencies. Near the upstream face the settlements are overestimated while toward the downstream side they are underestimated. As it could be inferred, this tendency is also observed in terms of stresses. The vertical stresses contours for full reservoir level is shown in figure A9, and a comparison for full reservoir level for load cells at B section is done in figure 5.

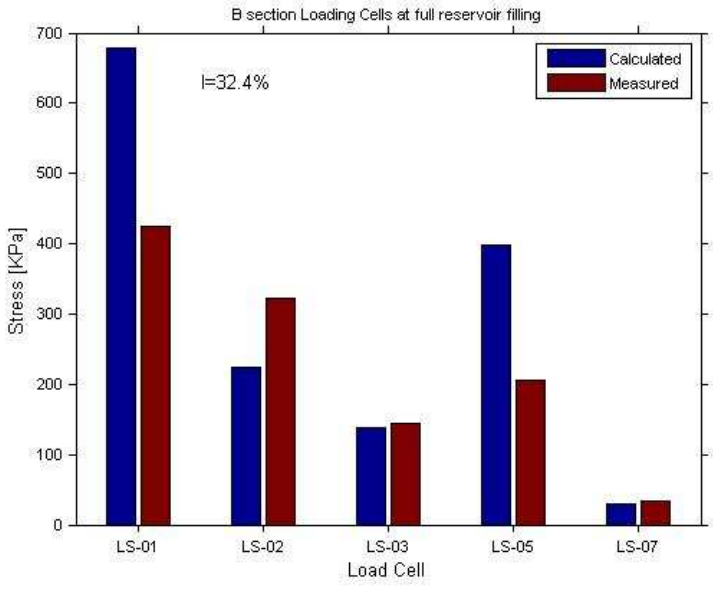

Figure 8. Vertical stress at load cells for full reservoir level.

Concrete face behaviour

The calculations were made until the EL. 2060. A problem due to the software ANSYS (not resolved by the end of august 2009) did not allow the extraction of the results for the maximum impoundment.

Our conclusion about the maximum impoundment will be done at the EL. 2060.
This conclusion is a short one: we just observed an important horizontal compressive strength near the slabs 17 and 18. The stress state of the interface is difficult to obtain (compressive stresses between 0.5 et 5 MPa, to be compared with the hydraulic gradient), but we know that the higher normal stress between the concrete face and the extremely stiff face is where the settlements are the biggest, so at the centre of the face.

The values of joint opening are estimated with the width of the slabs and the medium strain within each slab.

Some results are presented in appendix B.

Our computations about the concrete face behaviour will not be finished for the workshop, but we hope we will present some contributions to the discussion.

5 DISCUSSION

The simulation describes in an acceptable way the vertical displacements during construction and impoundment. However the u/s – d/s displacements during the impoundment are overestimated. Hereon, some reflexions are made in order to understand the differences between the simulated and observed behaviour of the dam, looking for identifying the consequences of simulation hypothesis.

It is reminded that the same stiffness modulus have been used for construction and impoundment stages. In order to reduce the difference between the model and the in situ data a stiffer modulus should be used for the impoundment simulations. It means that the mechanical behaviour of the dam is stiffer during impoundment than during construction, this remark is in accordance to the usual practice where the relation between impoundment and construction modulus are greater than one [2]. However, there is no a clear mechanical justification for this hypothesis.

The characteristics of a viscous behaviour could have affected the back-analysis, as a result of the increase of settlements at constant load that are traduced into a reduced stiffness modulus. This behaviour is evidenced by the instrumentation data at water level near to 2040 and 2060. At these water levels the settlement cells B14, B15, B16, B17 and B18 showed an increment of the settlements readings at constant water level, i.e. at constant load. In contrast to the behaviour observed the constitutive model used here does not take into account any time dependence.

The numerical model results show the cross valley displacements concentrated over the dam's upstream face, in contrast with the field data which reveals a quite symmetric pattern in reference to a middle line over the crest. This observation, and the behaviour just discussed, could lead to think that a kind of homogeneous settlement took place during the impounding stage. In consequence this behaviour may partially explain the differences between the horizontal displacements calculated and those measured. Because a homogeneous settlement gives more symmetric horizontal displacement contours in regard to the dam crest.

Apparently the total deformation for Mohale dam is composed of elastic, plastic and viscous components, and even if nowadays there exist constitutive models that take into accounts such effects, the assessment of the contribution corresponding to each type of deformation is not simple, especially in absence of reliable laboratory data. Unfortunately no information about piezometric pressure is available and no suggestions can be done about the influence of water in the mechanical behaviour, i.e. increase in particles crushing.

6 REFERENCES

[1] Marulanda C., Anthiniac P. (2009) *Theme B - Analysis of a concrete face rockfill dam including concrete face loading and deformation.* ICOLD 10th Benchmark on Numerical Analysis of Dams-Paris September 2009

[2] Johannesson P., Tohlang S.L. (2007) *Lessons learned from Mohale*. International Water Power & Dam Construction. August 2007. Pgs 16-25.

[3] Pritchard S.(2007) Taking the empirical approach. International Water Power & Dam Construction. February 2008.

[4] MA H., CAO K. (2007) *Key technical problems of extra-high concrete faced rockfill dam*. Science in China Series E: Technological Science. Oct 2007. Vol 50. Pgs 20-33.

[5] Gratwick C., Johannesson P., Tohlang S., Tente T., Monapathi N. (2000) *Mohale Dam, Lesotho*. Proceedings of the International Symposium on Concrete Faced Rockfill Dams. CIGB-ICOLD. Pgs 257-272.

[6] Frossard E. (2007) Barrages en enrochements à masque béton, *Fonctionnement structural du masque vis-à-vis des déformations de compression dans le remblais sous-jacent*, Mécanismes potentiels de rupture associées, Première partie : analyse structurale.

APPENDIX A

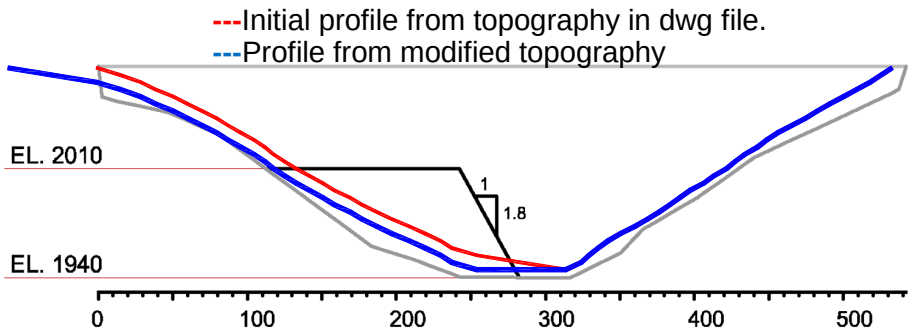

Figure A1. Geometric modification in left abutment.

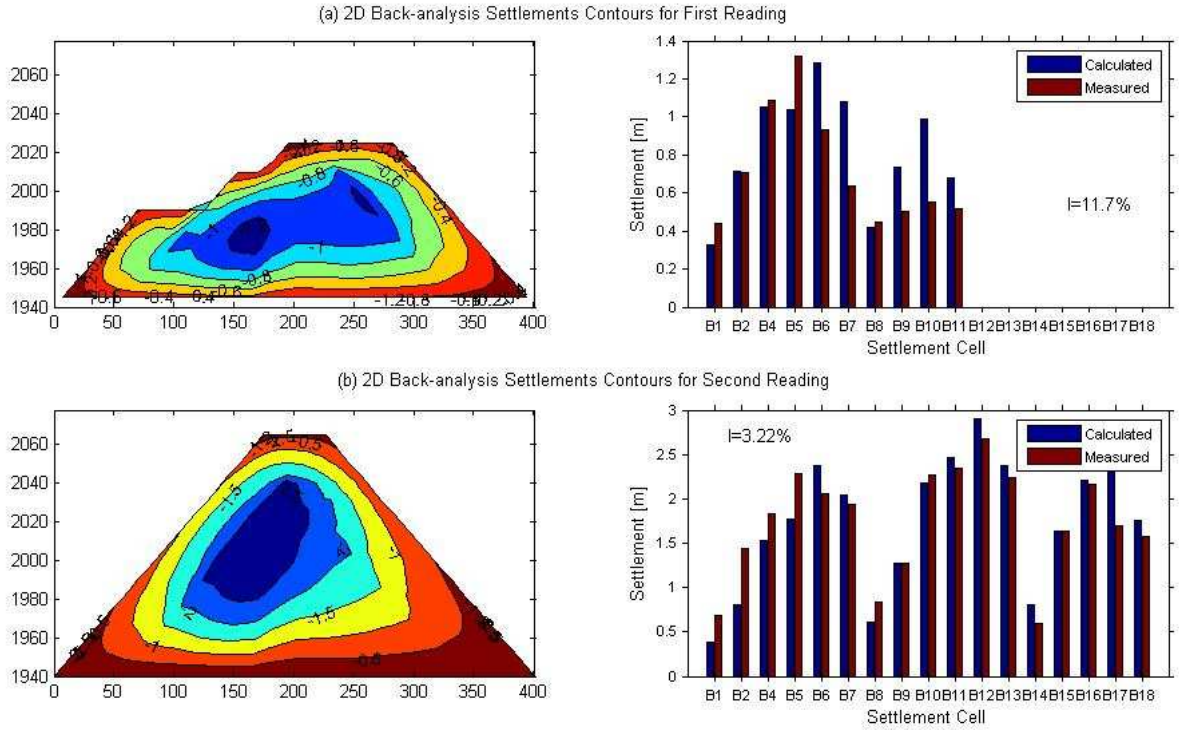

Figure A2. 2D Back-analysis results for construction stages.

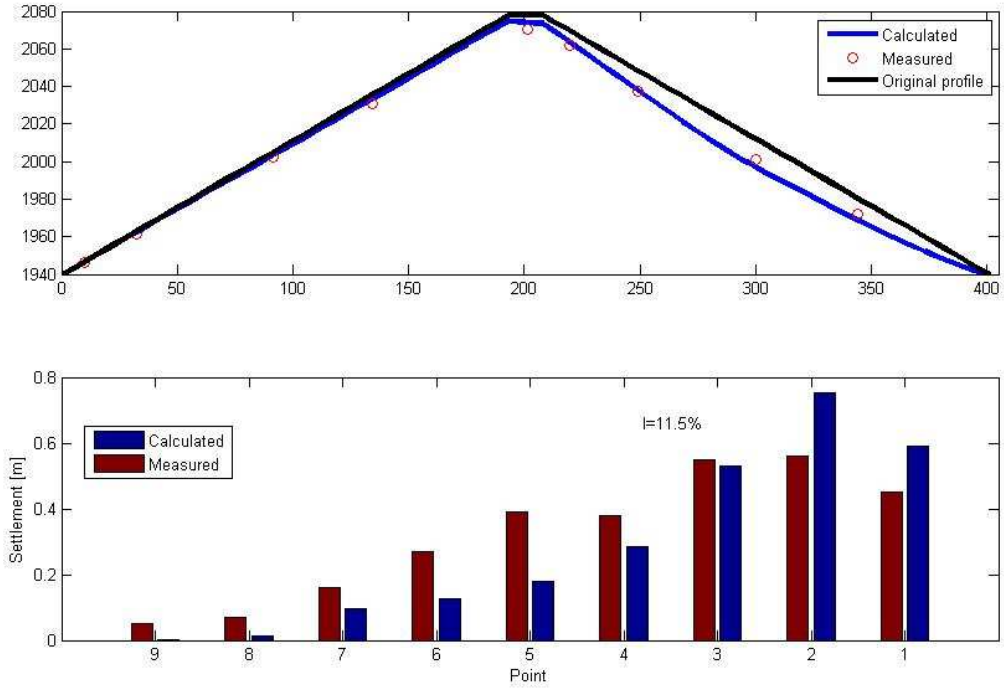

Figure A3. 2D Back-analysis results for impoundment stages.

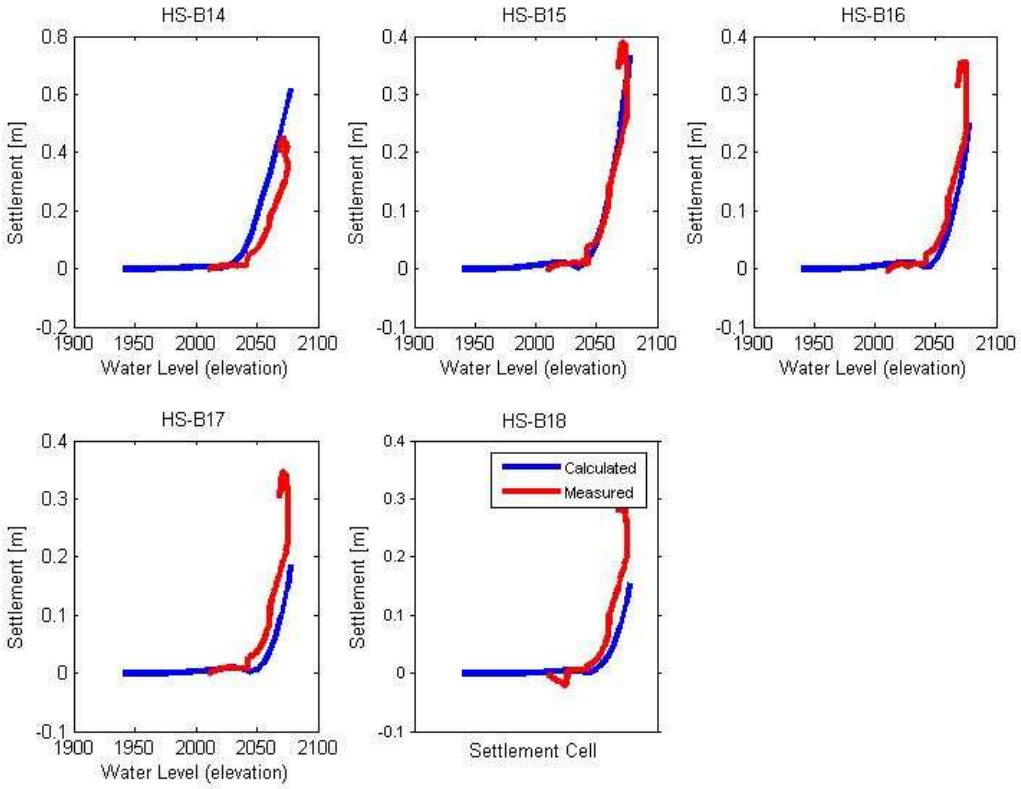

Figure A4. 2D Back-analysis result - Settlements evolution at measured points.

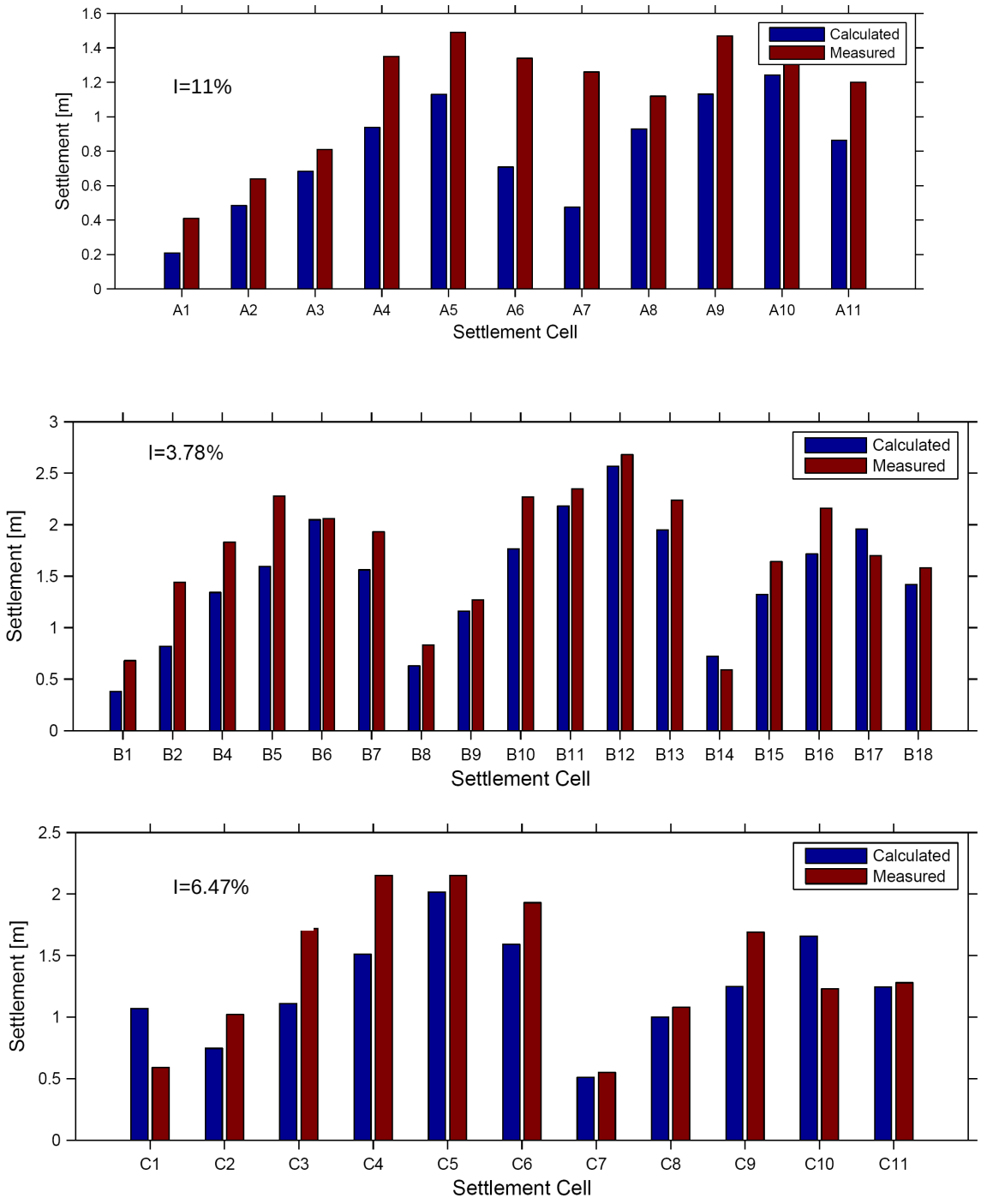

Figure A5. 3D simulated construction settlements comparison at second reading for (a) A section, (b) B section, and (c) C section from 3D model.

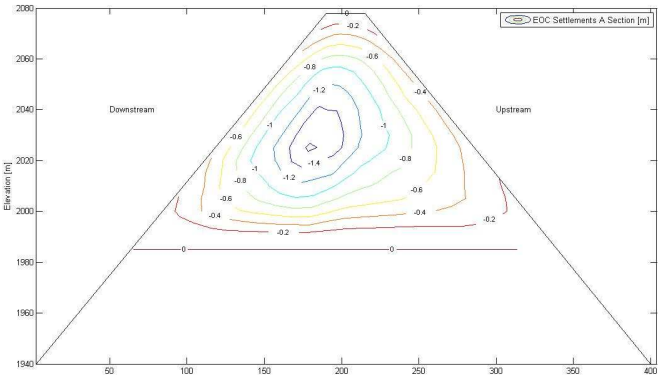

(a)

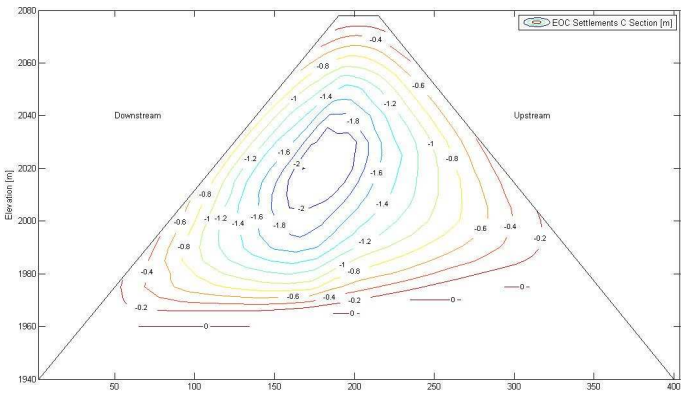

(c)

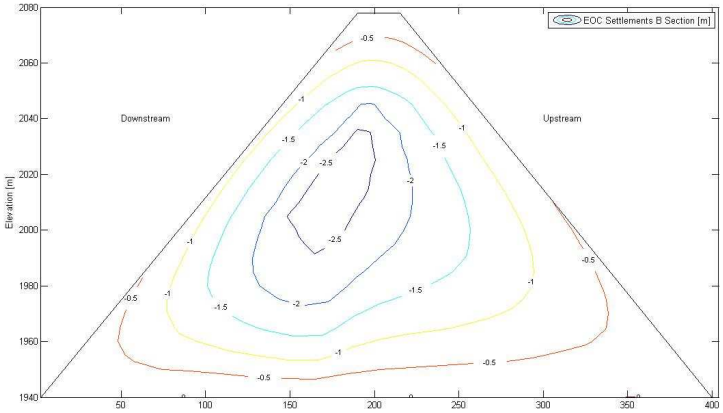

(d)

Figure A6. Settlements contours for impoundment at (a) A section, (b) B section and (c) C section from 3D model.

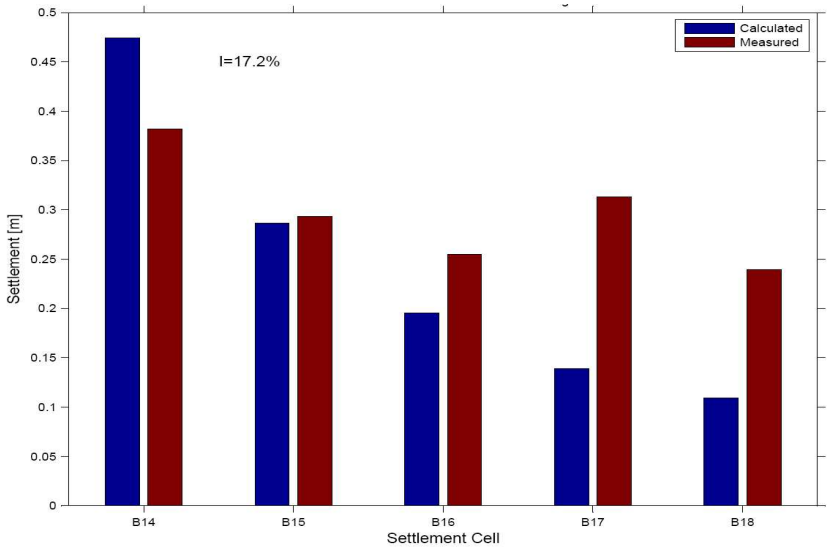

Figure A7. Settlement comparison for cells at B section water level 2070.

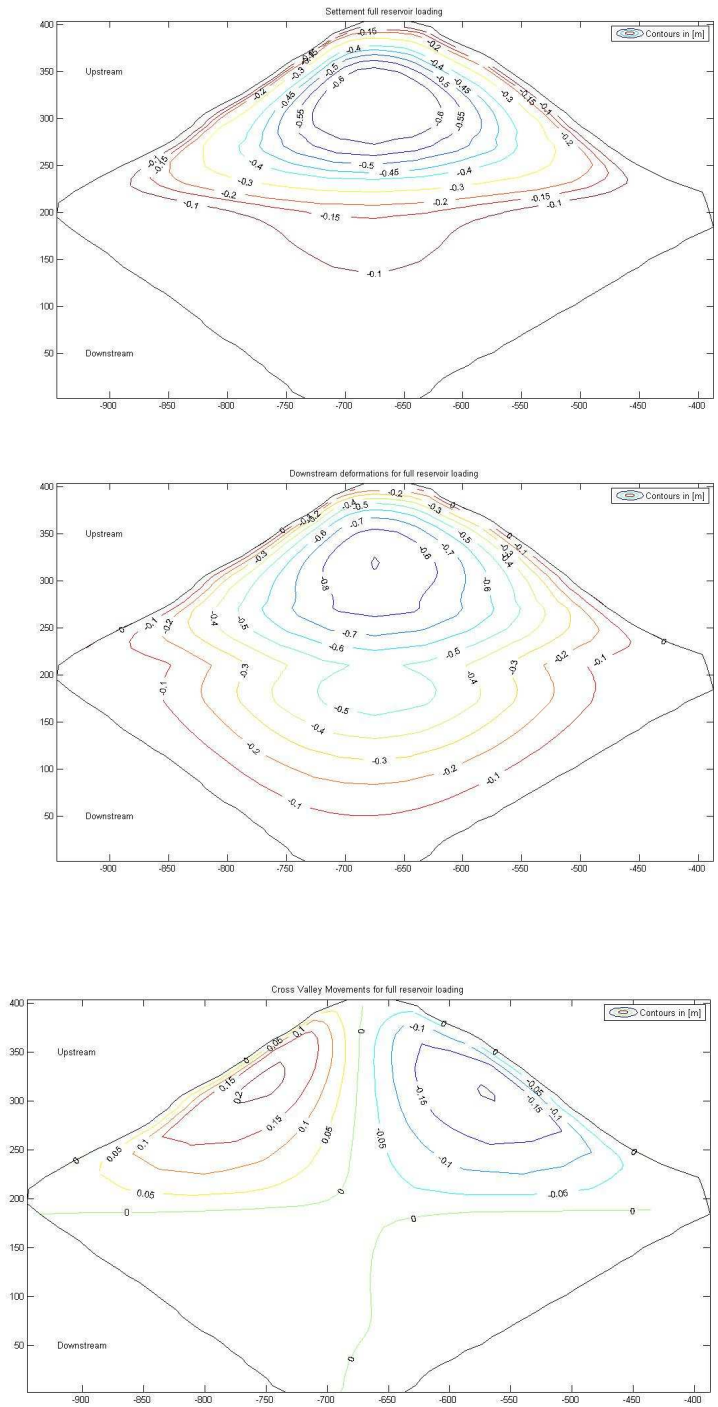

Figure A8. Contour lines for settlements, u/s – d/s displacements and cross-valley displacements 3D model.

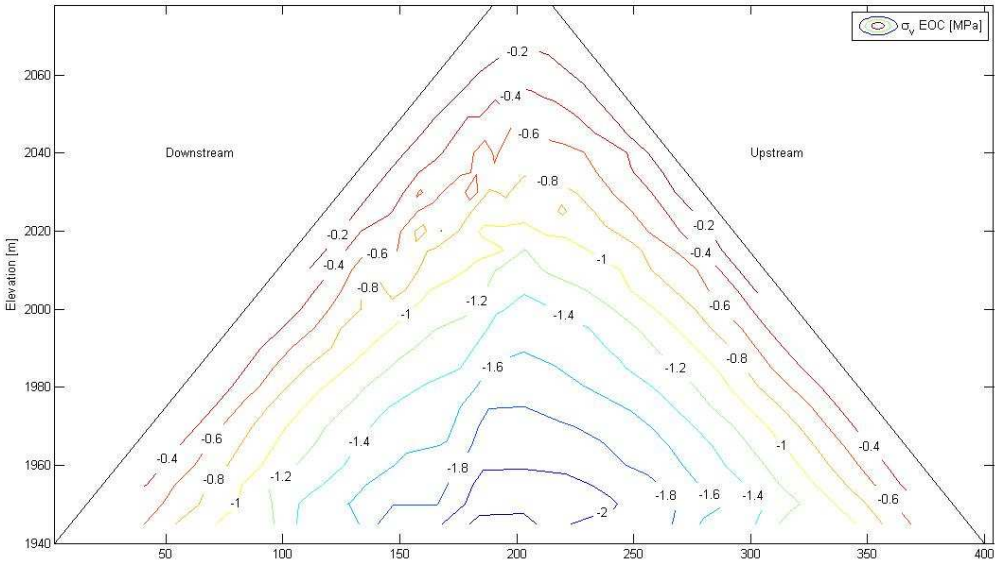

(a)

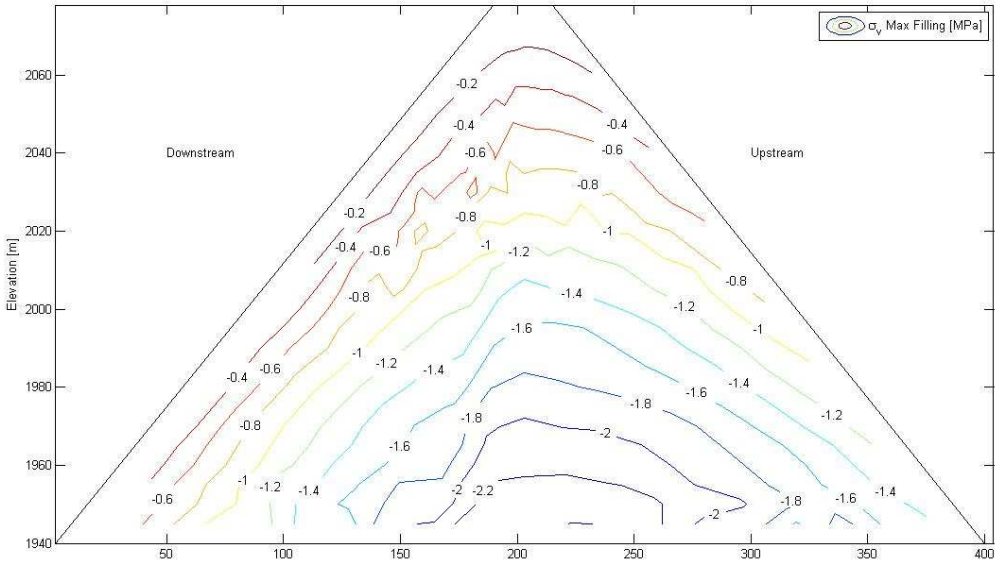

(b)

Figure A9. Contour lines for vertical stress at: (a) EOC, (b) Maximal water level.

APPENDIX B

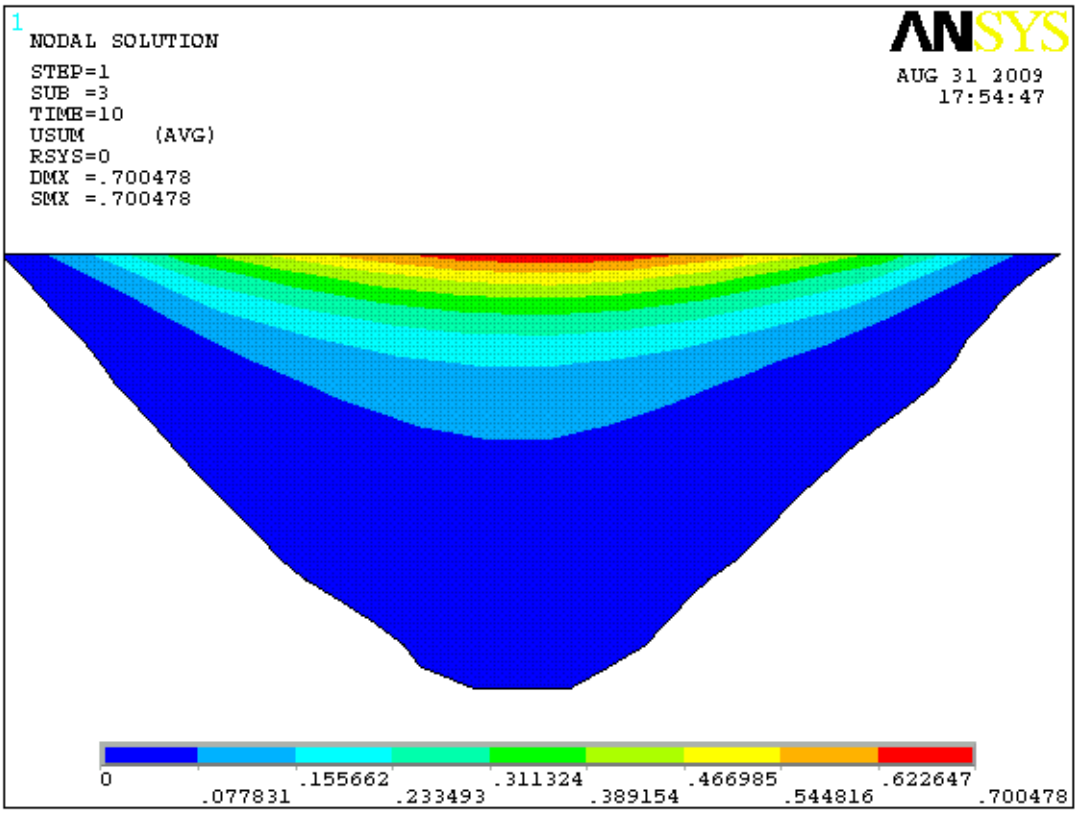

Figure B1 : Displacements applied on the concrete face below EL. 2040 at the end of construction

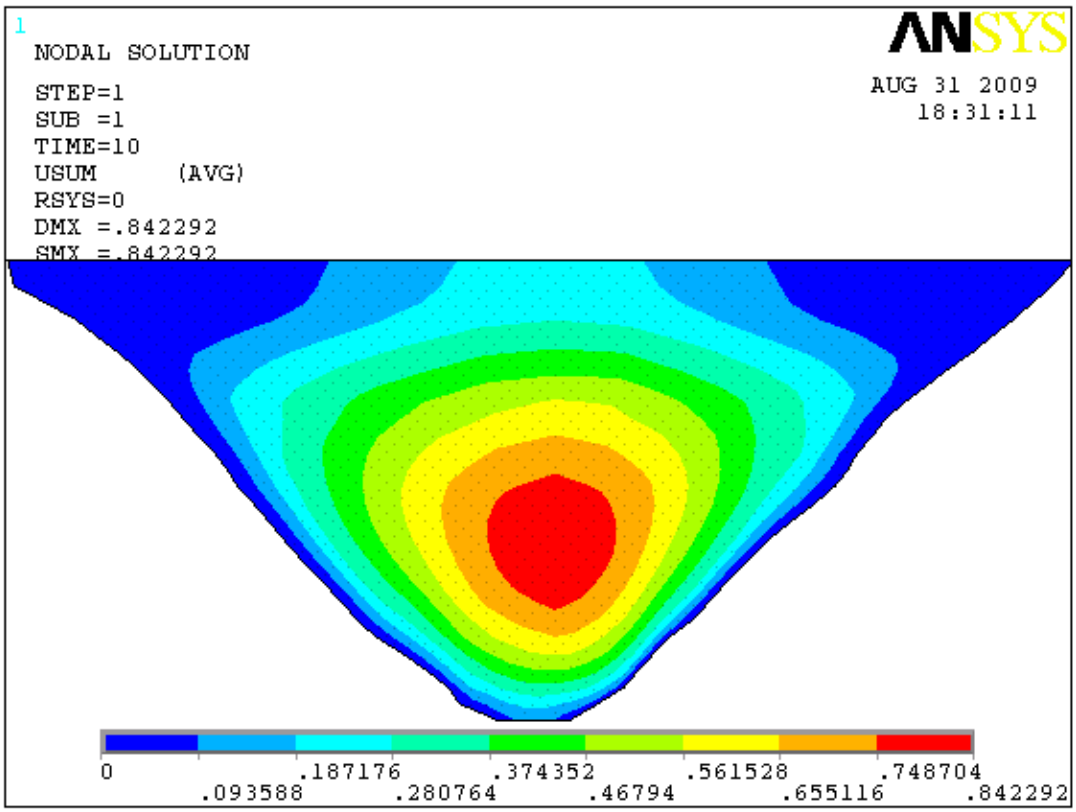

Figure B2 : Displacements applied on the concrete face after impounding at EL. 2060.

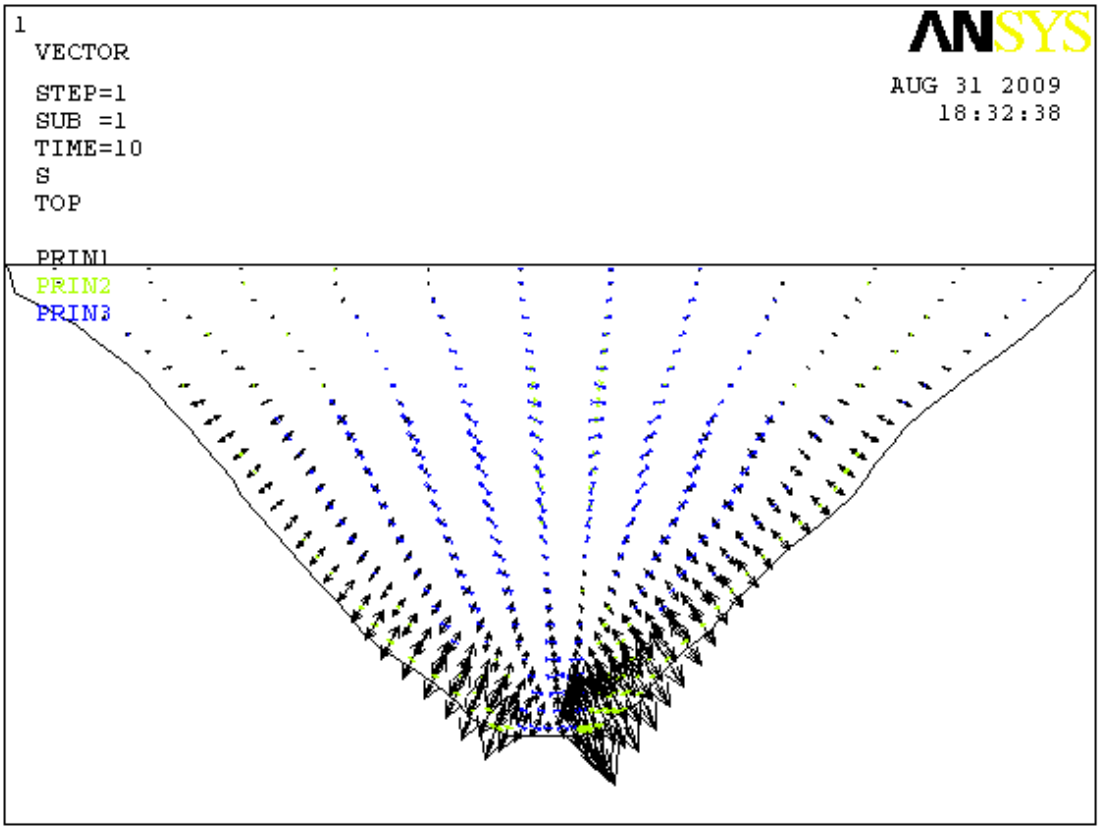

Figure B3 : Directions of the main stresses on the concrete face after impounding at EL. 2060.

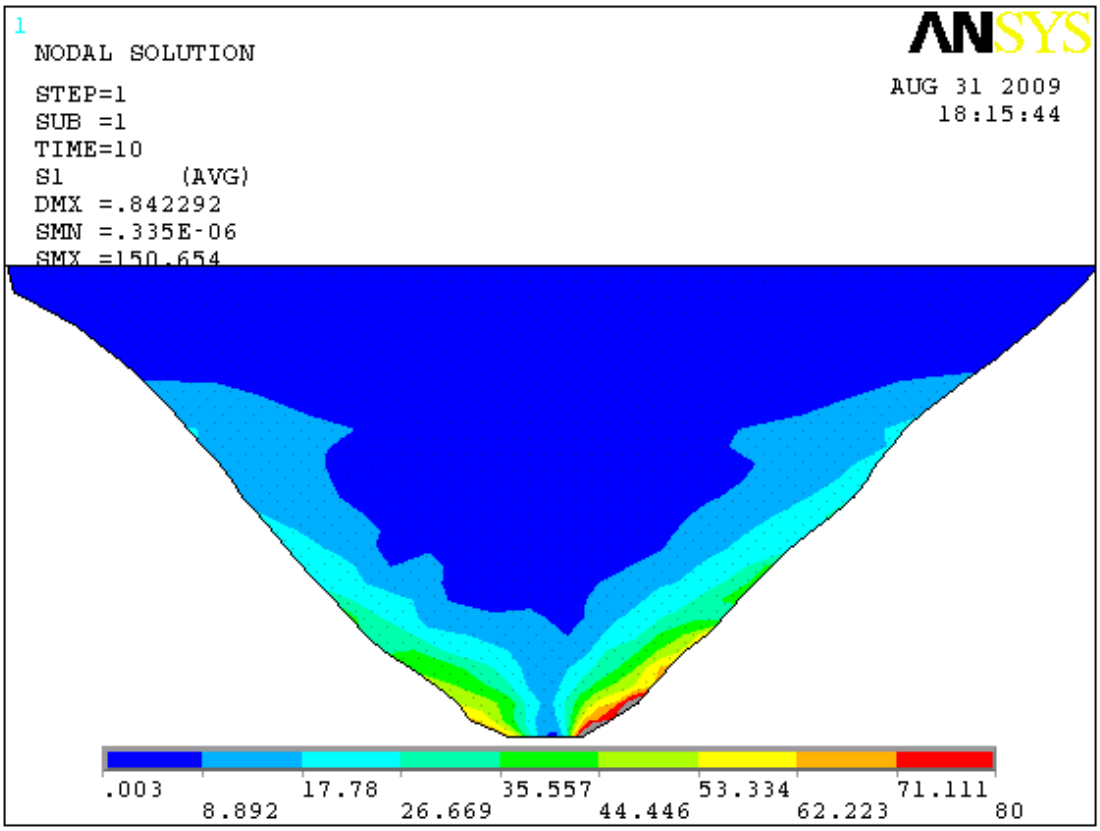

Figure B4 : Minor stress on the concrete face after impounding at EL. 2060 (the model follows an elastic law…)

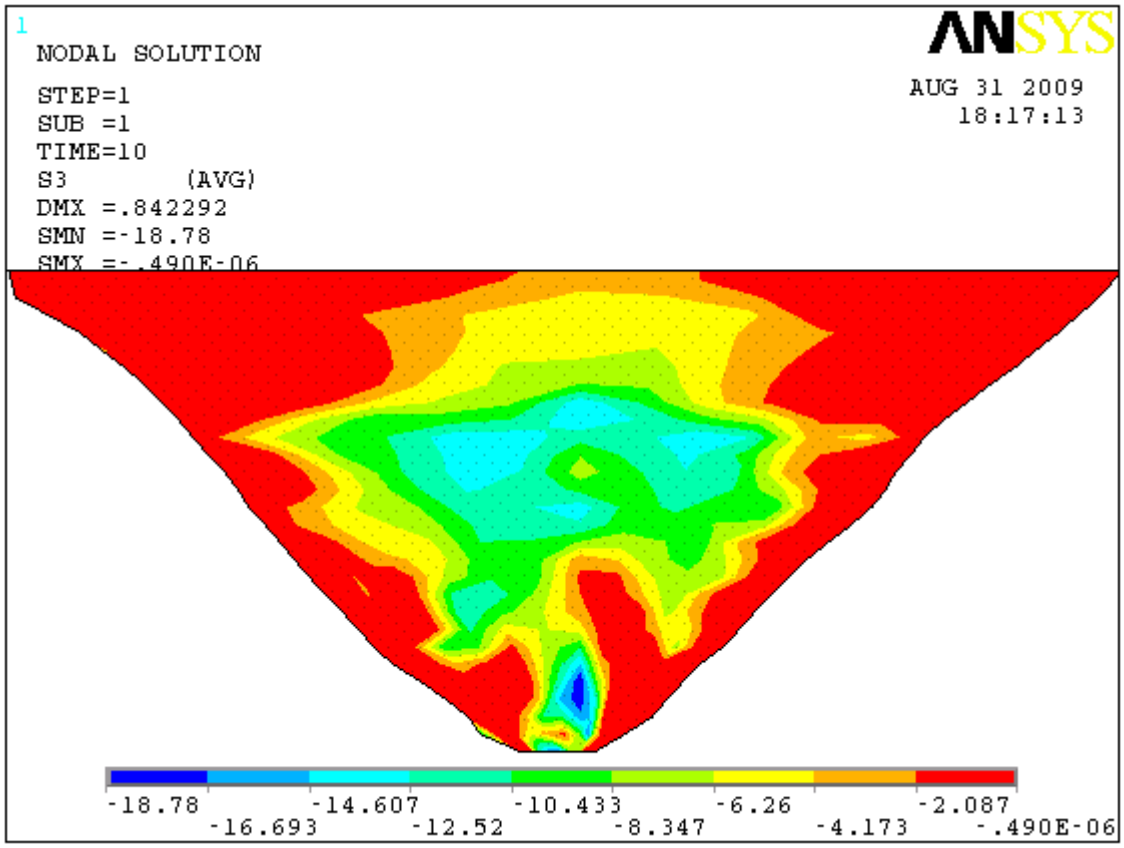

Figure B5 : Major stress on the concrete face after impounding at EL. 2060 (we observed a concentration of horizontal compression at the middle of the face).

DIANA ANALYSIS of a CONCRETE FACED ROCKFILL DAM

Gerd-Jan Schreppers[1], Giovanna Lilliu[1]
1, TNO DIANA BV, Schoemakerstraat 97 2613 DP Delft NL,
E-mail address: G.Schreppers@tnodiana.com, G.Lilliu@tnodiana.com

Abstract: Several concrete faced rockfill dams in the world present cracks in the concrete face. In this paper the authors make an attempt to predict formation of cracks in one of such dams, the Mohale dam in Lesotho, South Africa. Foundation of the dam, dam body and the concrete slab are modelled in 3D. A Cam-clay plasticity model with hardening is adopted for the rockfill. Contact bewteen the concrete face and rockfill is modelled with contact elements, with a Coulomb friction material constitutive model. Interface elements are used to model the vertical joints among the 37 panels that form the concrete face. For the concrete face a total strain crack model in combination with crushing is adopted. In the analysis the different construction stages have been considered, as well as the different impoundment stages. The results shown in this paper are displacement and stresses in the rockfill and the concrete face, crack patterns and crack strains in the concrete face, and openings of the vertical joints.
Key words: CFRD, Cracking, 3D.

1 Introduction

In CFRDs, settlements of the rockfill during and after construction can cause deformation and cracking of the concrete face. To prevent this, empirical rules have been formulated for controlling grading of the rockfill and compaction conditions. However, as higher and higher CFRDs are built in the world, numerical analysis is necessary to validate the empirical rules. Due to the complex physical mechanisms involved in the interaction of the different structural elements in a CFRD, and the need to consider 3D effects, there are not many comprehensive examples of numerical analysis of CFRDs. This has motivated the ICOLD Committee on Computational Aspects of Analysis and Design of Dams to propose the numerical analysis of a CFRD as one of the themes for the 10th Benchmark Workshop on Numerical Analysis of Dams [1]. Object of this benchmark is the Mohale dam in Lesotho, South-Africa. This is a 145 m high CFRD, with a crest length of 600 m, a concrete face surface of 73400 m^2 and a total fill volume of approximately 7.5 million m^3. The dam was built of basalt rockfill. After the reservoir was completely impounded, significant dam movements occurred and cracks developed in the concrete face, which caused leakage. Information provided in [1] is not sufficient for a quantitative comparison of numerical predictions and actual deformation and crack status in the Mohale dam. Nevertheless, this exercise has offered the authors the possibility to test the capability of the finite element package DIANA [2] to model the behaviour of CFRDs.

2 Modelling aspects

2.1 Finite Element Model

The finite element model of the dam body and the foundation is shown in Figure 1. The dam body is modelled with 4-node tetrahedral elements with 6 m edge size. This element size is chosen for limiting the number of degrees of freedom in the model. The total number of elements in the dam body is 184812, and the number of nodes is 36417. The foundation is modelled with 260900 elements, with 82321 nodes. The nodes at the outer and bottom surfaces of the foundation are constrained along the normal to the surface. Figure 2 shows the different construction stages of the dam body. The rock-fill phases are divided in a upstream half well-graded rockfill and a downstream half of poorly graded rockfill.

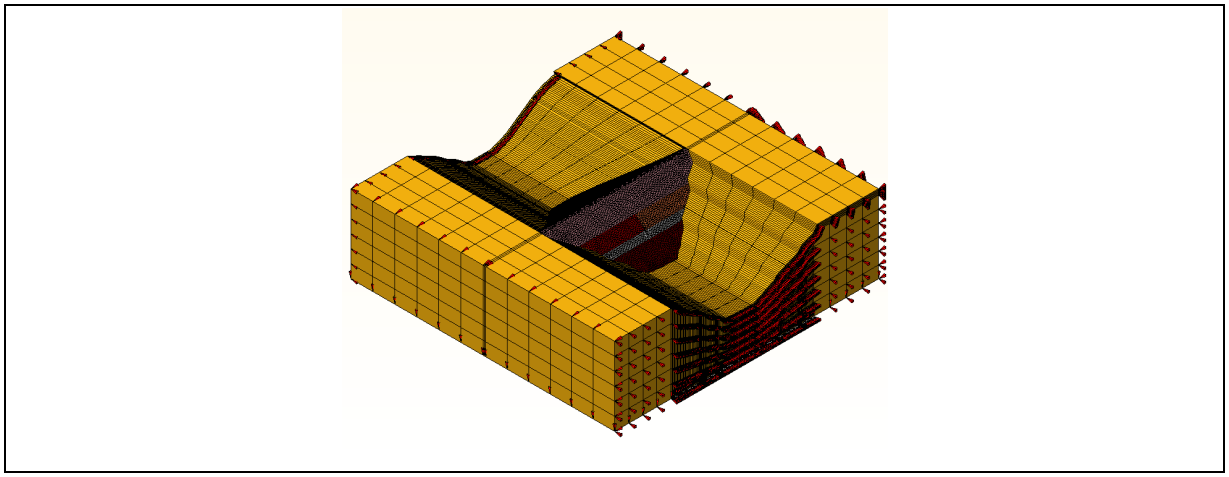

Figure 1. Finite element model of the dam body and foundation

The concrete slab is modelled with shell elements. The dam body has a complex shape, which cannot be easily meshed with a mapped mesh. For this reason, an automatic mesh generator has been used, which generates tetrahedral elements. However, quadrilateral elements are more suitable for modelling the concrete slab, as these elements account for the shear-stiffness in the slab more accurately. Furthermore, an element size smaller than 6 m is required in the concrete slab, for a more appropriate description of the failure behaviour of the slab. As a result, the quadrilateral mesh of the concrete slab, with 2.5 m element size, and the mesh of the rock fill are not compatible. Special contact elements that simulate the frictional interaction of rock fill and concrete slab are used to connect these two meshes. Line-shell interface elements between the concrete slab panels simulate the vertical joints. The concrete slab is constructed in two stages: in the first stage the concrete slab is casted up to a height of 100 m. Then a concrete beam is built at this height, for carrying paving equipment. The beam is modelled with beams elements with a cross section of 1 m^2. In the second stage the slab is casted until 178 m height. The thickness of the shell elements varies from 0.30 m at the crest of the dam until 0.735 m at the foot. (1942 m). The mesh of the concrete slab is shown in Figure 3.

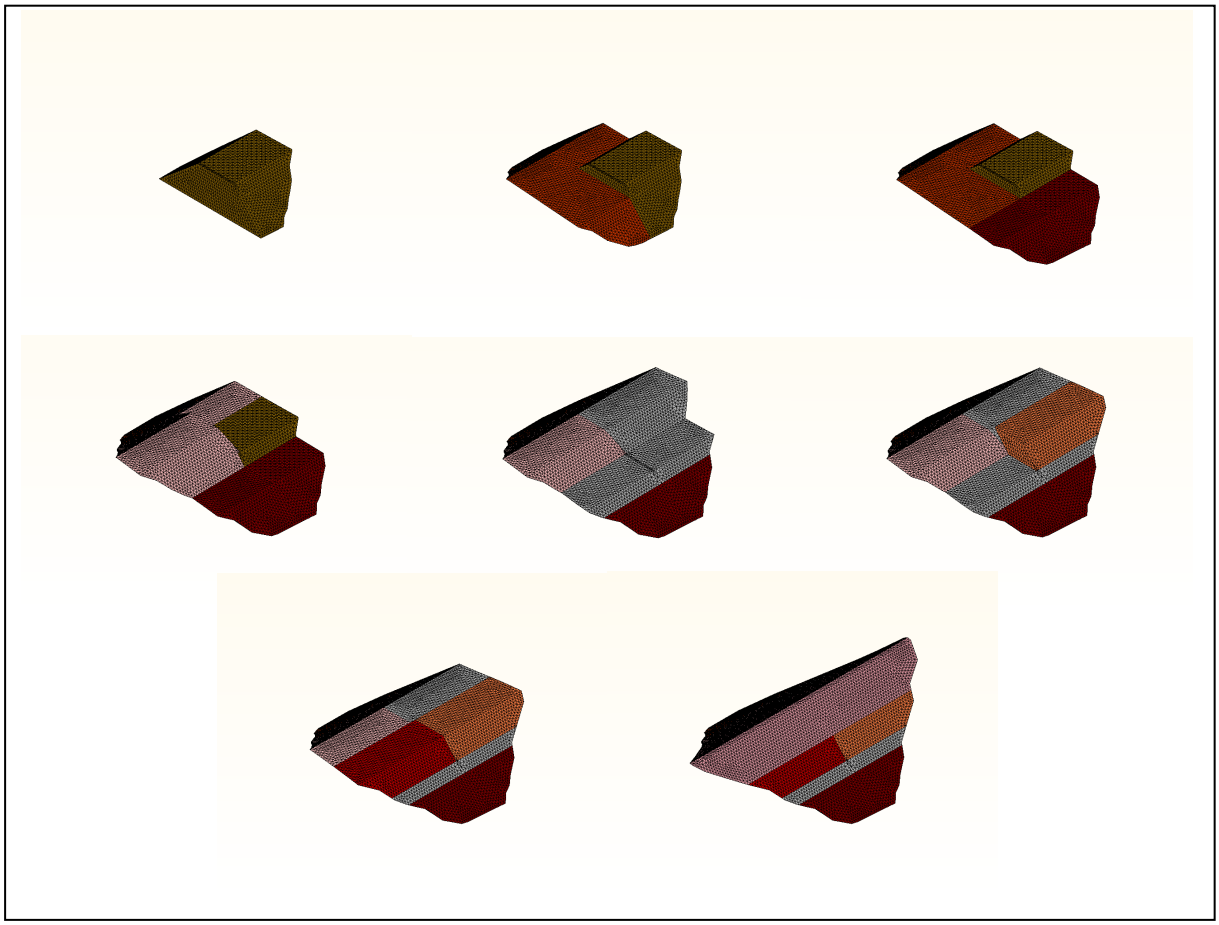

Figure 2. Construction stages of the dam body

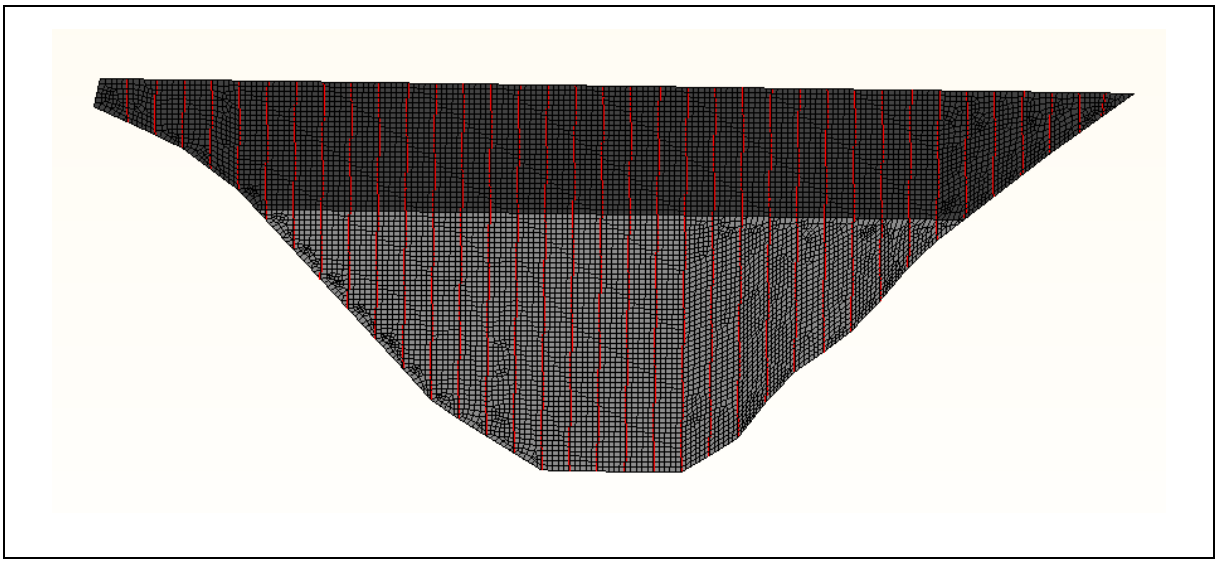

Figure 3. Mesh of the concrete slab

2.2 Material properties

Settlement/load data from two experiments, respectively for poorly graded and well graded basalt were available for characterizing the material. It was assumed that the experiments were confined compression tests, and that the material follows the Cam-clay plasticity model, with exponential elastic behavior and explonential plastic hardening. The material parameters derived for the basalt are summarized in Table 1. Figure 4 compares the data from laboratory experiments with the results obtained from DIANA analysis.

	Elastic hardening parameter	Poisson's ratio	Preconso-lidation stress	Friction angle	Plastic hardening parameter	Pressure shift
Poorly Graded	0.002	0.2	0.2 MPa	30^0	0.02	0.1 MPa
Well Graded	0.001	0.2	1.4 MPa	30^0	0.01	0.7 MPa

Table 1. Material parameters of the basaltic rockfill

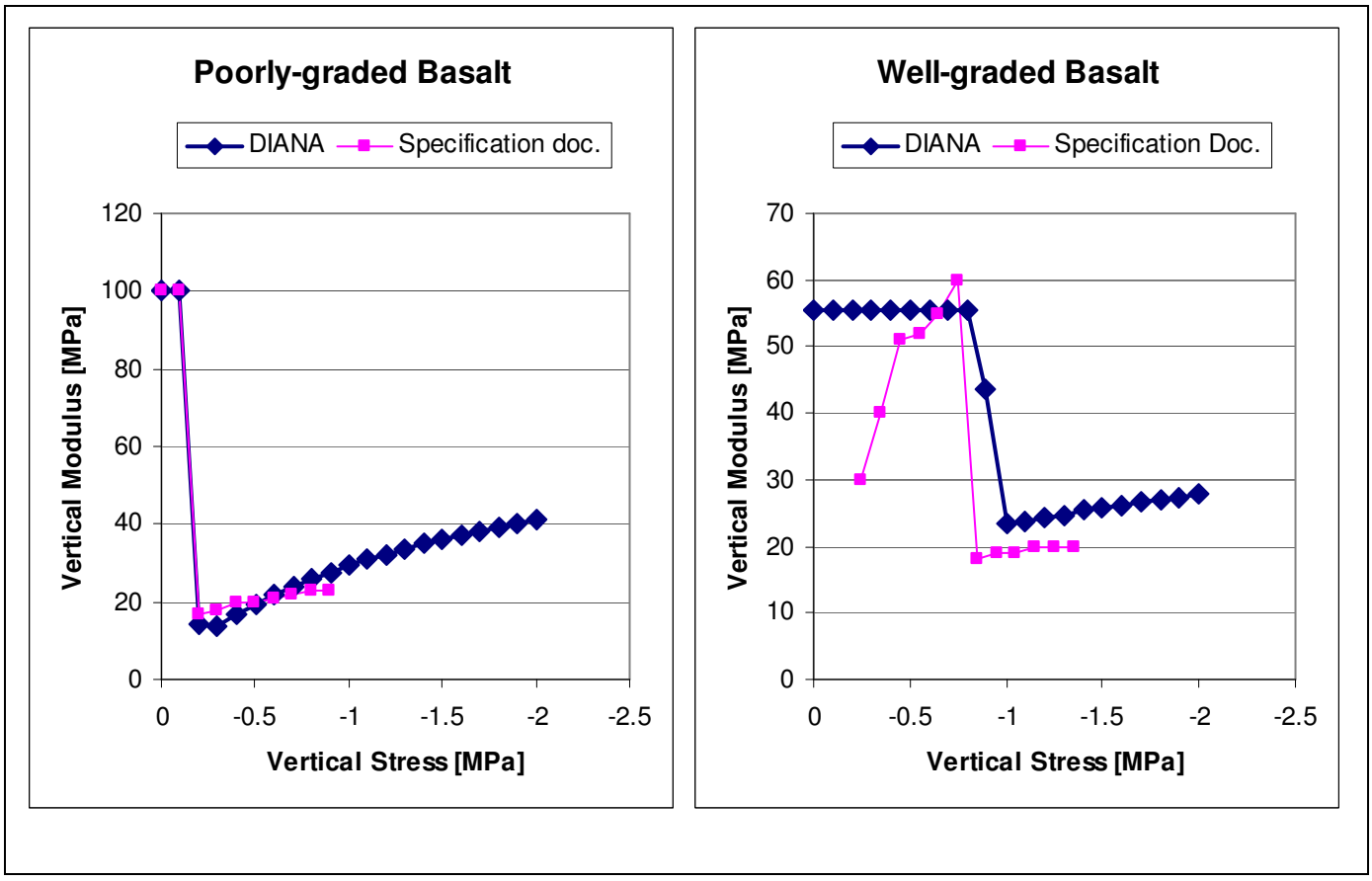

Figure 4. Calibration curves for the rockfill material

For the concrete slab a fixed total strain crack model with linear softening and Thorenfeld compressive failure is adopted. The material parameters corresponding to the C20, which were used for the concrete

slab, are listed in Table 2. A higher Young's modulus has been used in order to account for the effect of steel reinforcement grids.

	Young's modulus	Poisson's ratio	Tensile strength	Compressive strength	Ultimate crack strain
C20	40000 MPa	0.2	1.25 MPa	20 MPa	0.001

Table 2. Concrete material parameters

For the foundation it is assumed that this behaves linear elastically, with Young's modulus 5.0 GPa and Poisson's ratio 0.2. For the contact elements between rockfill and concrete slab cohesion and dilatancy are assumed null, and the friction angle is 40^0. A tensile strength of 0.5 MPa is assumed for the interface elements in the vertical joints.

2.3 Construction stages and loading

The analysis includes 16 phases. Phase 1 corresponds to the situation before construction of the dam. In this phase only the foundation element are activate elements in the analysis, and the only load considered is the own weight of the foundation. Starting from Phase 2 until Phase 6, the dam body is built as specified in Figure 2. In Phase 7, the concrete slab is casted up to a height of 100 m and the concrete beam is built. From Phase 8 until Phase 10 the construction of the dam body is completed. In Phase 11 the concrete slab is casted until the final height. From Phase 12 until Phase 16 the reservoir is impounded, and the water levels reach 85 m, 105 m, 120 m, 125 m and 138 m.

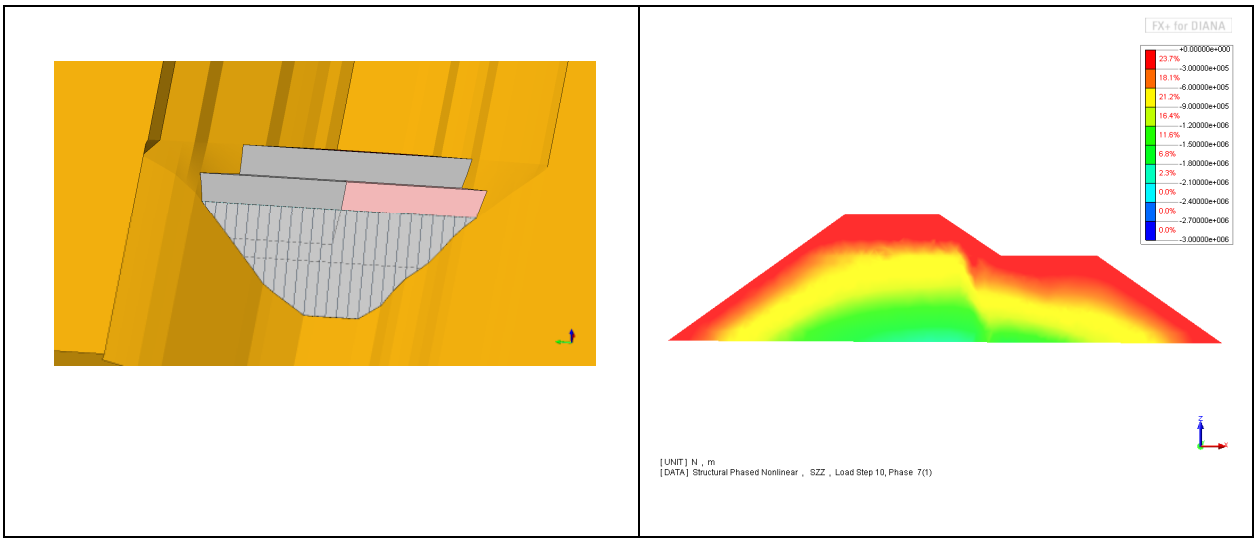

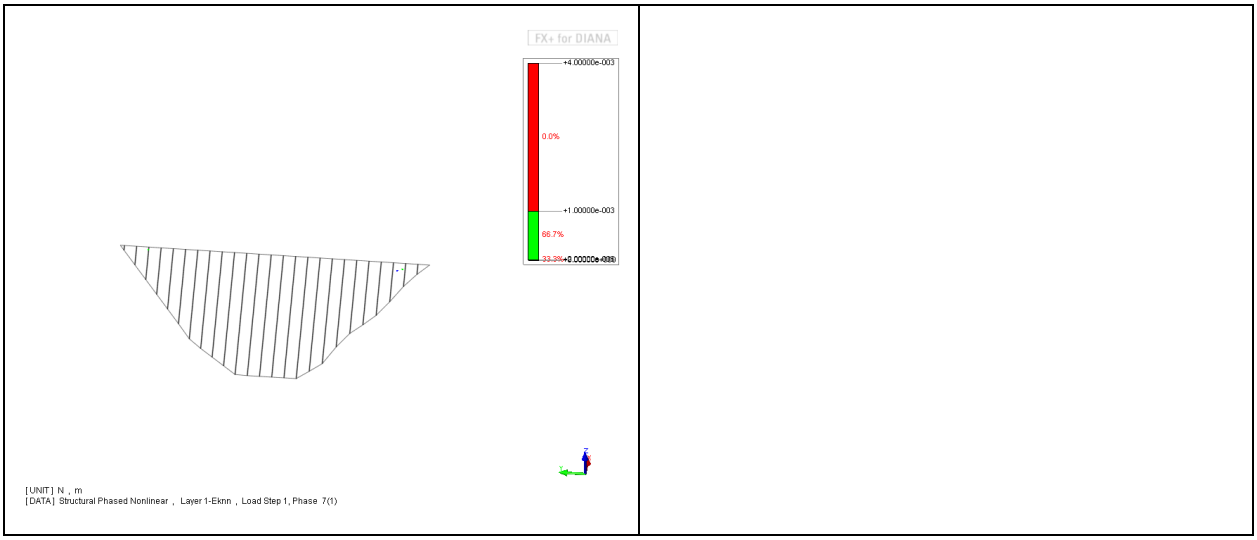

Figure 5. Results at the end of Phase 7

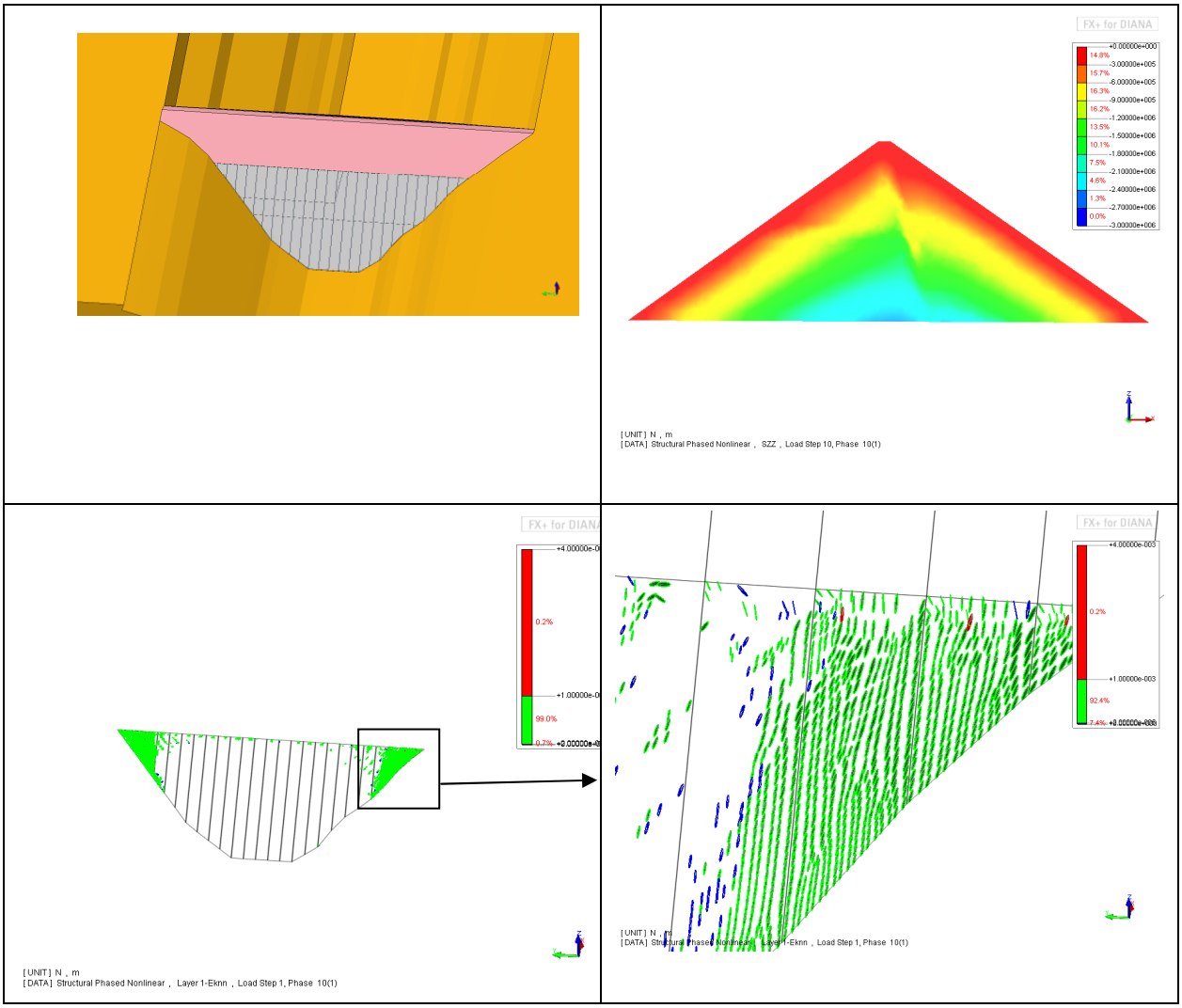

Figure 6. Results at the end of Phase 10

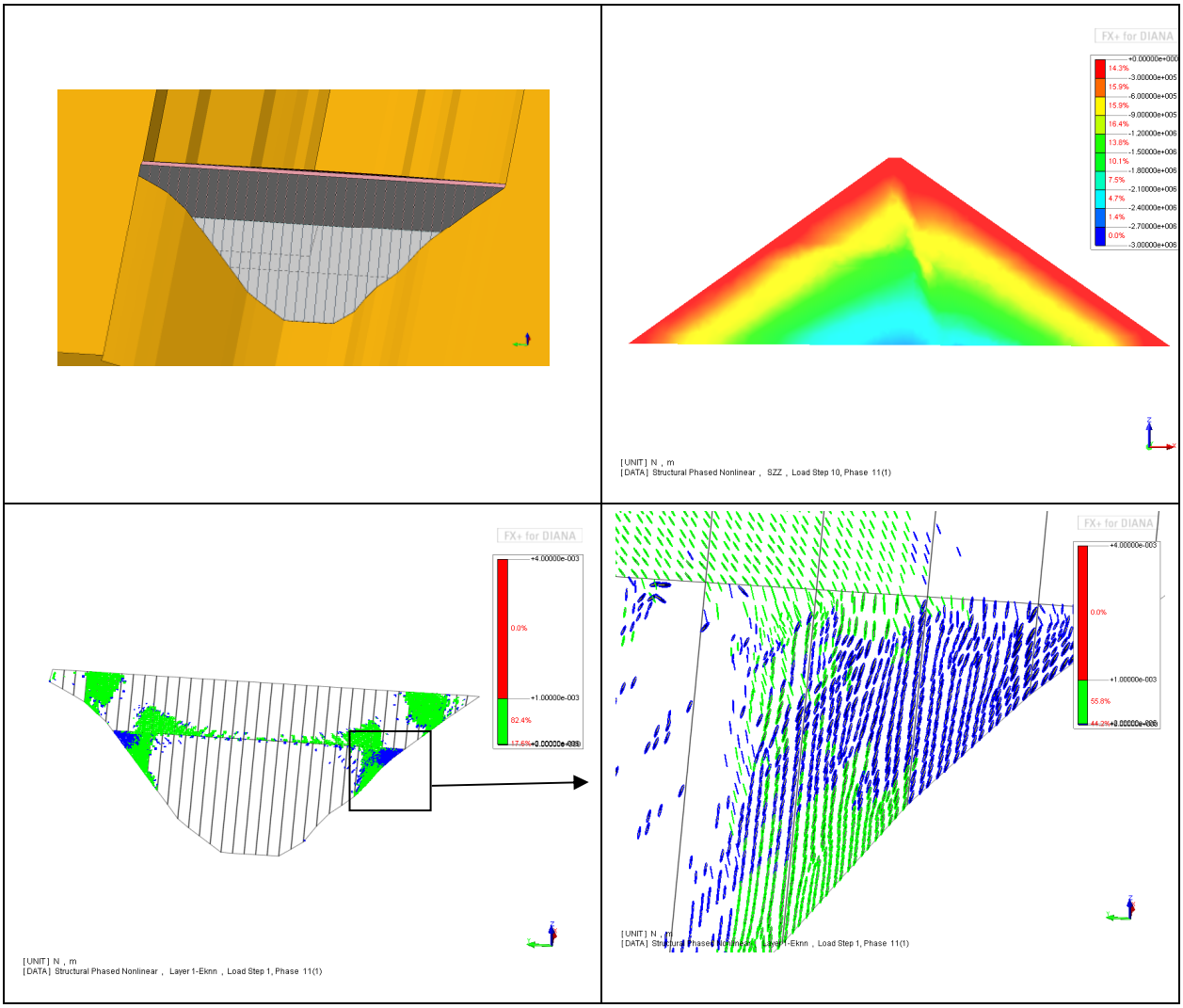

Figure 7. Results at the end of Phase 11

3 Results

The analysis was performed on a 8-processors LINUX system. The calculation time is about 3.5 hours. For sake of space, only part of the results for the analysis conducted assuming well graded rockfill and C20 concrete type are shown in this paper.

In Figure 5 are the results of Phase 7, when the first casting of the slab is completed. At the left is the geometry of the active part of the model, at the top right is the contour plot of the vertical stresses in the rock fill, at the bottom right is the crack plot in the concrete slab. But in this stage of the analysis hardly any cracks were found. The cracks are represented with discs laying on the crack surface. The different colours of the discs correspond to different crack strains. Red corresponds to a crack strain of larger then the ultimate crack strain $1 \cdot 10^{-3}$, namely to a crack opening of 3.0 mm..

At the end of Phase 10, when the dam body has been completed, but only the lower half of the slab is present, cracks appear at the lateral ends of the concrete slab, as shown in Figure 6. The detail picture in the lower-right-hand of figure 6 shows the orientation of the cracks, which are mainly in vertical direction. These cracks are caused as result of the ongoing elevation of the rock-fill after

the lower half of the concrete has already been put in place. As result of the ongoing elevation of the rockfill the slab is pushed downward, leading to tensile loading at the lateral ends and compressive horizontal stresses in the central part.

However, further cracking occurs in Phase 11, after the concrete slab has been completely casted, see Figure 7. In this phase the crack-strain in the lateral ends of the lower slab is reduced already (now blue, before green) as result of the load of the top-half of the slab.

In Phase 12, which corresponds to first impounding of the reservoir (water level 85 m), cracks form also at the base of the concrete slab, as consequence of the bending induced by the hydrostatic pressure.

At the end of the second impounding the water level is at the height of the concrete beam (Phase 13). In this phase a horizontal crack at the location of the beam is found, starting at the left-side of the slab and diagonal cracks parallel to the plinth in the lower slab were found. These crack patterns agree very well with observations. The principal stresses at the top-face in the slab in this stage are shown in the lower-left-hand picture of figure 8. Blue represent compressive stresses and red tensile stresses. The picture shows the high compressive stresses in lateral direction in the central part of the lower slab up to 18 MPa, where as the stresses in the upper slab are considerable lower, because the lower slab was already loaded at the time that the upper slab was constructed. The lower-right hand picture of figure 8 displays joint openings (red) and compactions (blue). In this phase the maximum joint opening is 0.5 cm.

During the sequent phases, cracks that have formed in the previous phase tend to close, and new discrete vertical cracks are initiated at the lateral ends of upper-slab when the reservoir is completely full.

Figure 8 and Figure 9 show the results in Phase 13 and Phase 16. The bottom right-hand pictures show the contour plots of the joints openings, and of their relative displacement normal to the concrete slab. Also the deformed shape of the concrete slab is shown. From the pictures of the vertical displacements the transition from well-graded rockfill (up-stream half of dam) and poorly graded rockfill (down-stream half of dam) can be recognized.

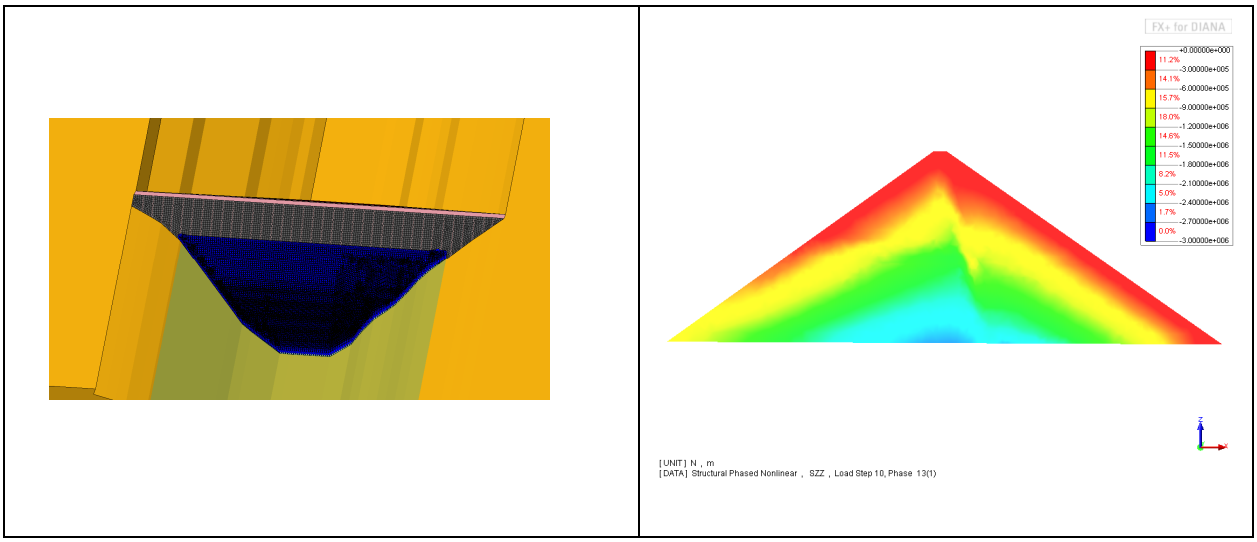

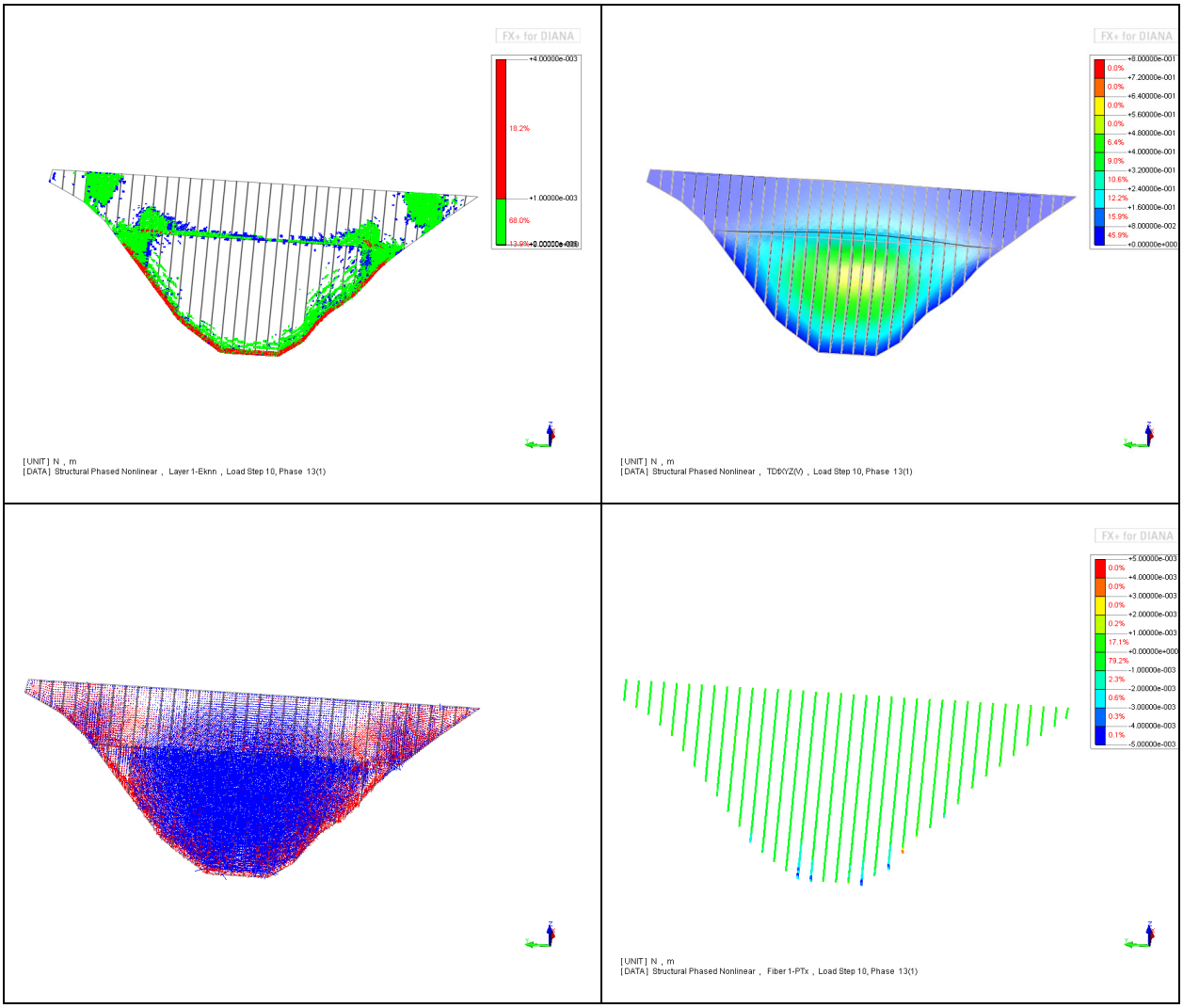

Figure 8. Results at the end of Phase 13

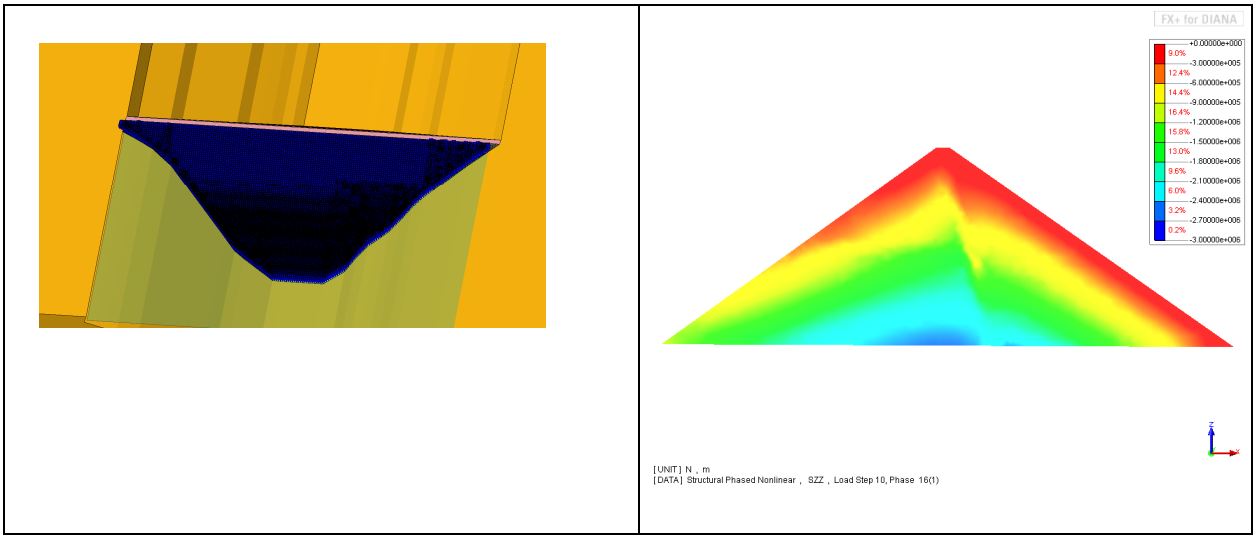

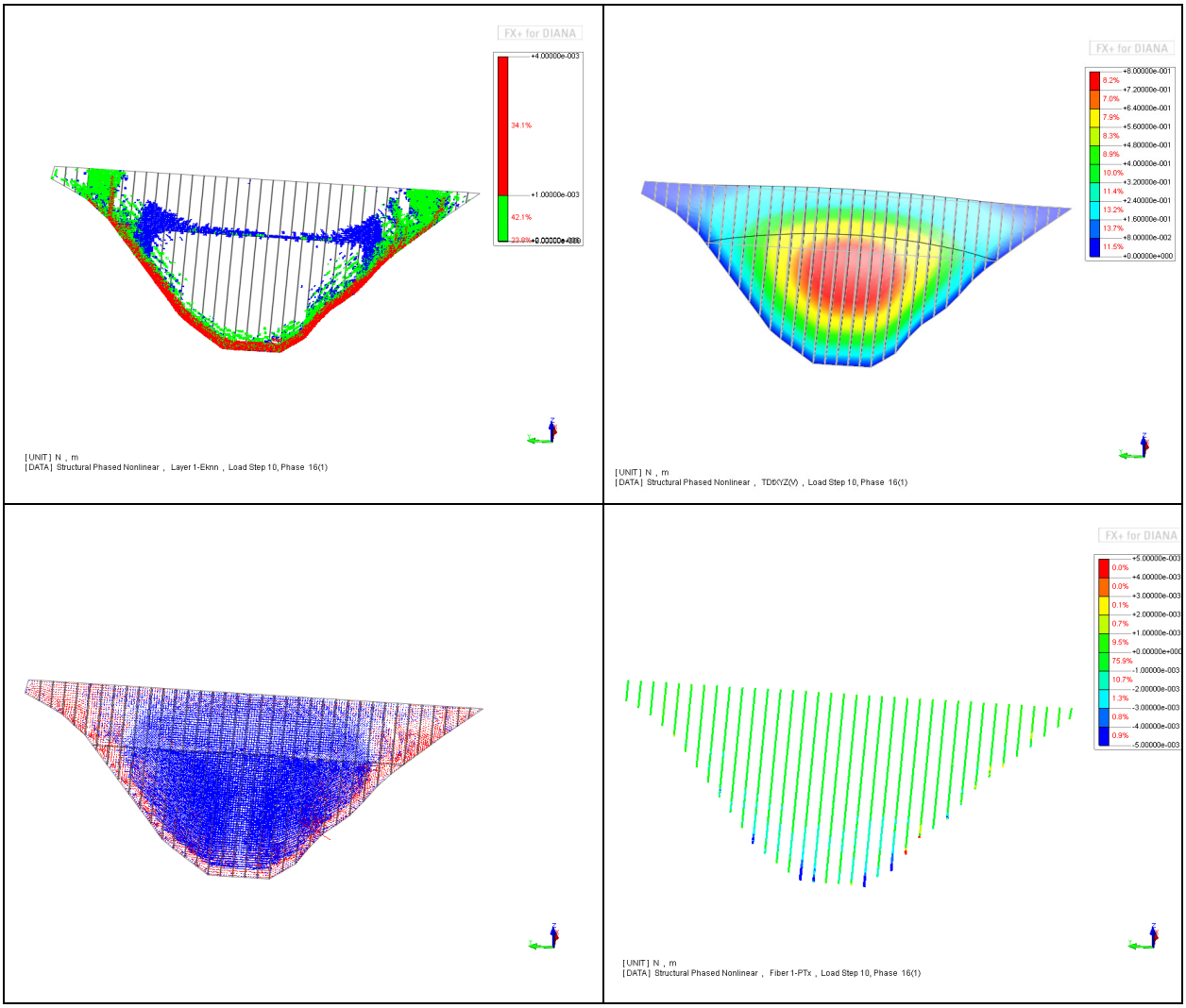

Figure 9. Results at the end of Phase 16

4 Conclusions

In this paper a concrete faced rockfill dam has been modeled in 3D and analyzed with the finite element package DIANA. Nonlinear compaction of the rockfill, effects of the construction stages, frictional slip between rock-fill and concrete slab, cracking and crushing of concrete, opening and out of plane slipping of the vertical joints are taken into account. The results of the numerical analysis show that the general deformation of and stresses in the dam can be well predicted with this model, as well as the most important observed crack-patterns. The analysis predicts strong lateral compaction stresses (18 MPa) in the lower half of the slab, which remain under the failure stress of 20 MPa and as a consequence the observed compressive failure in one of the central slabs was not predicted. When the compressive failure-stress of the concrete would be lower in practice then the applied value of 20 MPa, the model would be able to predict this compressive failure, leading to larger displacements and joint-openings.

References

[1] C. Marulanda and P. Anthiniac, Analysis of a Concrete Faced Rockfill Dam including Concrete Face Loading and Deformation, 10th Benchmark Workshop on Numerical Analysis of Dams, September 16-18, 2009, Paris, France. International Commission of Large Dams (ICOLD).

[2] DIANA User's Manual, Release 9.3.

Theme B

ANALYSIS OF A CONCRETE FACE ROCKFILL DAM INCLUDING CONCRETE FACE LOADING AND DEFORMATION USING PROGRAM PACKAGE SOFiSTiK

Gjorgi KOKALANOV, Professor, Faculty of Civil Eng., Skopje, Republic of Macedonia
Ljubomir TANČEV, Professor, Faculty of Civil Eng., Skopje, Republic of Macedonia
Stevcho MITOVSKI, Assistant, Faculty of Civil Eng., Skopje, Republic of Macedonia
Slobodan LAKOČEVIĆ, Civ. Eng., Faculty of Civil Eng., Skopje, Republic of Macedonia

INTRODUCTION

Mohale dam is concrete face rockfill dam, with height H=145 m, length of the dam crest 600 m and total fill volume of 7.5 millions m^3. In the process of reservoir impounding, when the reservoir level reached maximum elevation, significant dam movements occurred, this in turn increased the compressive stresses within the center portion of the concrete face, resulting in shear failure of the slab. The main objective of this analysis is to gain data for the deformation-stress state of the dam, including and the observed cracking pattern of the concrete face, using three-dimensional model with simplified topography, incorporation of the concrete face with use of the dam zoning and construction sequence. In other words, the history of the behaviour of the structure (related to construction sequence, water level histories and appearance of the cracking failure), should be followed by means of numerical experiments. These data would serve for comparison with the measured results that will be followed by interpretation of the obtained data and in the end conclusions concerning the obtained results and the behaviour of the dam.

DESCRIPTION OF THE THREE DIMENSIONAL NUMERICAL MODEL OF ANALYSIS

GENERAL PART

The used computer software SOFiSTiK for stress-strain analyses, produced in Munich (Germany), is based on the finite element method. It has a wide range of possibilities for simulation of dam behaviour and inclusion in the analyses of all necessary fenomena, important for real simulation of the dam behaviour, such as: an automatic discretization of the dam body taking into account the iregularities in the geometry of the dam base, application of different constitutive models for materials, simulation of the dam body construction and reservoir filling in increments, and so on. The program has rich possibilities for presentation of the output results. In our work, mainly plane graphical presentation was used, showing the output results in the required cross and longitudinal sections, and also in the required slab failure points. On Fig. 1 is shown the general view of the layout of the dam, Fig. 2 shows the typical cross section of the dam. In Table 1 are given the materials included in the dam body.

Table 1. Materials included in dam zoning, according to Figure 2.

Zone	Description	Lift height [m]
1A	Impervious fill	0.3
1B	Random fill	0.6
1C	Impervious fill	0.3
2A	Fine filter	0.4
2B	Durable crushed doleritic basalt	0.4
3A	Selected small quarry run rock	0.4
3B	Quarry run rockfill	1.0
3C	Quarry run rockfill	2.0
3D	Selected durable rock	NA
3E	Quarry run doleritic basalt	1.0/2.0

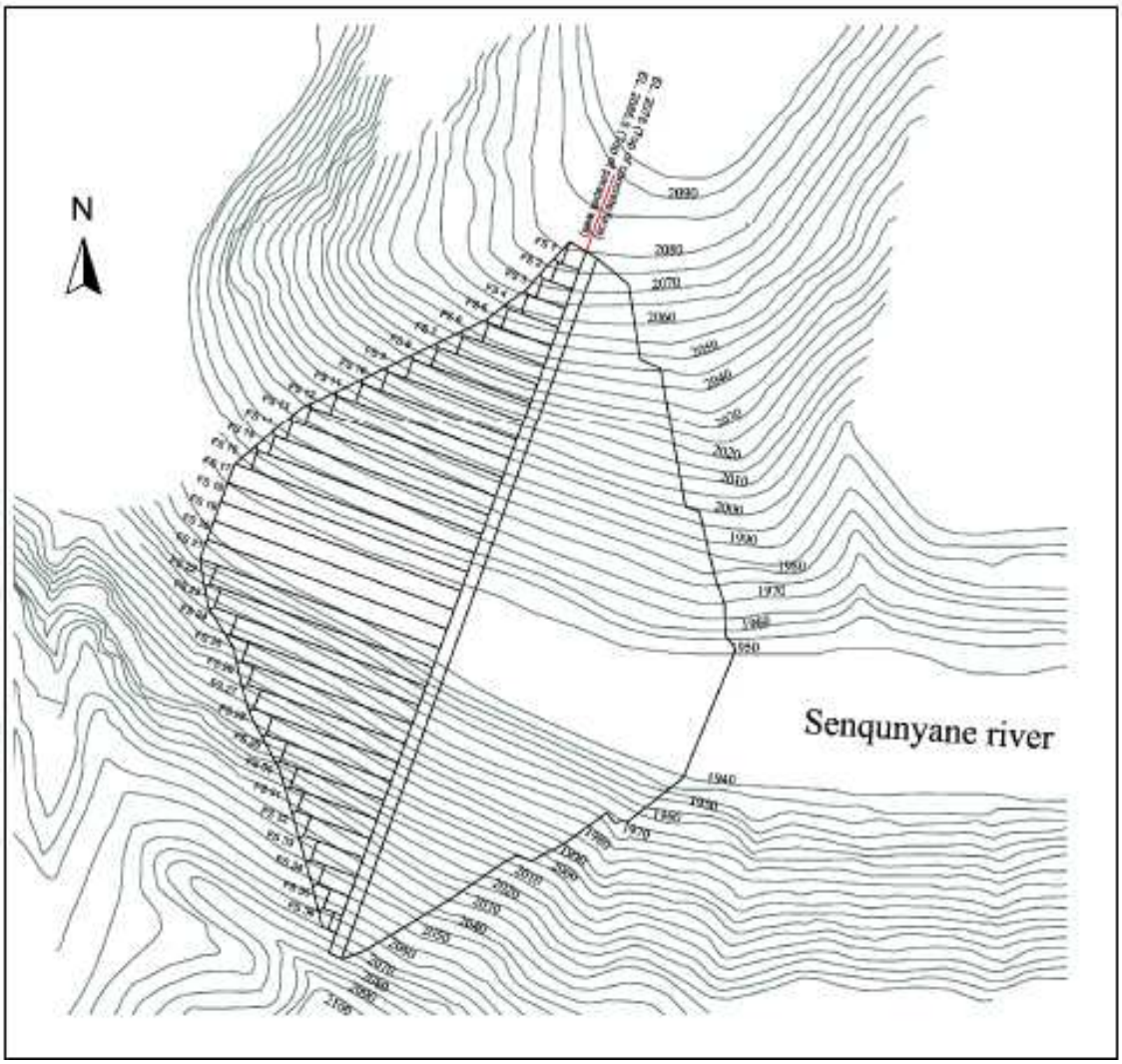

Figure 1. Layout of dam Mohale.

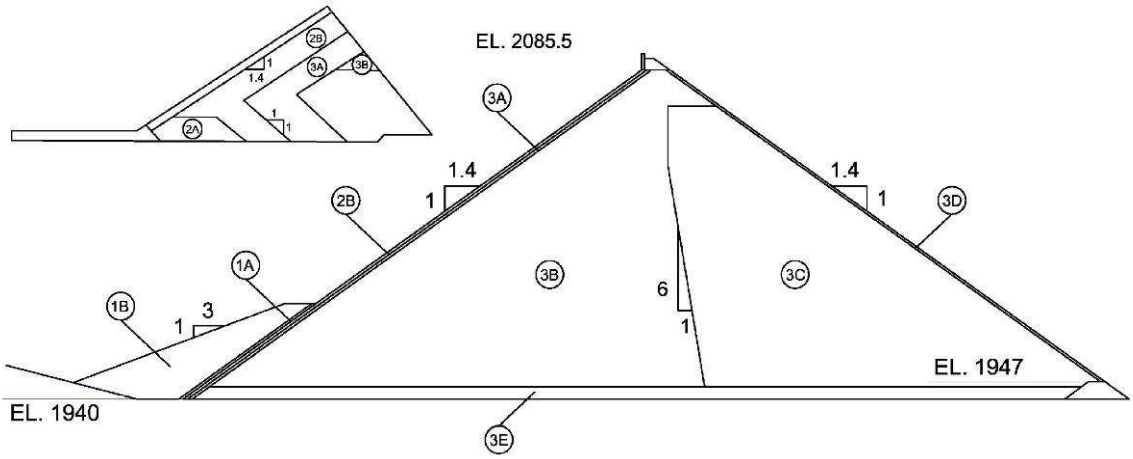

Figure 2. Typical cross section of dam Mohale with detail of the foundation slab of the concrete face.

CONSTITUTIVE RELATIONSHIP AND PARAMETERS OF THE MATERIALS

The choice of the parameters for the materials is one of the most important, but in same time and most complex tasks in the numerical analyses of dams. The rockfill body of the dam was built of three different materials with similar properties. In the analytical model they are presented with constitutive material model GRAN from the library of SOFiSTiK. That

is extended elastoplastic material with an optimized hardening rule (*single* and *double hardening*) for soil materials. Hardening is limited by the material's strength, represented by the classic Mohr/Coulomb failure criterion (Fig. 3a). The hardening rule is based on the hyperbolic stress-strain relationship proposed by Kondner/Zelasko, which was derived from triaxial testing (Fig. 3b). Additionally, the model accounts for the stress dependent stiffness according to equations (1−3). A further essential feature is the model's ability to capture the loading state and can therefore automatically account for the different stiffness in primary loading and un−/reloading paths.

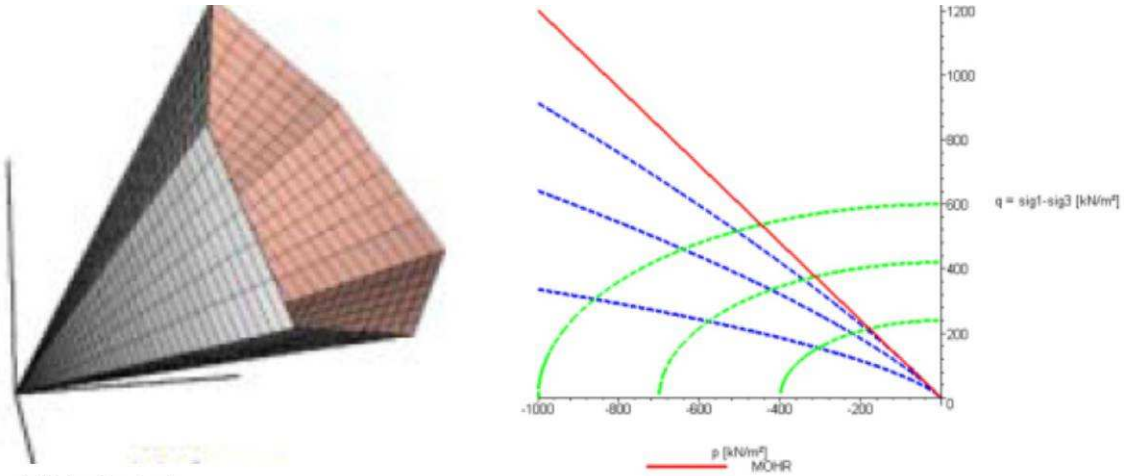

a) Mohr-Coulomb

b) Kondner-Zelasko hyperbolic relation

Figure 3. Mohr-Coulomb failure criterion and hyperbolic stress-strain relationship.

Rockfill material shows stiffness behaviour dependent of the stress state. The oedometric modulus magnitude depends on the effective axial stress state according to the following relationships, equation (1):

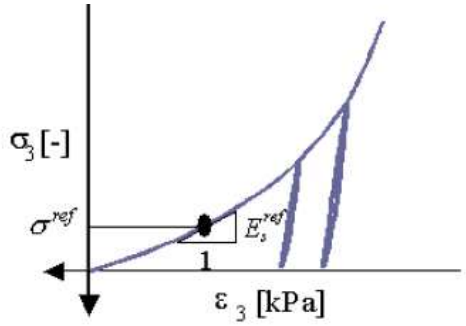

$$E_s = E_{s,ref} \cdot \left(\frac{|\sigma_3| \cdot \sin\varphi + c \cdot \cos\varphi}{p_{ref} \cdot \sin\varphi + c \cdot \cos\varphi} \right)^m \quad (1)$$

E_{50} is defined as secant stiffness that corresponds to a 50−percent mobilisation of the maximum shear capacity, given by equation (2).

$$E_{50} = E_{50,ref} \cdot \left(\frac{|\sigma_1| \cdot \sin\varphi + c \cdot \cos\varphi}{p_{ref} \cdot \sin\varphi + c \cdot \cos\varphi} \right)^m \quad (2)$$

An analogous approach for the elastic un−/reloading stiffness yields, given by equation (3):

$$E_{ur} = E_{ur,ref} \cdot \left(\frac{|\sigma_1| \cdot \sin\varphi + c \cdot \cos\varphi}{p_{ref} \cdot \sin\varphi + c \cdot \cos\varphi} \right)^n \quad (3)$$

The face of the dam was built of the concrete C 25. There was no date of the laboratory test of the concrete and the reinforcement, so the standard concrete and steel properties where adopted (Fig. 4 and Fig. 5).

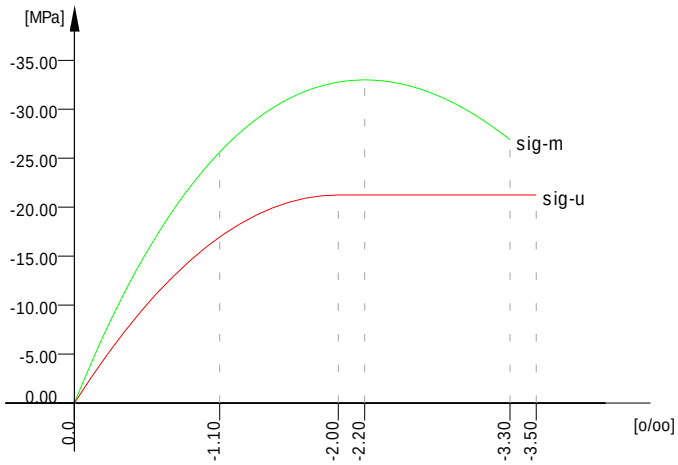

Figure 4. Stress-strain relationship of concrete C 25.

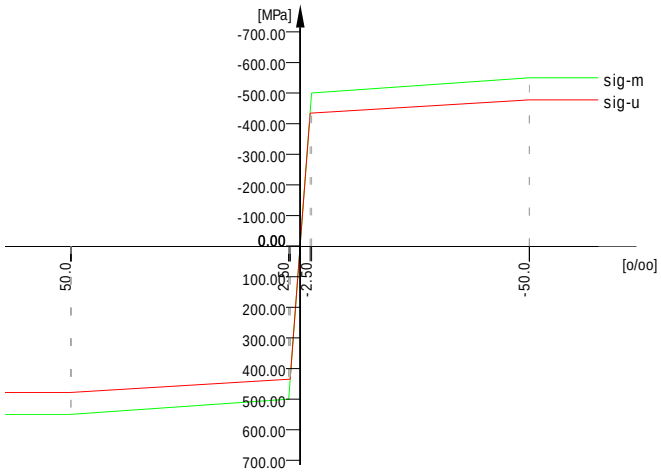

Figure 5. Stress-strain relationship of steel S 500.

NUMERICAL MODEL

Using the given data three-dimensional (3D) mathematical model of the dam was build (Fig. 6). The finite element mesh was generated using SOFiSTiK automatic mesh generator. Three types of element were used to model the dam's body: BRIC and QUAD elements. The body of the rockfill dam was modelled with 3D solid elements (8th node issoparametric).The solid element of SOFiSTiK is the BRIC (volume) element (Fig. 7), a general six-sided element with eight nodes.

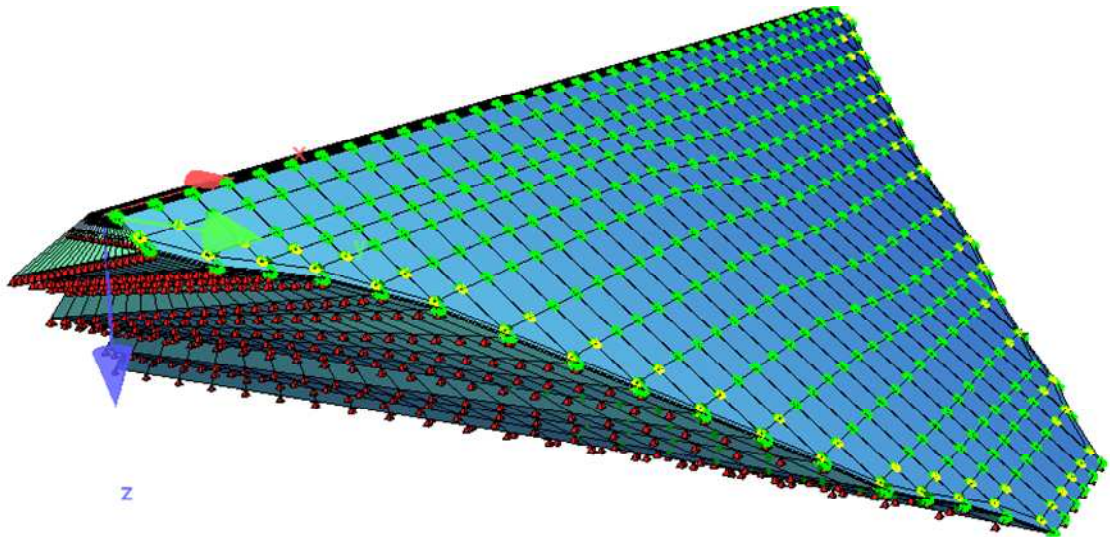

Figure 6. General view of the 3-D model of the dam-foundation system.

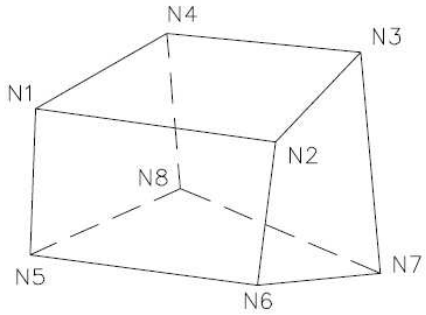

Figure 7. BRIC element.

The plane element QUAD (shell) (Fig. 8) is a general quadrilateral element with four nodes. The surfaces of the BRIC element can be described by special QUAD-elements, which can also be employed for the display of stresses in BRIC-elements. The QUAD-elements are introduced in order to simplify the process of generation of the water pressure loads.

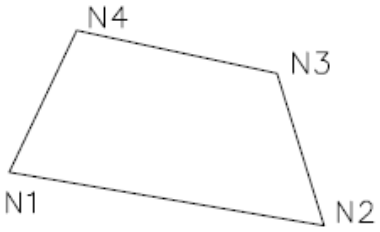

Figure 8. QUAD element.

The input data in the analysis were the given data regarding the geometry of the dam and the material properties. In order to simulate the construction sequences the body of the dam was modelled with 18 construction stages (horizontal layers). The concrete face of the dam was modelled by shell elements. It was applied at the body in two construction stages. The face elements are with variable thickness. The thickness of the concrete was determined as a function of the hydrostatic pressure, following the equation e=0.30+0.00H. Adopted reinforcement is 0.4% in vertical direction and 0.35% in horizontal direction. The concrete face was built in several strips (15 m width) and joint gaps between the strips were adapted 2 cm (Fig. 9). For the needs of the nonlinear analysis the shell element are treated as layered in 10 concrete layers, (Fig. 10). The reinforcement is also simulated by smeared layers. That model is able to reproduce the 3D crack pattern developing. Construction stages where simulated in the following sequences

CS 1 ÷ CS 11	- rockfill body up to elevation 2040
CS 12	- rockfill body + concrete face up to elevation 2040
CS 13 ÷ CS 17	- rockfill body up to elevation 2078 + concrete face up to elevation 2040
CS 17	- rockfill body + concrete face up to elevation 2078

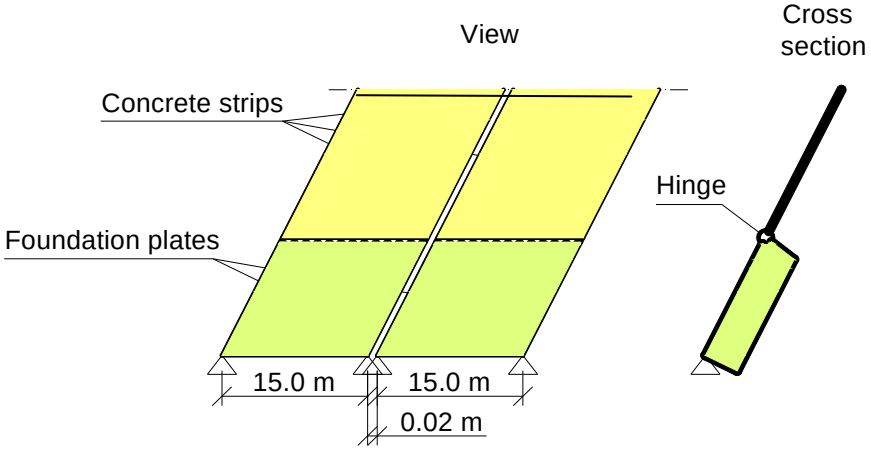

Figure 9. Display of the concrete face discretization.

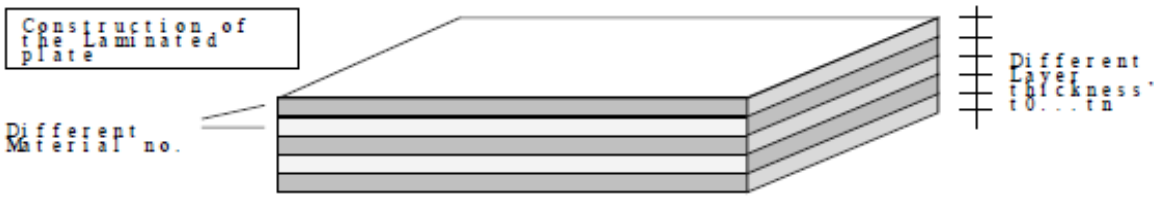

Figure 10. Simulation of the construction of the shell elements in layers.

The numerical model gives two possibilities for simulation of the supports:

- Simply support connection where there are no movements in the supported points.
- Supports by linear/nonlinear bedding. With this type of supports some effects characteristic for soli-structure interaction can be simulated (sliding of the dam body, lifting in the case of the tension, linear/nonlinear friction and similar).

The strips of the concrete face are connected with stiffer foundations. The interface between these elements is with edges hinge that allowed independent rotation of strips and foundation along the common edges, but keep the connection between the both.

INTERFACE

The dam was build of elements with very different stiffness. In order to avoid numerical problem during nonlinear analyses, rigid connection of that type of element should be avoided. The strips faced element initially has gap of 2 cm (Fig. 11). During the construction and impounding, free movement between neighbour points happened till the points contact each other. After that the point moved together without, and some forces can be transferred between the points. This type of the interface was simulated with nonlinear spring that cannot transfer tension forces. The spring will be activated in the moment when the distance between the points became equal to the gap (2 cm).

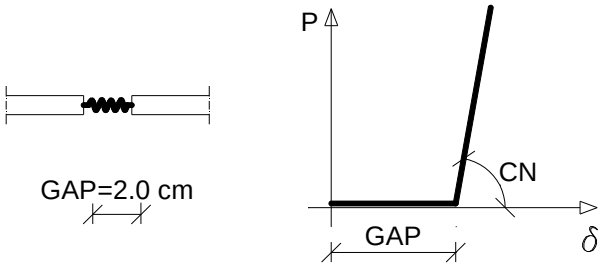

Figure 11. Spring-force displacement relation.

The connection between the concrete strips and the rockfill body was simulated with nonlinear distributed springs. The characteristics of these springs are as follow (Fig. 12):

- CN – axial spring constant. Usually very large number to preserve contact between the strips and the body in the normal direction.
- CT – lateral spring constant. That constant can allow movement between the interface surfaces. The value of that constant dependent of the friction between the two surfaces.
- CRAC – failure load. In the case CRAC = 0, no tension between the surface is allowed.
- GAP – the spring will be activated when the distance between the points became equal to the gap's value.

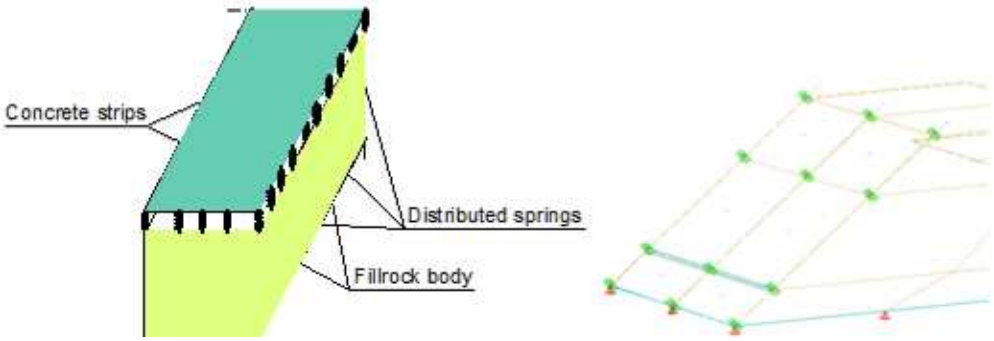

Figure 12. Connection between the concrete strips and the rockfill body.

LOADING OF THE DAM

According to the given data, appropriate loads from self weight and water pressure were created. SOFiSTiK has very efficient tools for load generation. The self weight loads are applied with the values of the unit weight of the materials in the dam body and division of the dam body in appropriate construction sequences, according to the given data, with command to act in the gravity direction. The simulation of the dam construction in layers is displayed on Fig. 13. The temperature, and the creep and shrinking effects were not taken into consideration.

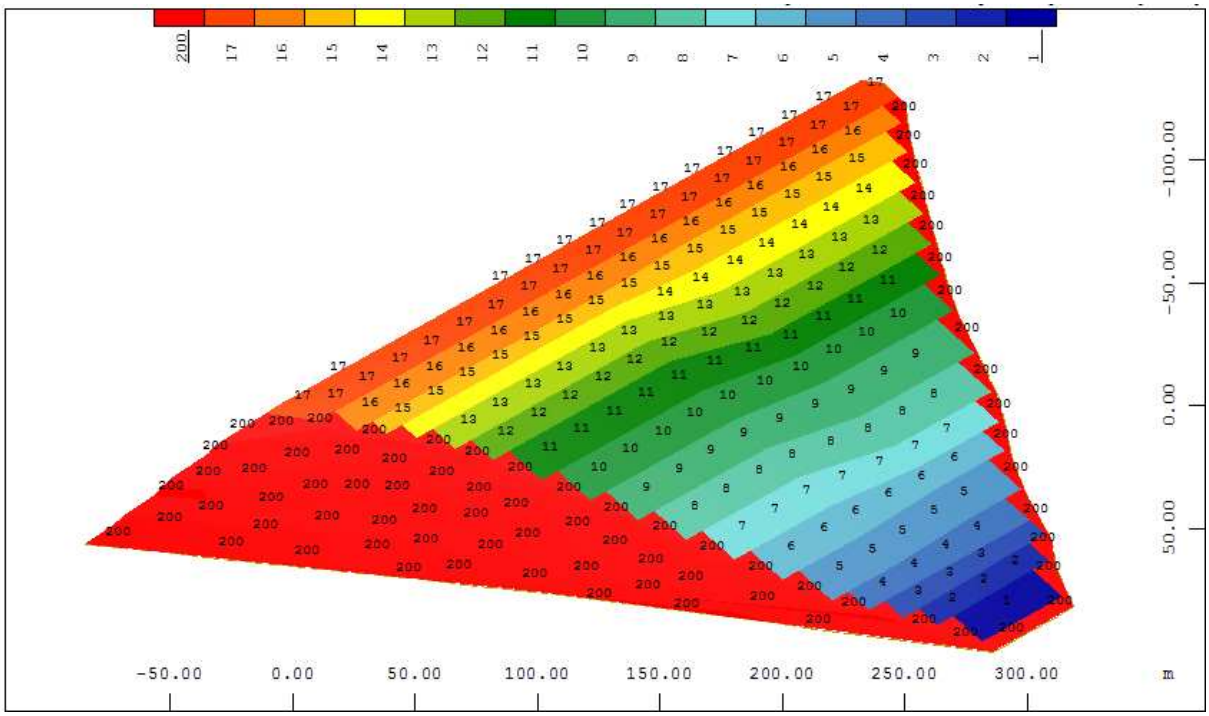

Figure 13. Simulation of dam construction in layers.

With the VOLU-statement, a loading on volumes, group of BRIC-elements or all QUAD-elements within the volume is enabled. The changes of the pressure load along tree edges are specified. All referenced elements of the group or the volume will be loaded. The selection of elements is only by a sheared cube (Fig. 14), defined by three selectable directions p_1-p, p_3-p_2, p_5-p_4, which must not be collinear. For transfer of the water pressure loads, some QUAD elements faces on the upstream of the dam's body was created, that are enabling to introduce the concrete face in the analysis and to apply the water load adequately (Fig. 15 and 16). This elements has only geometrical values, they have no contribution on the total structure stiffness. Referencing these QUAD elements in the VALU statement cause simple transfer of the water pressure in appropriate node loads. The water load is applied as hydrostatic pressure in increments.

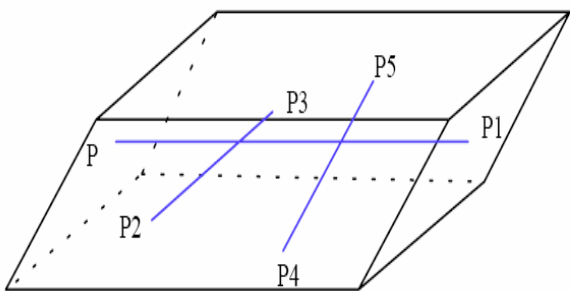

Figure 14. Sheared cube.

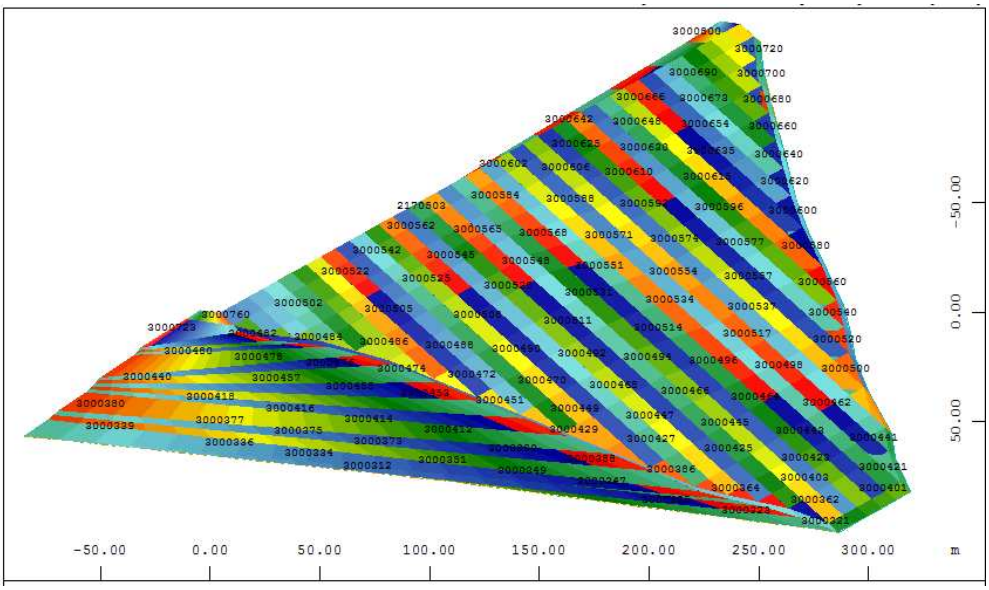

Figure 15. QUAD elements faces on the 3-D model of the dam's body.

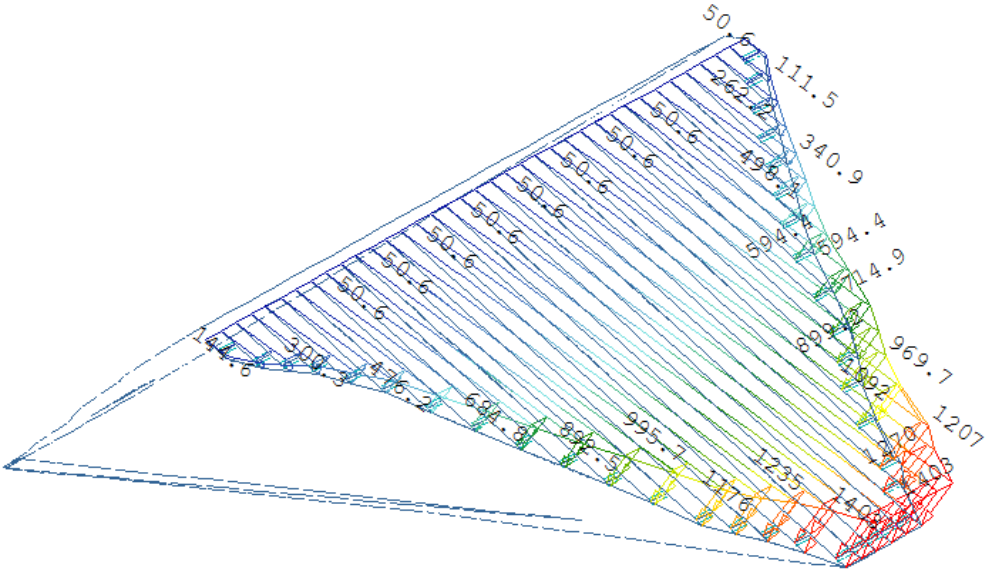

Figure 16.. Full water load applied on the 3D model of the dam, step 20.

ANALYSES OF THE DAM

Fill settlements

The dam was analyzed on statically action of self weight and water pressure loads. In order to obtain complete information about the stress-deformation state of the dam, in the following are displayed the obtained results for the displacements and the stresses in the dam body in the required cross sections for two loading stages (Fig. 17): stage after the end of dam construction and stage after the impounding of the reservoir.

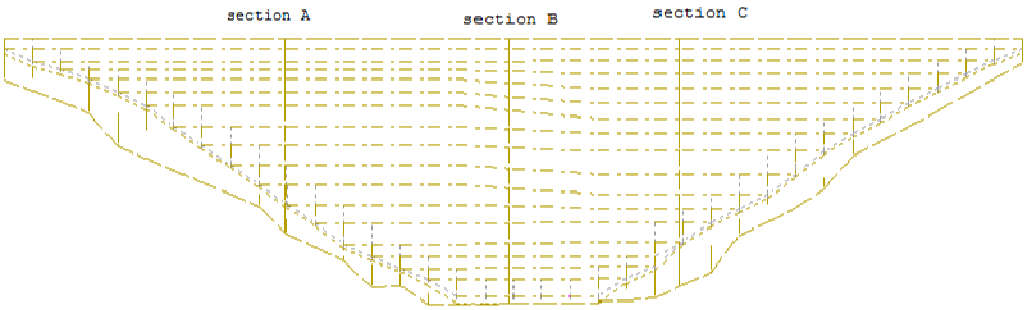

Figure 17. Location of the sections A, B and C in the dam.

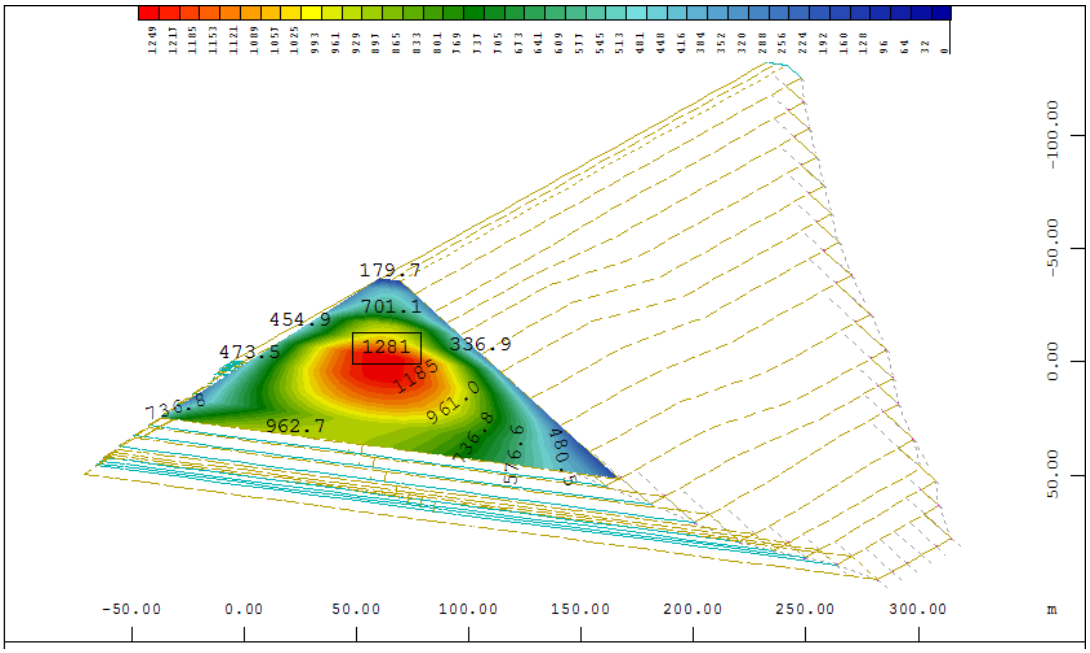

Figure 18. Vertical displacements after the dam construction, section A, Y = (0.0 ÷ 1281) mm, (-) is displacement opposite of the gravity direction, (+) is displacement in gravity direction.

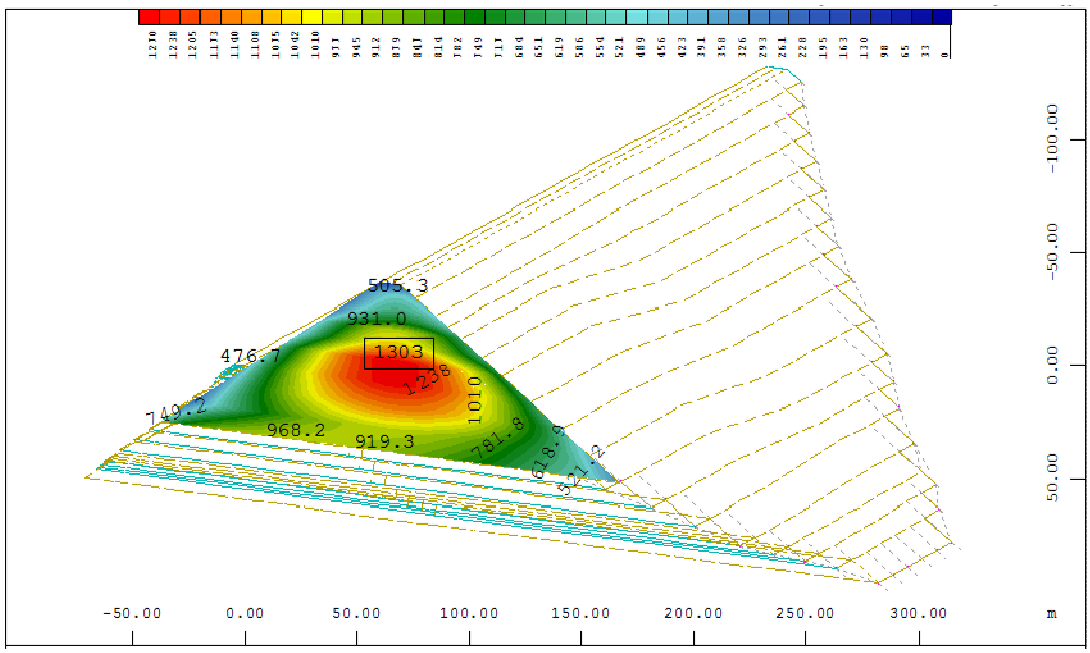

Figure 19. Vertical displacements after reservoir impounding, section A, Y = (0.0 ÷ 1303) mm, (-) is displacement opposite of the gravity direction, (+) is displacement in gravity direction.

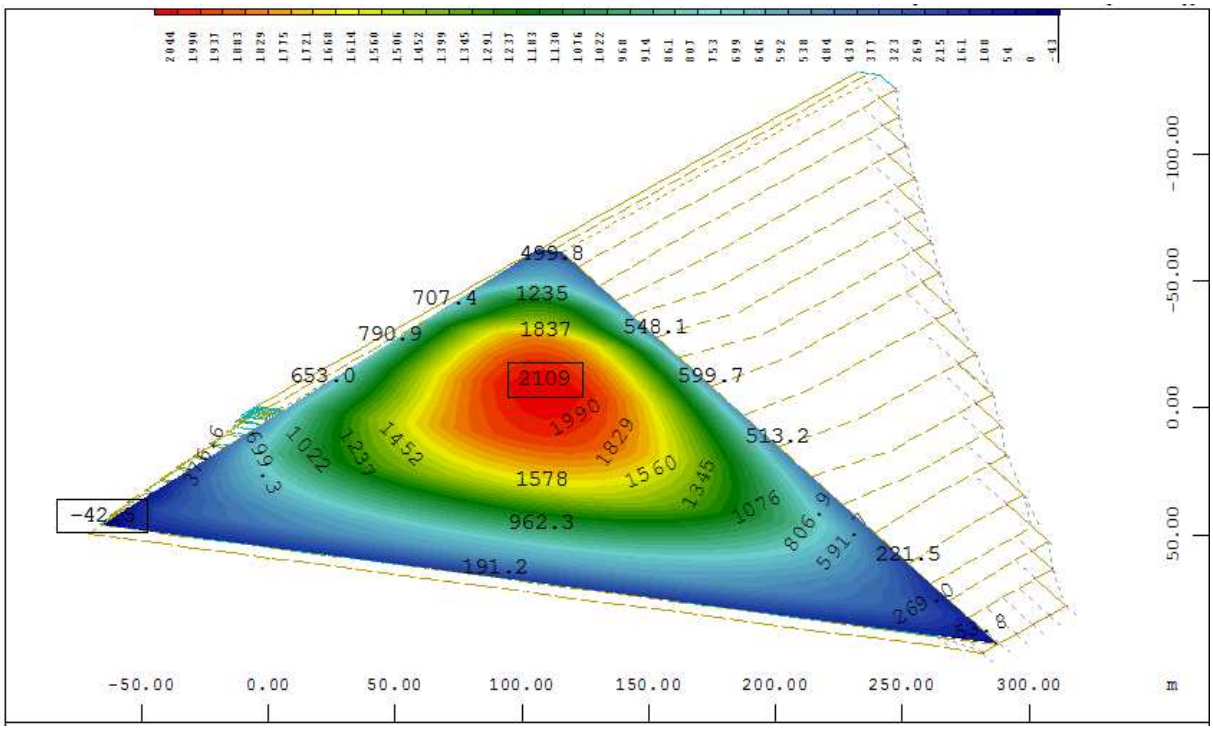

Figure 20. Vertical displacements after the dam construction, section B, Y = (0.0 ÷ 2109) mm, (-) is displacement opposite of the gravity direction, (+) is displacement in gravity direction.

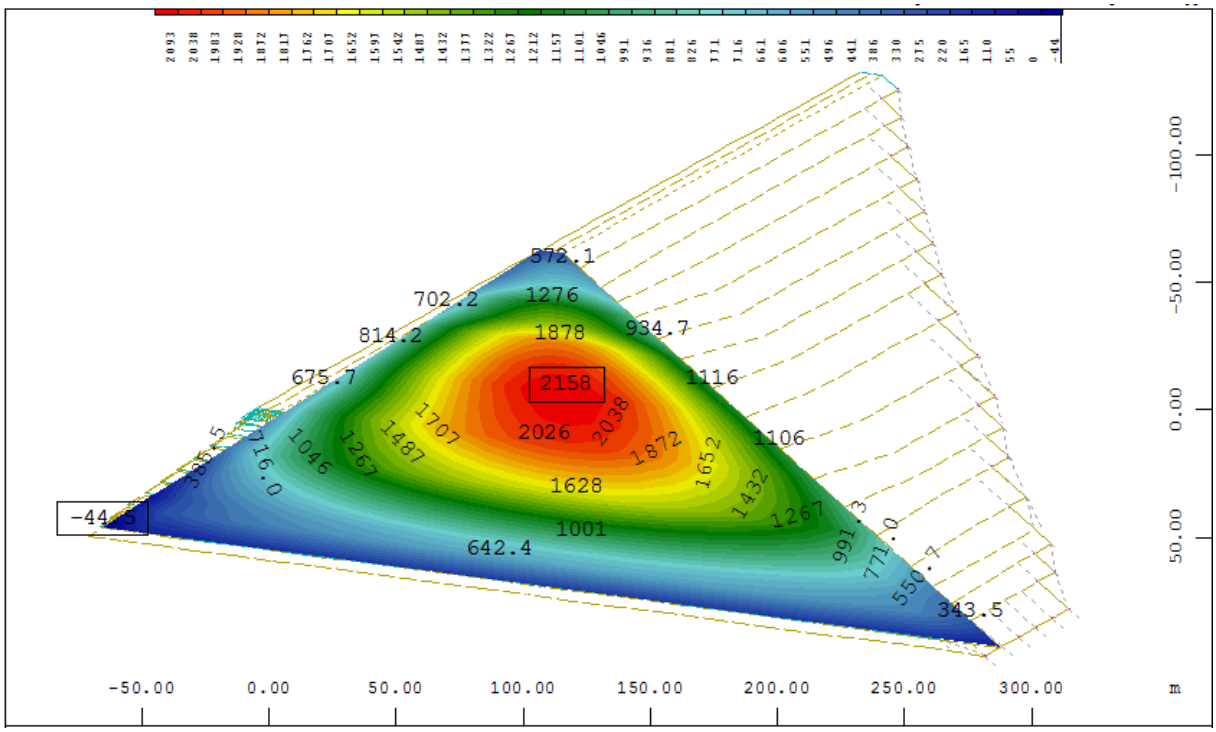

Figure 21. Vertical displacements after reservoir impounding, section B, Y = (0.0 ÷ 2158) mm, (-) is displacement opposite of the gravity direction, (+) is displacement in gravity direction.

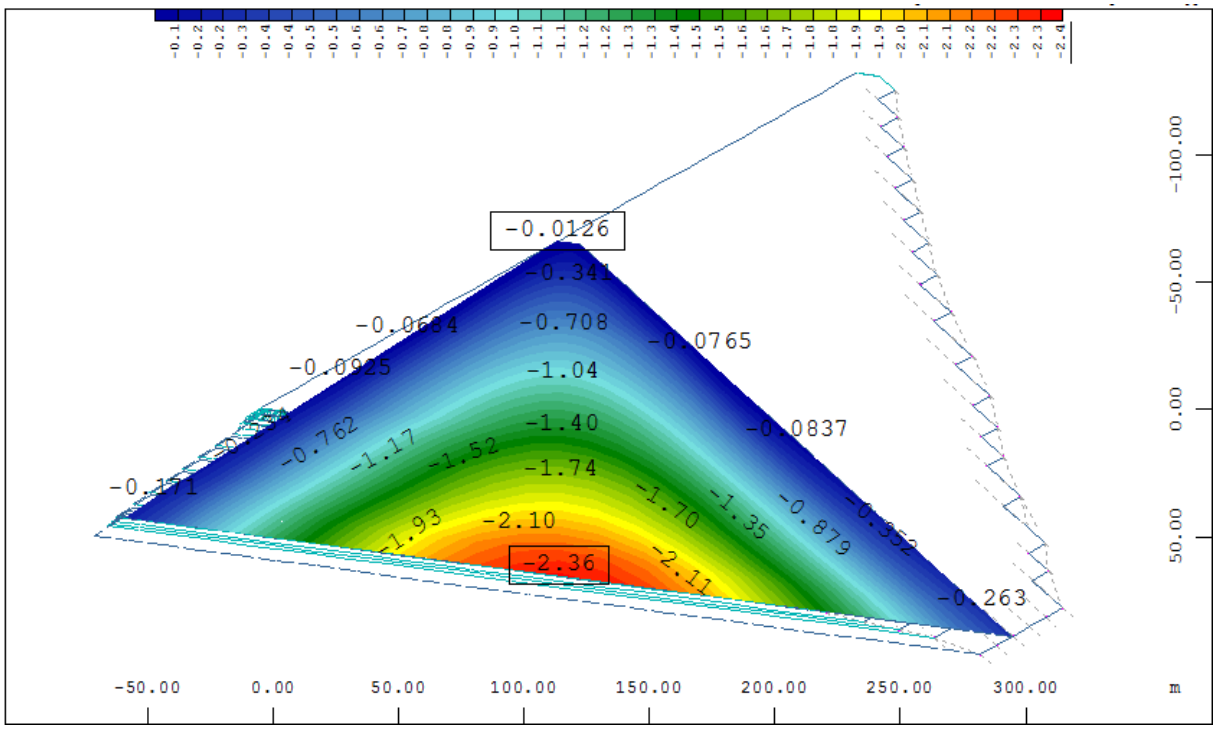

Figure 22. Vertical stresses after dam construction, section B, σ_Y= (-0.0126 ÷ -2.36) MPa.

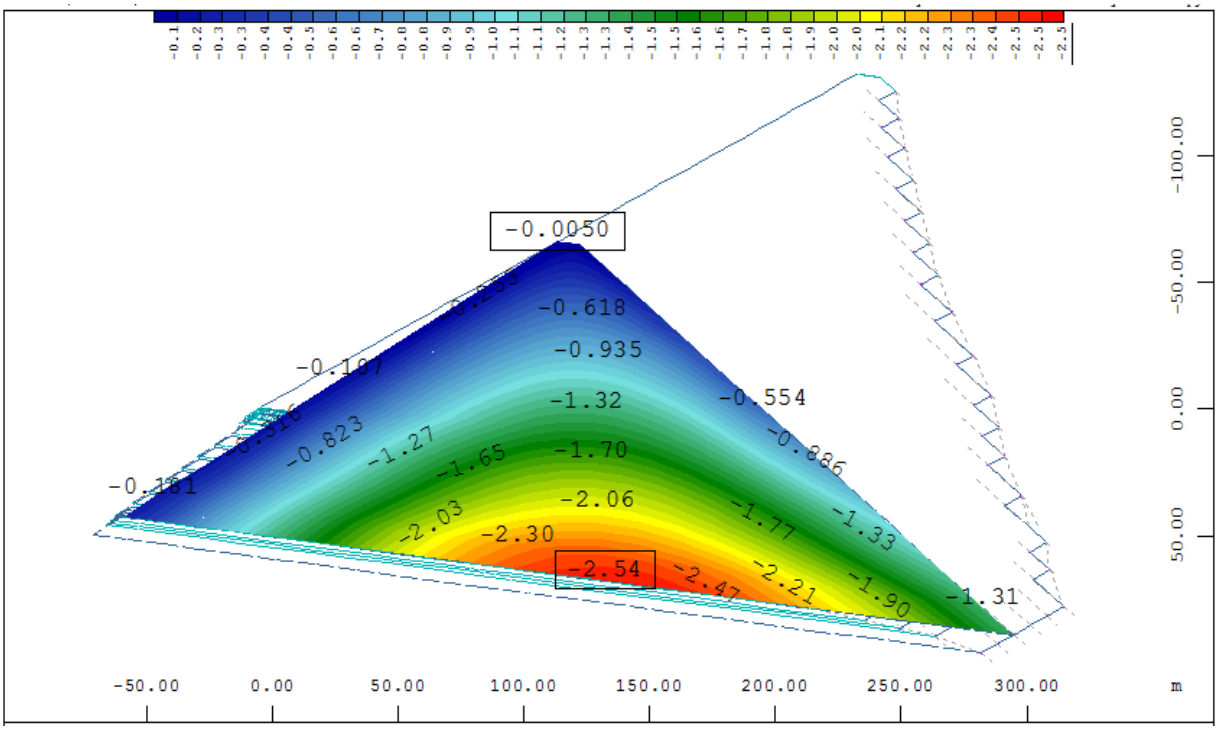

Figure 23. Vertical stresses after reservoir impounding, section B, σ_Y= (-0.005 ÷ -2.54) MPa.

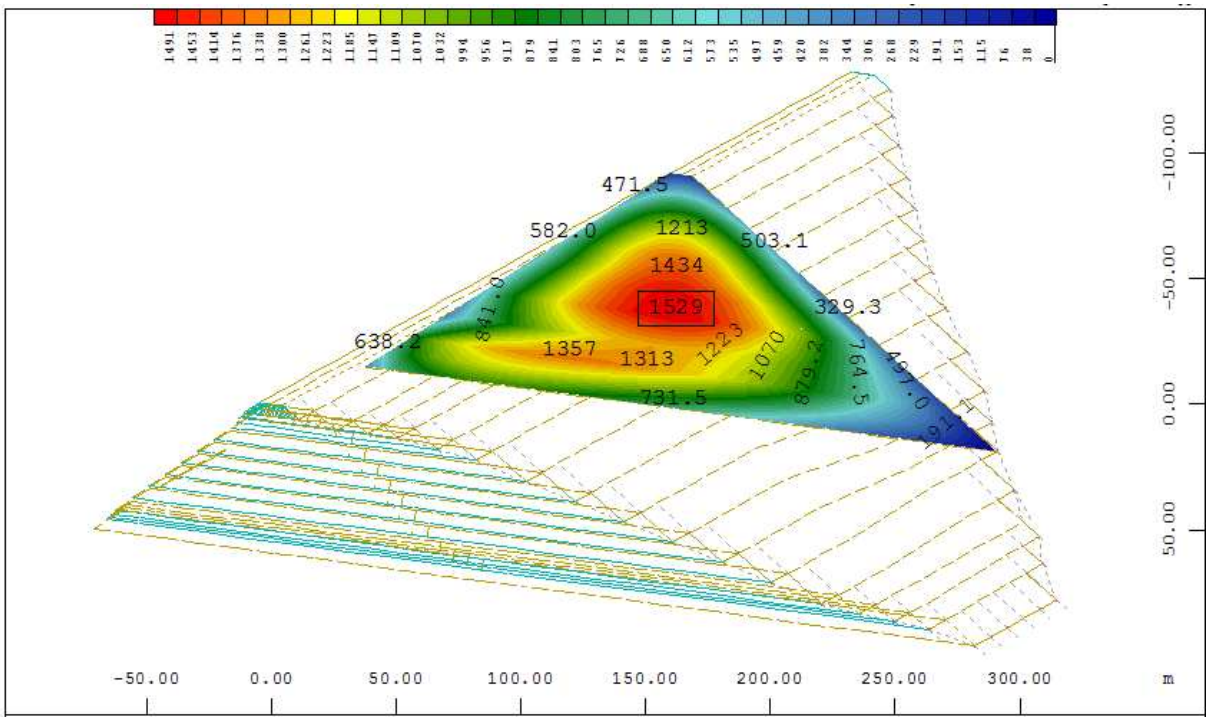

Figure 24. Vertical displacements after the dam construction, section C, Y = (0.0 ÷ 1529) mm, (-) is displacement opposite of the gravity direction, (+) is displacement in gravity direction.

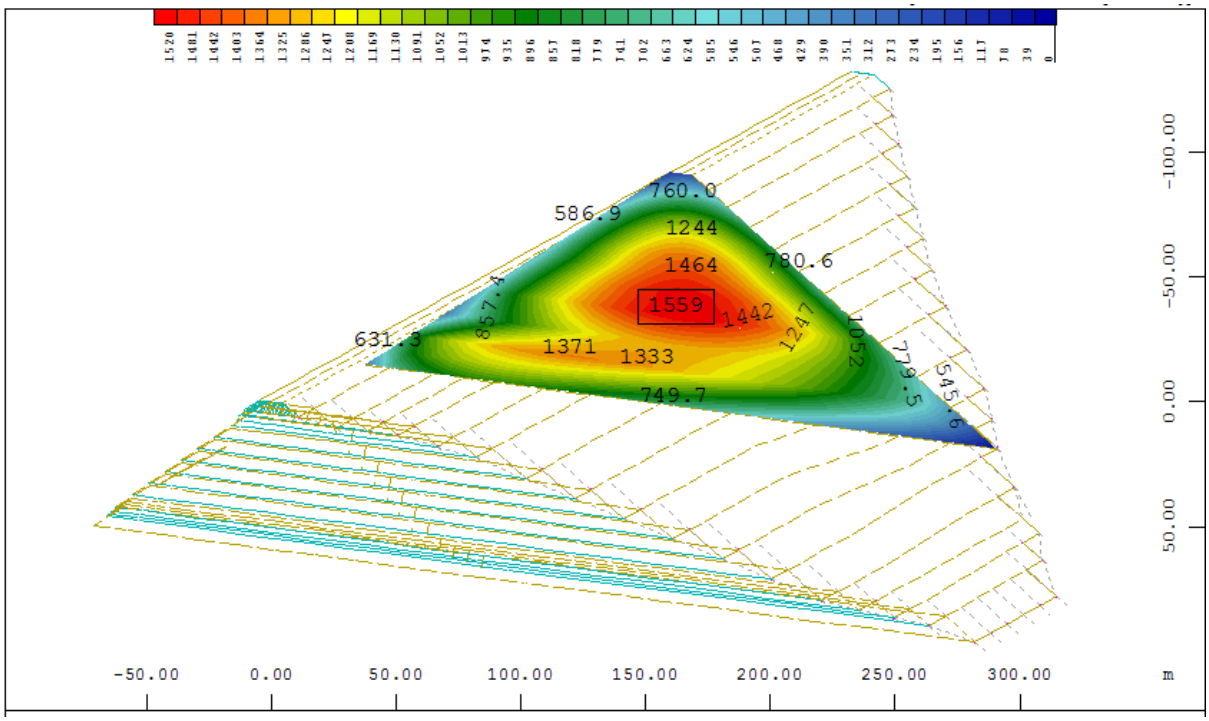

Figure 25. Vertical displacements after reservoir impounding, section C, Y = (0.0 ÷ 1559) mm, (-) is displacement opposite of the gravity direction, (+) is displacement in gravity direction.

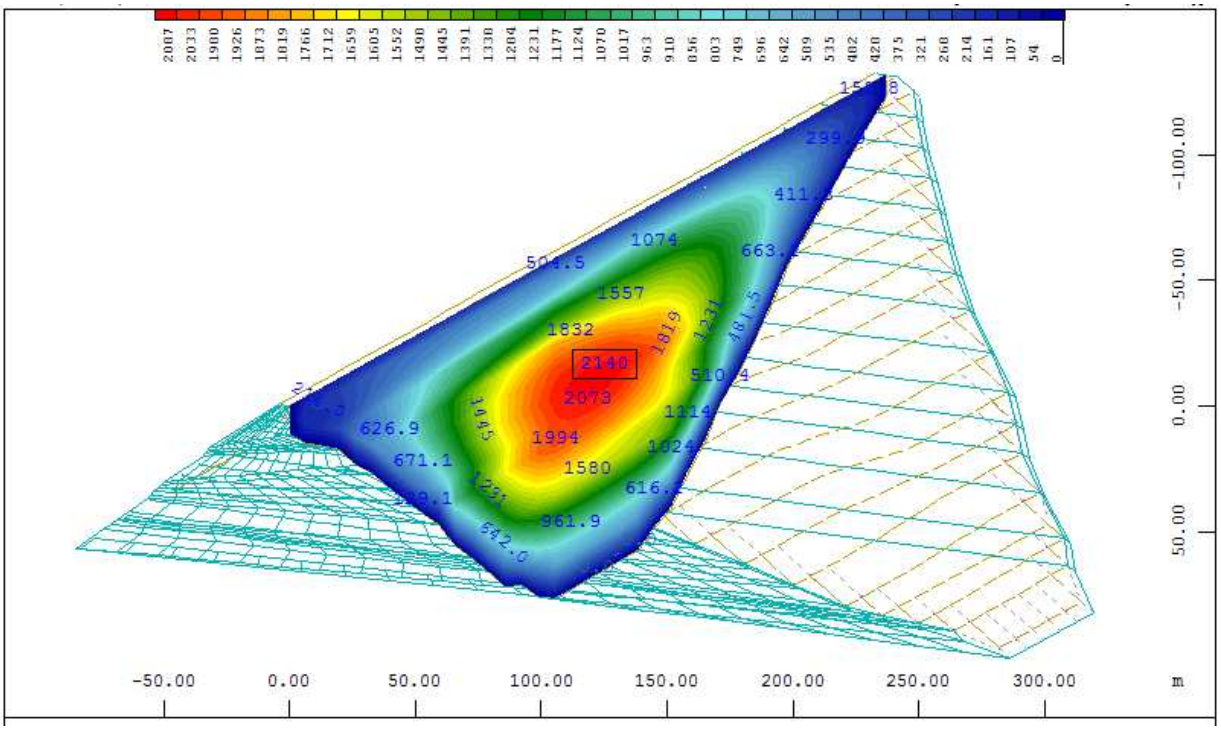

Figure 26. Vertical displacements after dam construction, longitudinal section of the dam, Y = (0.0 ÷ 2140) mm, (-) is displacement opposite of the gravity direction, (+) is displacement in gravity direction.

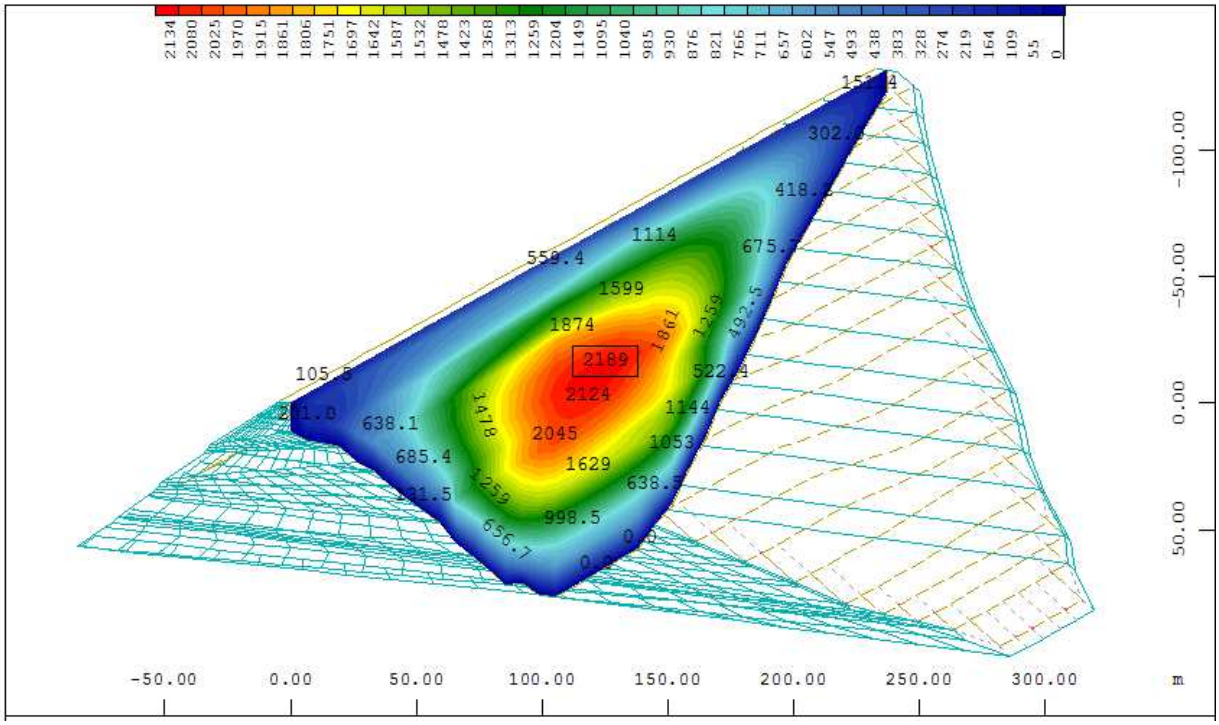

Figure 27. Vertical displacements after reservoir impounding, longitudinal section of the dam, Y = (0.0 ÷ 2189) mm, (-) is displacement opposite of the gravity direction, (+) is displacement in gravity direction.

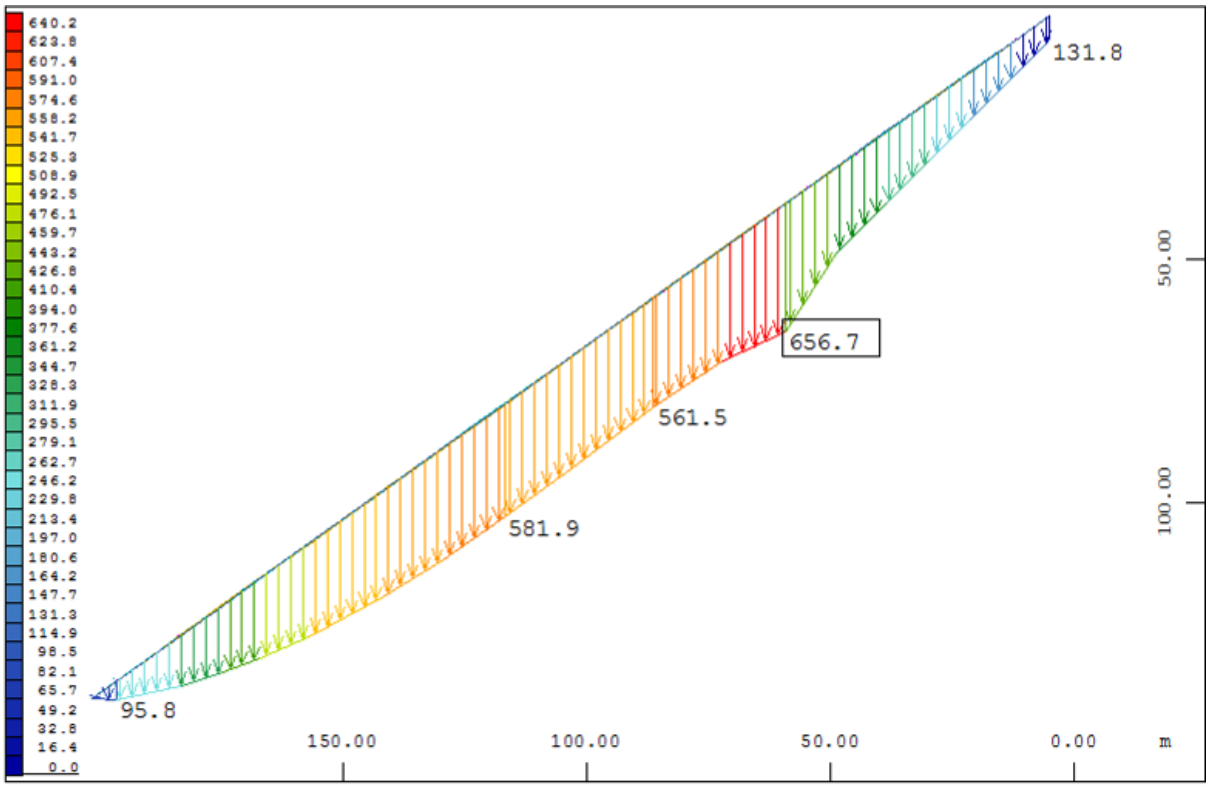

Figure 28. Surface settlements for lake level at EL 2075, upstream side.

Strains and stresses within the Concrete Face

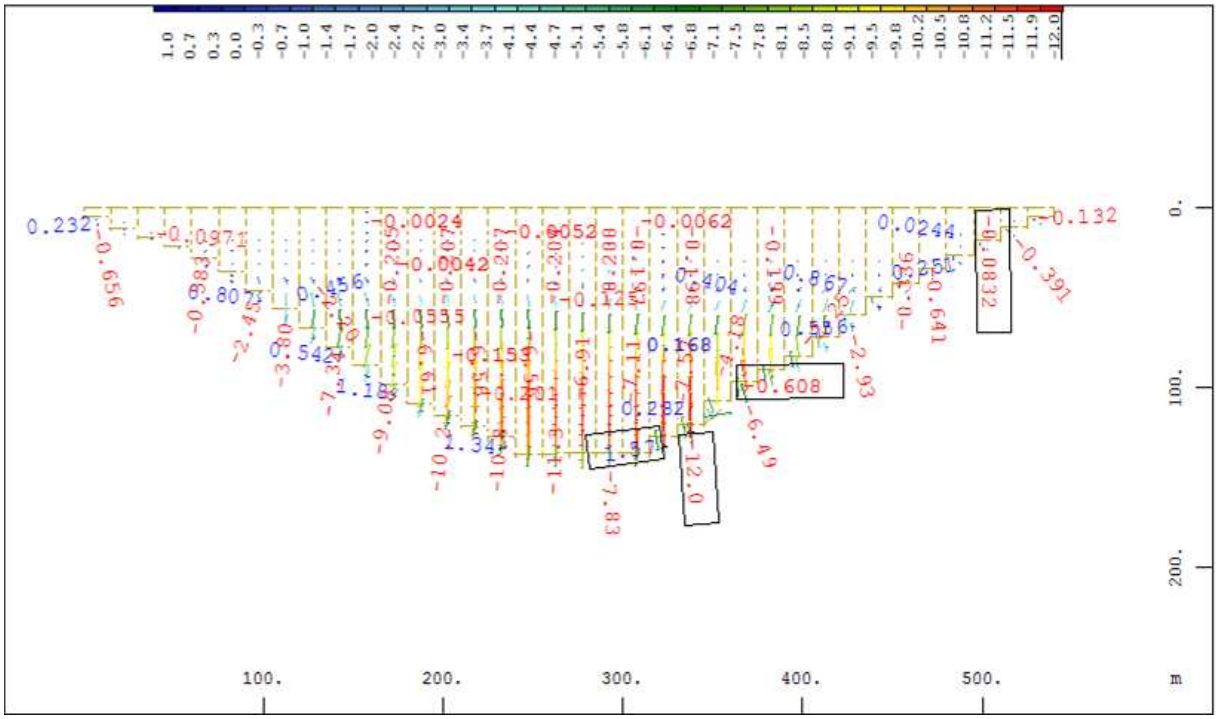

Figure 29. Top non-linear principal stress in the concrete face after dam construction, σ=(0.083 ÷ -12.0) MPa.

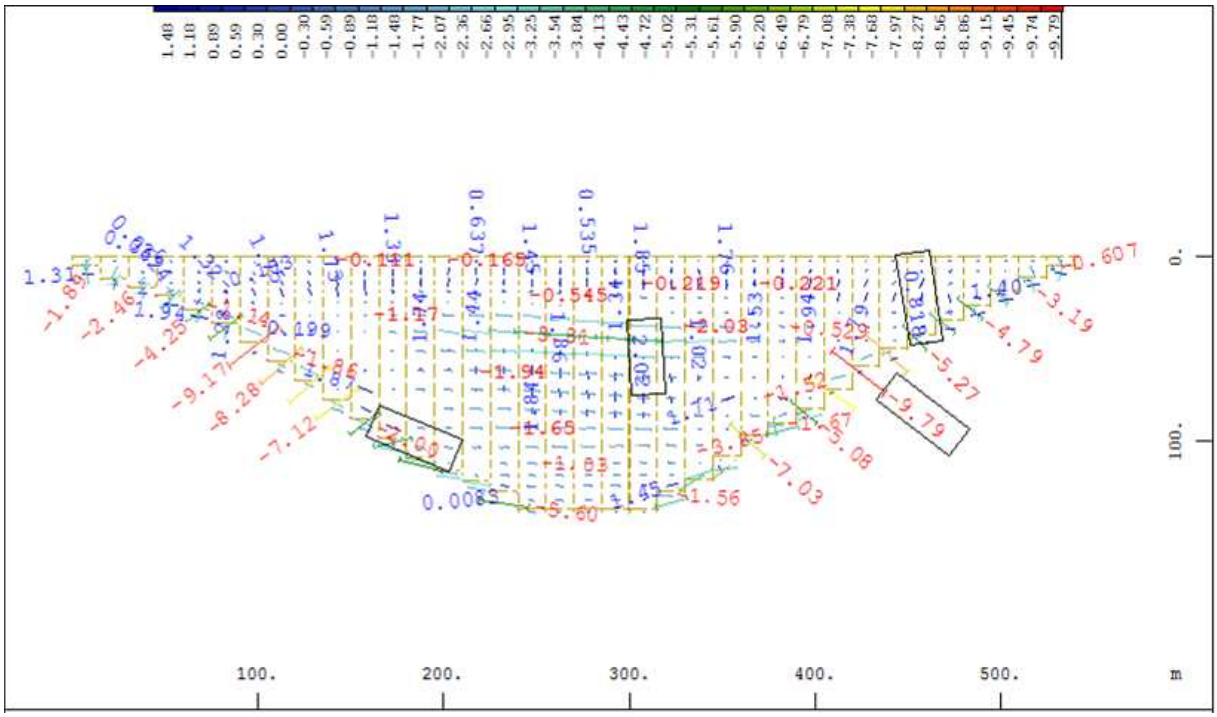

Figure 30. Top non-linear principal stress in the concrete face after reservoir impounding, σ = (1.48 ÷ -9.79) MPa.

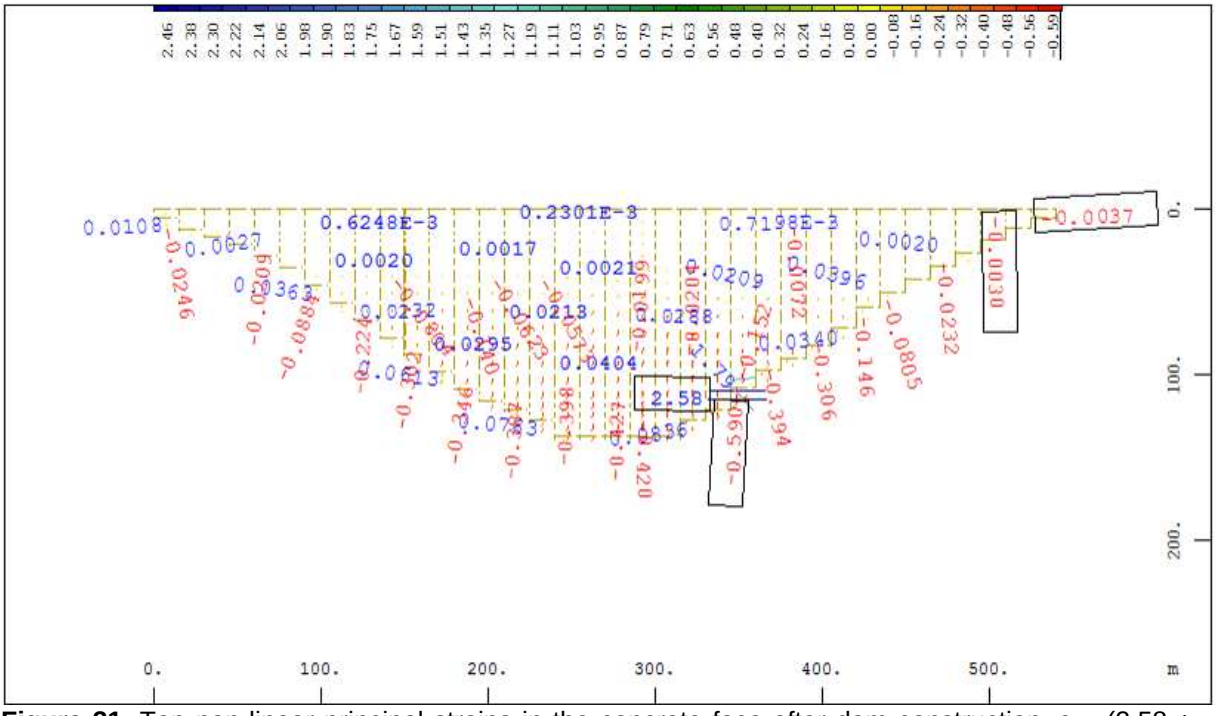

Figure 31. Top non-linear principal strains in the concrete face after dam construction, ε = (2.58 ÷ -0.59) ‰.

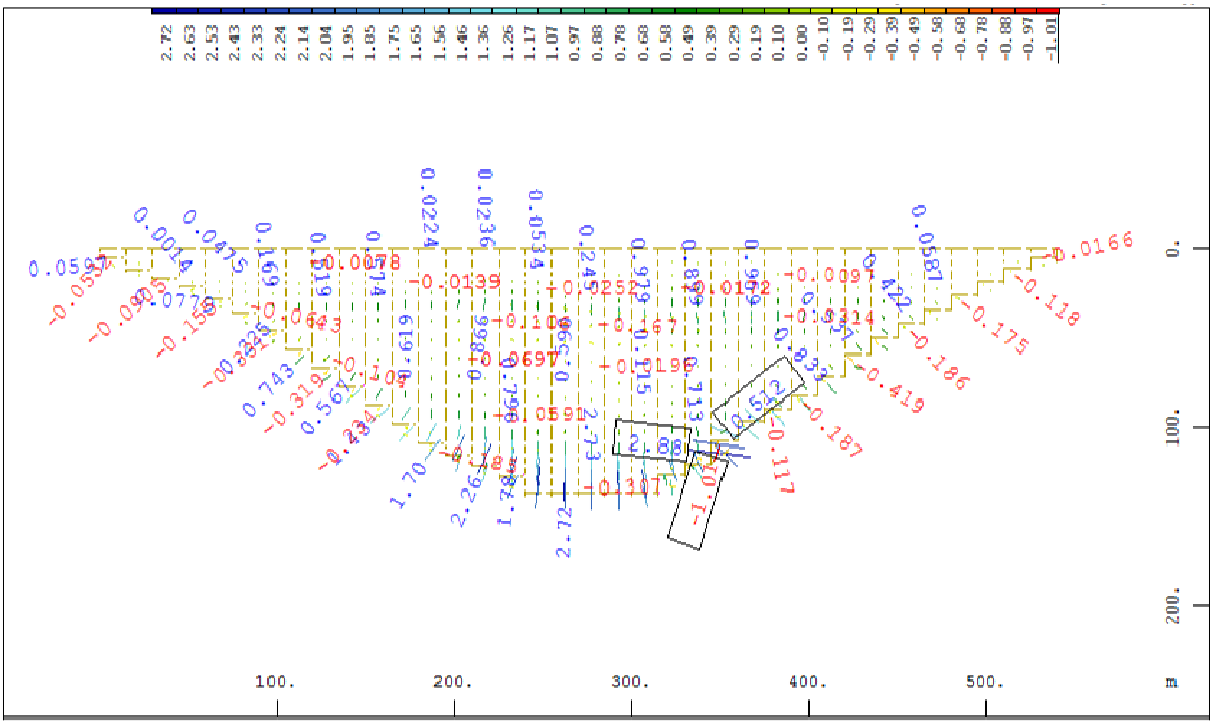

Figure 32. Top non-linear principal strains in the concrete face after reservoir impounding, ε = (2.72 ÷ -1.01) ‰.

Face deflections

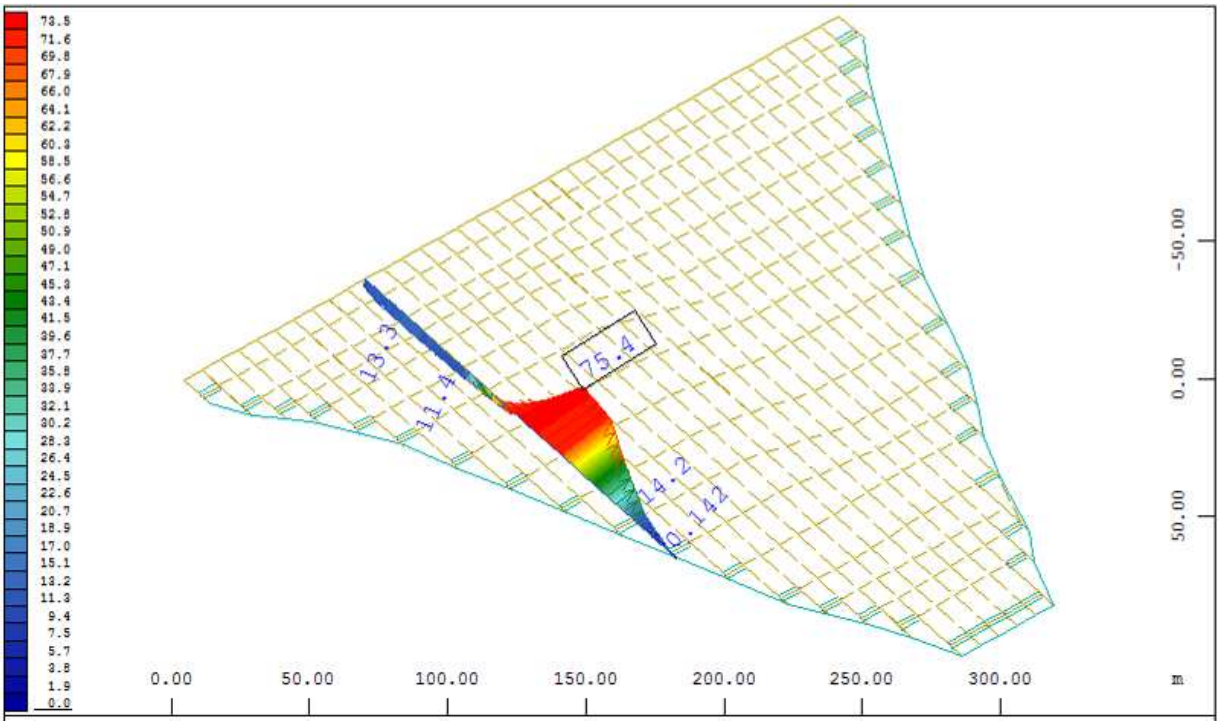

Figure 33. Face deflection after dam construction, section A, D=(0.0 ÷ 75.4) mm.

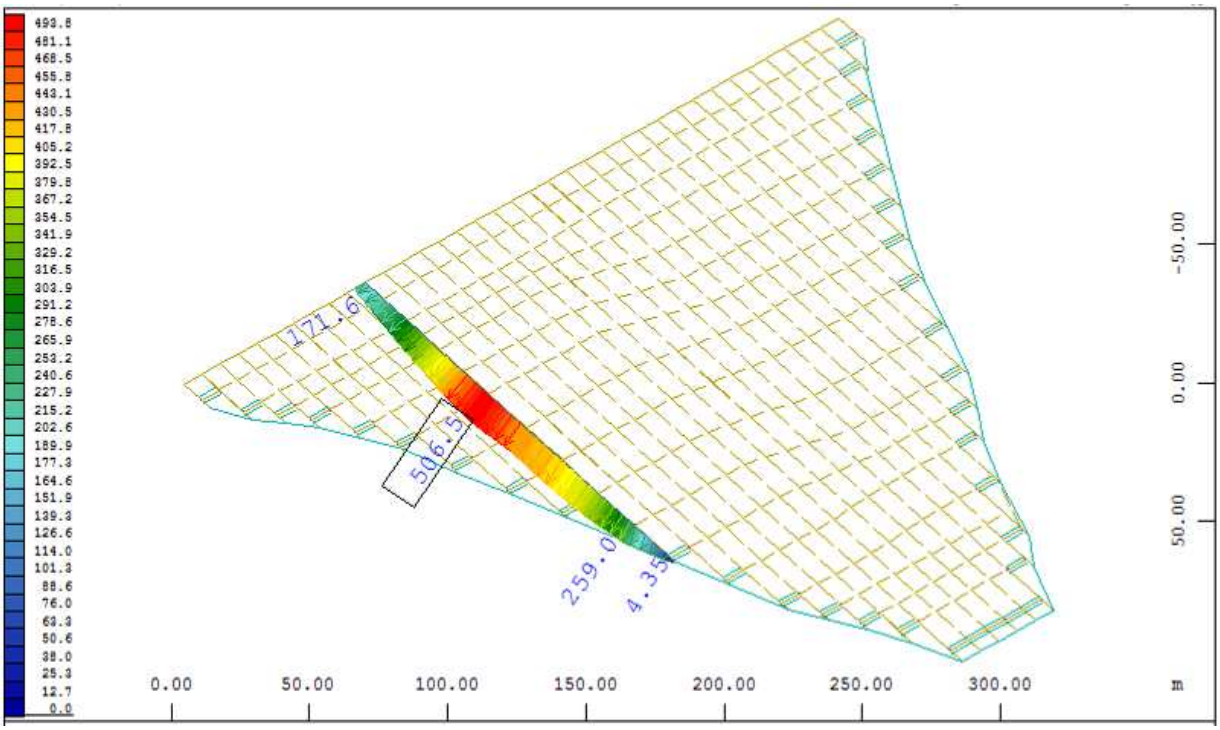

Figure 34. Face deflection after reservoir impounding, section A, D=(0.0 ÷ 506.5) mm.

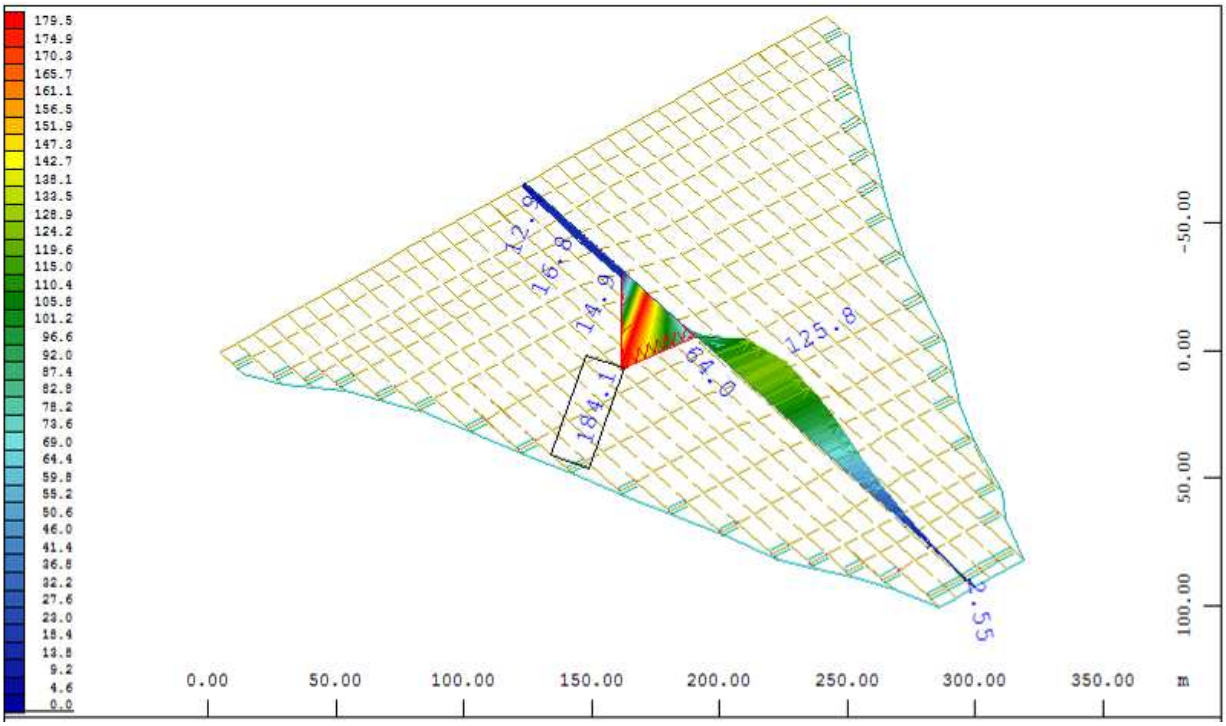

Figure 35. Face deflection after dam construction, section B, D=(0.0 ÷ 184.1) mm.

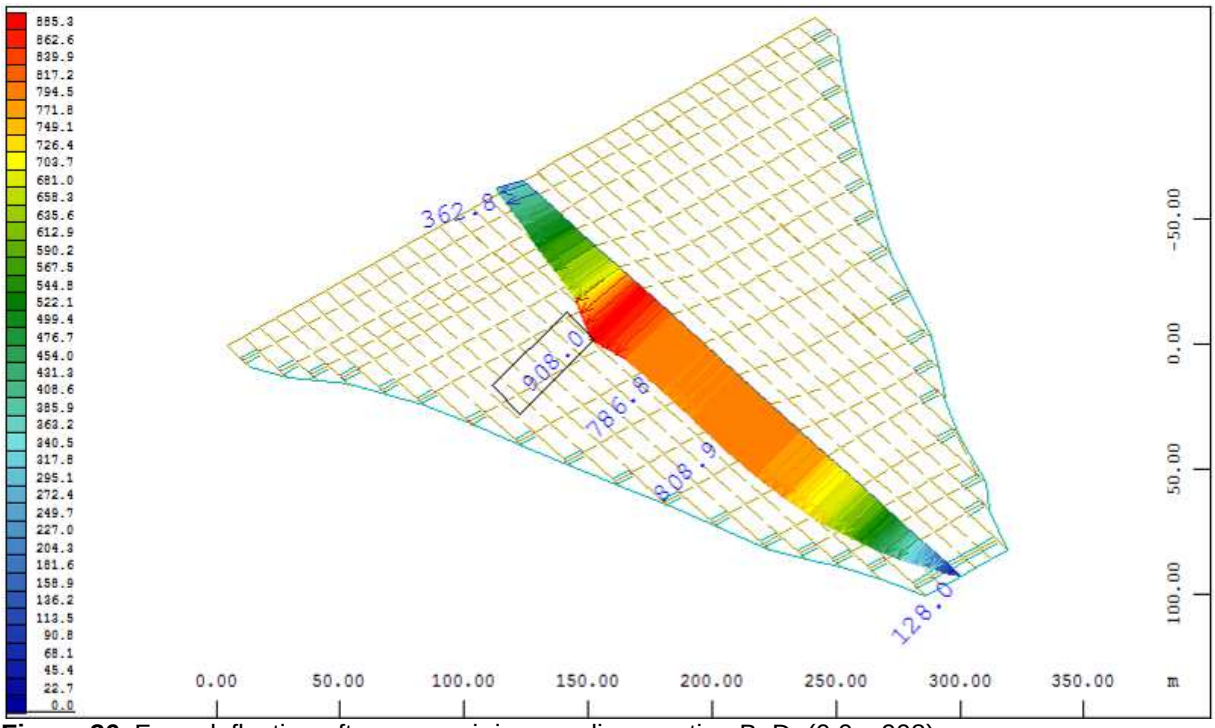

Figure 36. Face deflection after reservoir impounding, section B, D=(0.0 ÷ 908) mm.

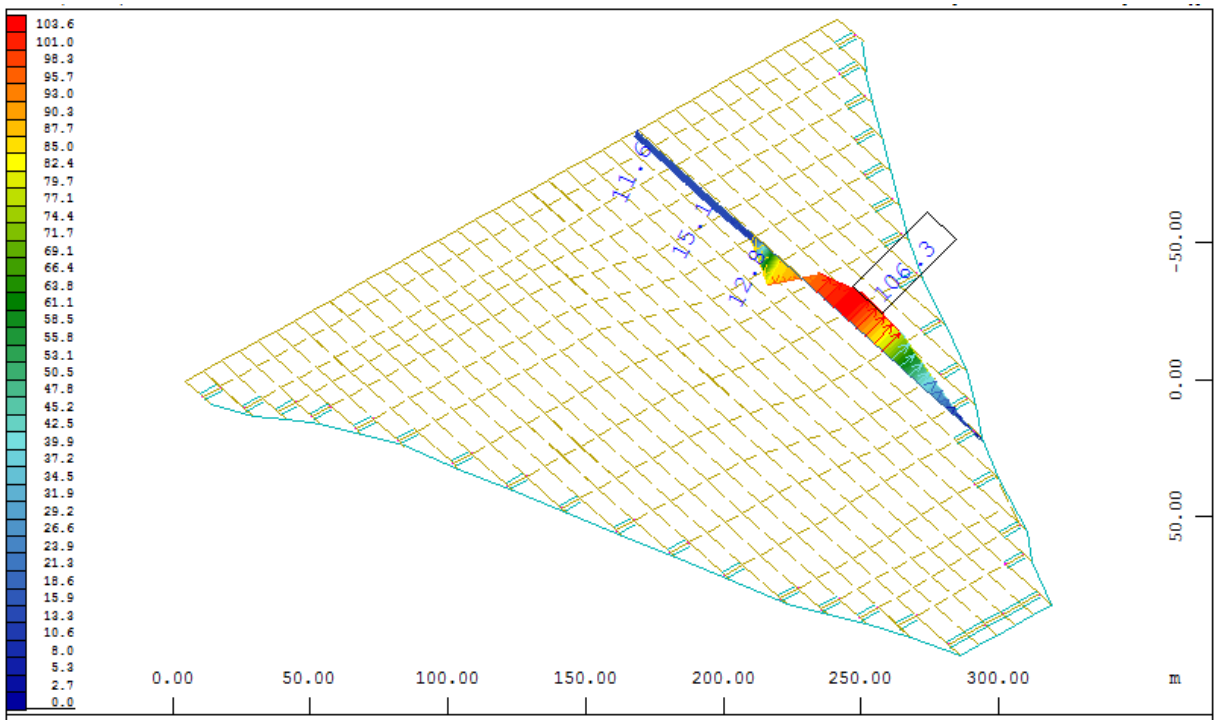

Figure 37. Face deflection after dam construction, section C, D=(0.0 ÷ 106.3) mm.

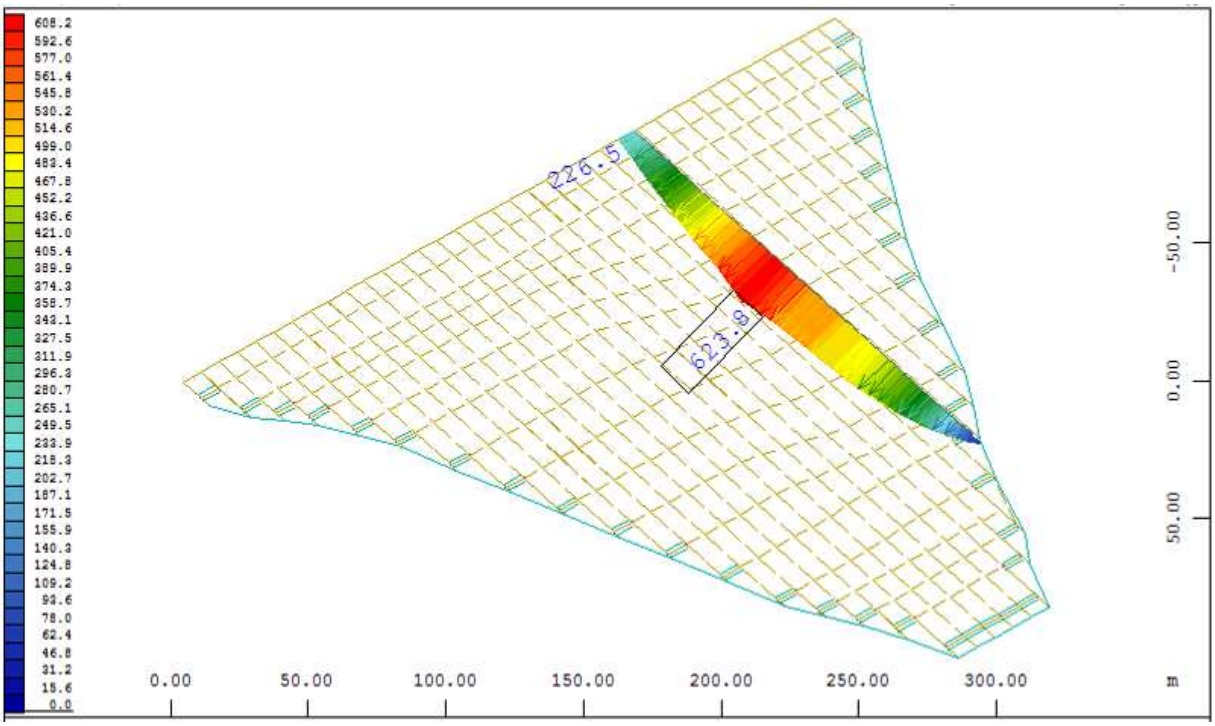

Figure 38. Face deflection after reservoir impounding, section C, D=(0.0 ÷ 623.8) mm.

CONCLUSIONS

From the performed analysis following main conclusions could be drawn out:

→ Program package SOFiSTiK is powerful tool for complex three-dimensional analysis of dams. It has rich possibilities for modeling of the dam body, and also possibilities for application of different constitutive laws, as well as for complex load influences.

→ From the analysis of dam behaviour for the loading states (state after dam construction and state after reservoir impounding), obtained values and distribution of the dam settlements and vertical stresses are usual for this type of dam. The maximal vertical settlement is in the intermediate part of the dam, located approximately at 60% of the dam height, with value 2.138 m at point HS B11, while the measured value at the same point is 2.32 m. This shows good accordance between these values. Maximal vertical stresses are at the bottom, in the central part of the, with value of 2.36 MPa.

→ From the comparison of the measured values for surface settlements for lake level at EL 2075 (Fig. 16 from the given data) and obtained values from the analysis (only for the upstream side, Fig. 28 from the analysis) it can be noticed that the diagram and the values of the settlements are very similar and also shows good accordance.

→ Up to now, with calibration of the numerical model, using some of the advanced features of the program SOFiSTiK, it was possible to explain some of the results obtained by the performed measurements. But, to explain the complete behaviour of the dam including the crack pattern, it is necessary to do additional improvement and calibration of the already complex numerical model with the measured data.

ANALYSIS OF A CONCRETE FACE ROCKFILL DAM INCLUDING CONCRETE FACE LOADING AND DEFORMATION

10th Benchmark Workshop on Numerical Analysis of Dams

September 16-18, 2009. Paris, France

C. Marulanda[1], E. Leon[1]

[1]INGETEC Cra 6 No 30a-30, Bogota-Colombia.

Abstract

The analysis of the behaviour of a concrete face rockfill dam described herein was carried out by four independent engineering teams. The case under consideration corresponds to "Theme B" formulated by the authors to the 10th Benchmark Workshop on Numerical Analysis of Dams, which took place in Paris (France) in September 2009 and was organized by the ICOLD Committee on Computational Aspects of Analysis and Design of Dams.

The theme titled "Analysis of a concrete face rockfill dam including concrete face loading and deformation" was based on available information on the performance of Mohale dam, located in Lesotho.

Four independent groups presented their results: 1) Civil engineering school of Skopje (Republic of Macedonia), 2) Coyne et Bellier (France), 3) TNO Diana (The Netherlands), and 4) INGETEC (Colombia).

Introduction

The construction of Concrete Face Rockfill Dams (hereafter referred to as CFRD) has increased in the last decades. This enthusiasm for CFRDs has its origin in both its inherent stability characteristics and its construction and schedule features. Also, its foundation requirements and treatments that are less strict and more straightforward to carry out, particularly when compared to gravity or arch dams, have made this type of dam a very attractive solution. As a consequence, the CFRD is currently a very common type of dam with several projects recently finished or under construction, with heights above 180 m. The design and development of CFRD dams, have been based primarily on precedent and empiricism, however, recent incidents have shown that the extrapolation of precedents with the current procedures can have serious consequences. Recent events have shown the need to improve the current design approaches and evolve beyond empiricism, including the development of analytical methodologies to analyze the behaviour of this type of dams.

Numerical analyses are now a common tool to predict dam behaviour, including the behaviour of the concrete face. However, the physical mechanisms involved in the interaction of the different structural components of a CFRD dam are a very complex problem to model. The theme titled "Analysis of a concrete face rockfill dam including concrete face loading and deformation" and studied in this document, aims at identifying

the key physical mechanisms that should be included in a numerical analysis to adequately predict the behaviour of a CFRD. In order to identify the key mechanisms, the analysis seeks to reproduce, in a three dimensional model, the cracking pattern observed on the upstream face of a high CFRD

The problem consists in predicting the development of deformations and stresses on the concrete face during construction and reservoir impoundment. Since the concrete face is a very slender element, it behaves as a shell and its displacements are controlled by the deformation of the rockfill. The development of stresses in the slabs is essentially caused by the deformation of the rockfill due to its own weight and the hydrostatic load of the reservoir. In addition, stresses, due to concrete curing and temperature gradients, will develop in the concrete face. The design of a concrete face should consider all the mechanisms that contribute to the development of stresses in the face. These mechanisms include the development of friction between the rockfill and the concrete face, the three dimensional deformation of the concrete face during construction and the reservoir impounding. Nevertheless, the difficulty in obtaining analytical solutions that include all of these mechanisms, and the absence of computational tools that allowed the calculations of the combined effect of the mechanisms acting on the slabs, contributed to the development of design procedures that were based primarily on precedent and empiricism. This tendency is exemplified in the determination of the concrete slab thickness, which is essentially based on precedent.

The proposed exercise was inspired by the recent incidents of cracks in the concrete face observed in high CFRD dams. The incidents include the following dams: Barra Grande (186 m high, 665 m crest length, concrete face area 108,000 m², rockfill volume 11.8 million m³ made of highly compressible basalt), Campos Novos (202 m high, crest length 590 m, concrete face area 105,000 m², rockfill volume 12.9 million m³ made of highly compressible basalt) both in Brazil and Mohale dam in Lesotho (145 m high, crest length 600 m, concrete face area 73,400 m², rockfill volume 7.5 million m³). The general characteristics of the recent incidents, where cracking has occurred, have been described in Johannesson [1], Pinto [6] and Sobrinho et al.[7].

The names of the participants and their papers are listed below (Table 1). The contributions of the participants are greatly appreciated.

Table 1 Full list of participants

Title	Authors	Company/Institution
Analysis of a concrete face rockfill dam including concrete face loading and deformation using program package SOFiSTiK	Gjorgi Kokalanov Ljubomir Tančev Stevcho Mitovski Slobodan Lakočević	Civil engineering school of Skopje.
DIANA Analysis of a concrete faced rockfill dam	Gerd-Jan Schreppers Giovanna Lilliu	TNO DIANA, Delft NL.
A CFRD case using 3D modelling	C. Nieto J-C. Philippe M. Werst P. Anthiniac	Tractebel Engineering-Coyne Et Bellier. Gennevilliers Cedex, France.
Analysis of a concrete face rockfill dam including concrete face loading and deformation	C. Marulanda E. Leon	INGETEC, Colombia.

Scope of the workshop

The chosen case history to be analyzed in this theme is the Mohale dam in Lesotho, which was completed in 2000. This 145 m high CFRD, with a crest length of 600 m and a total fill volume of approximately 7.5 million m³, is the highest dam of this type in Africa. The dam was constructed of basalt rockfill. The impounding stage started by the end of 2002, reaching the reservoir elevation (El.2060) in April 2005, illustrating that the entire impounding was extremely slow due to weather conditions

During the heavy rains that hit the region in early February 2006, the reservoir level reached spilling conditions (El.2078) and the dam suffered significant displacements, which in turn increased the compressive stresses in the concrete face. As a result, slab cracking was observed between slabs 17 and 18 including a 78 mm overlapping movement at crest level [1] (see Figure 1 and Figure 2), which increased significantly both inter-slab and perimeter joint openings. After this incident, seepage increased considerably, peaking at around 600 l/s. Reportedly, the deformation characteristics of the fill material exhibit initial high deformation modulus (100 MPa) that dropped afterwards (up to 20 MPa) when certain level of confining stress was reached. The basalt rockfill used for the dam was strong, however very angular, poorly graded and with high void ratio. Initially the rockfill produces an apparent strong interlocking and generating an apparent modulus in the range of 100 MPa. However, based on settlement readings; once the load (vertical stress) reaches values of approximately 0.2 MPa, grain breakages occurred and a considerably drop in fill stiffness occurred.

Figure 1: Crack seen from above between slabs 17 and 18

Figure 2: Slabs 17 and 18 after removing sheared concrete

Even though, the behaviour of geomaterials is regularly described as stress-dependent, this sudden reduction is only explained by grain breakage due the angular shape of the basalt particles. Similar experiences have been gained in Káranjúkar (Iceland), a CFRD constructed of fine graded basalt [1].

The information provided to the participants was aimed at calibrating the numerical models and reproduce the cracking observed in the central part of the concrete face when the reservoir level reached an elevation of 2078 masl in February, 2006

Given the fact that this type of dam is being widely used, the information gained from this incident, supported with the instrumentation data and dam details, is of crucial interest from a numerical analysis and design point of view. Taking into consideration the amount of information provided, each participant had a free choice of the data to incorporate in his models. The requested results from these analyses can be summarized as follows: (a) Fill settlements for two intermediate construction stages, at the end of construction and after reservoir impoundment,(b) Rockfill stresses at four levels of impoundment,(c) Horizontal and vertical stresses in face slabs 18 and 21 for four levels of impoundment, (d) Vertical fill stresses at the end of construction and when the reservoir level reached EL.2078, (e) Inter-slab joint openings at the end of construction and reservoir level at El.2078, and (f) Perimeter joint openings after full impounding.

Summary of given data

The following information was provided to all participants, which was based on different published information [1][2][8][9]. Details of this information can be found on the theme formulation provided to all participants [4].

a. Dam geometry
   - Cross section of the dam, including detailed geometry of the parapet wall and rockfill zoning.
   - Plan view of the location of the dam, dam axis and topographic map.
b. Construction sequence
   - 15 stages describing rockfill placement and five levels of impoundment extracted from construction sketches and images.
   - Location of a concrete beam at EL.2040 that was constructed for carrying pavement equipment.
   - Reservoir levels versus time
c. Material characterization
   - Rockfill placement requirements
   - Results of instrumentation data on rockfill vertical deformation modulus versus confining stress at two different locations within the dam body (Settlement cells HS-A9 and HS-A4, respectively).
   - Gradation requirements and index properties of rockfill
d. Instrumentation data
   - Settlements
   - Location of settlement cells along three cross sections of the dam body and level of rockfill at the time of readings.
   - Settlement readings during construction.
   - Surface settlements for reservoir level at EL.2075.
   - Interpolated contours of vertical, cross valley and downstream displacements induced by full reservoir.
   - Local settlements with respect to reservoir level in five settlement cells located along the central cross section.
   - Load cells

- Location of load cells along the cross sections of the dam body
- Vertical stresses versus time
    - Calculated based on Strain gauges measurements
- Location of strain gauges along face slabs 18 and 21.
- Horizontal and vertical stresses with respect to time.
    - Joint meters
- Location of inter-slab and perimeter joints
- Readings of inter-slab and perimeter joint openings
    - Face deformation
- Face deflection for slabs 21 and 27 at the end of construction
- Displacements normal to slope for curb and face slabs at EL.2040 (1st stage of concrete face)
- Cross valley displacements at crest level for EL.2060 and EL.2078
- Downstream and vertical displacements at crest level for EL.2060, EL.2065 and EL.2078.
- Crack pattern observed in concrete slabs when reservoir reached EL.2078.

In spite of the fact that considerable information was obtained through different publications, there still remained uncertainties regarding the properties and thickness of the curb, the extent of the excavations of the plinth, and the properties of the rockfill. However, neither of the participants elaborated on the relevance of this information.

Characteristics of the team models

The description of the models developed by each team focuses on the construction sequence, interfaces between the rockfill and concrete face, constitutive relationships for concrete and rockfill, and modelling of joints.

1) The Skopje team developed a three dimensional model using the software SOFiSTiK. Its main characteristics can be summarized as follows: The construction sequence for the dam body consisted in 18 horizontal layers of rockfill that did not conform to the proposed sequence, besides that, it did not describe a construction method realistic for this type of dam. Hence, the concrete face was placed in two stages at the end of the rockfill placement, which diverged from what was really done. The dam body was modelled using hexahedral solid elements with eight nodes, even as shell elements were used for the concrete face. The interface between the concrete face and the curb was modelled using a series of nonlinear axial and lateral springs. Axial springs transmit no tension load and its stiffness in compression shifts to a larger value when the distance between the two surfaces is less than 2 cm. The stiffness of the lateral spring depends upon the friction coefficient between the two surfaces. However, no information was provided on the parameters adopted for these springs.

An elastoplastic model with a hardening rule that follows a hyperbolic stress-strain relationship limited by the Mohr-Coulomb criterion was used to model the rockfill. No information was provided on the parameters involved and the calibration process. The concrete face was modelled using an elastoplastic stress-strain curve that yields in

compression at 20 MPa for concrete. An elasto-plastic stress-strain curve yielding at 500 MPa for both compression and tension was chosen for the rebars.

Finally, inter-slab joints were modelled as hinges that act along the slab edges, which allow rotation but no separation between slabs. The interface between the plinth and the perimeter joint was not considered.

2) TNO DIANA BV used their Finite Element software DIANA 9.3. The geometry of the canyon was simplified following the contour of the concrete face, the foundation was included in the model and the construction sequence includes 11 out of the 15 provided steps. However, no comments were made on the reasons for this simplification. Five levels of impounding were included. The dam body was modelled with 4-node tetrahedral elements with 6 m edge size and the concrete slab was modelled with shell elements using a quadrilateral mesh of 2.5 m element size. The outer and bottom face of the foundation were fully constrained.

Contact between the concrete face and the rockfill was modelled with contact elements, using a Coulomb friction material constitutive model with a friction angle of 40°. Interface elements were used to model the vertical joints among the 37 slabs that form the concrete face. No information was provided on the boundary conditions between the rockfill and the foundation.

The rockfill was modelled using a Cam-clay plasticity model with hardening using the parameters presented in Table 2. A pressure shift parameter is included in the model to describe the vertical stress at which the observed drop in stiffness takes place (0.1 MPa for poorly graded and 0.7 MPa for well-graded basalt). Properties of well-graded and poorly-graded basalt were assumed to describe the behaviour of upstream and downstream fill, respectively.

Table 2 DIANA - Material parameters of the basaltic rockfill

	Elastic hardening parameter	Poisson's ratio	Preconsolidation stress [MPa]	Friction angle	Plastic hardening parameter	Pressure shift [MPa]
Poorly graded	0.002	0.2	0.2	30°	0.02	0.1
Well graded	0.001	0.2	1.4	30°	0.01	0.7

It should be noted that this theme described the rockfill behaviour through a model that was developed for clay soils. No information was provided on how this model was calibrated and these parameters were obtained. The reported friction angles are unrealistic for a rockfill dam, and no description was provided of how the concept of preconsolidation stress for a rockfill material was conceived. The concrete face was assumed to follow a fixed total strain crack model with linear softening and Thorefeld compressive failure, (see Table 3). No description of this model was included. The foundation was assumed to behave elastically with Young's modulus of 5.0 GPa and Poisson's ratio of 0.2.

Table 3 DIANA - Material parameters of concrete

Material	Young's modulus [MPa]	Poisson's ratio	Tensile strength [MPa]	Tensile strength [MPa]	Ultimate crack strain
C20	40000	0.2	1.25	20	0.001

3) Coyne et Bellier presented two complementary models, the first model was performed using the software GEFDyn, a Finite Element Software developed by Coyne et Bellier and other partners, specialised in geotechnical structures with non linear behaviour. The second model was developed using ANSYS Finite Element Code which focuses only on the behaviour of the concrete face. The displacement field predicted for the rockfill in the first analysis was applied as an external boundary condition to the model of the concrete face. A sliding interface governed by a Coulomb-friction law was included between the concrete face and the displacement field derived from the rockfill deformation with the purpose of describing the stress transfer between these two elements. The modelling of inter-slab joints was not described.

The construction sequence for the rockfill incorporated in their model comprises only three out of the fifteen provided steps. The reservoir impounding was simplified also to four steps. The GEFDyn code adopted to describe the rockfill behaviour is an elastoplastic model with a non-associative flow rule and isotropic hardening was. This team did not elaborate on the effect of the development of stresses on the rockfill, considering that considerable larger loading stages were performed. The calibration of parameters was carried out through an iterative procedure to minimize discrepancies with local values of observed settlements during construction. Since the three-dimensional model was found to be exceptionally time consuming, the calibration of parameters was carried out using a two-dimensional model. The summary of model parameters is presented in Table 4. The concrete face is governed by linear elasticity.

Table 4. COB - Rockfill model parameters

Elasticity			
Material	**3B1**	**3B2**	**3C**
K_{ref} [MPa]*	30,1	21,8	17,1
G_{ref} [MPa]*	19,3	12	11,1
ν	0,2	0,2	0,3
p_{ref} [MPa]	1	1	1
Critical state and Plasticity			
ϕ_{pp}[°]**	38	38	38
β	17	17	17
D	2.5	2.5	2.5
B	0,2	0,2	0,2
p_{co}[MPa]	1,5	1,5	1,5
Flow rule and Isotropic hardening			
ψ [°]	35	35	35
α_{ψ}	1	1	1
a_m	1,8e-2	1,8e-2	1,8e-2

a_{cyc}	2e-4	2e-4	2e-4
C	1e-4	1e-4	1e-4
c_{cyc}	5e-5	5e-5	5e-5
M	1	1	1

4) INGETEC developed the model using the multipurpose Finite Element code ABAQUS. The model included the entire 20 construction stages; in which the concrete face is placed in two stages and the reservoir level was raised in five different stages. The dam body was modelled using tetrahedral elements, and hexahedral elements were used to model the concrete face.

Four interfaces were considered in the model. For the bedrock-rockfill interface, INGETEC carried out a series of simplified analyses to evaluate the effect of the inclination of the abutments in the predicted behaviour, finding out that significant relative displacements take place when the inclination of the abutments is greater than 45°. This aspect was calibrated using several case histories. It was concluded that for the abutment angles of the Mohale canyon (~30°), in combination with the high normal pressures acting on the abutments of the dam, the rockfill-foundation interface could be modeled as a zone where movements are restricted. Hence, no relative displacements were allowed between the foundation and the dam body.

The contact between concrete face and curb was modelled with special interface elements that follow a Coulomb friction law. Thus, relative displacements occur when external forces exceed the shear strength given by the normal stress applied at the interface and the friction coefficient between the two surfaces. The behaviour of the perimeter joint was described by using an interface between the slabs and the plinth, in which only compressive stresses are transferred. The inter-slab joints at the tension joints allow free opening and rotation.

Based on the experience in similar projects, and on the registered deformation modulus of various rockfill materials [5], is evident that the deformation characteristics of the rockfill for this type of dams exhibit an anisotropic behaviour. This behaviour has been reported by several authors, including Pinto and Marques [5]. This behaviour is considered to be developed by the rockfill placement procedure, which generates inevitably some level of segregation, creating a difference between the so called transverse moduli [5] and the vertical modulus of deformation. The INGETEC rockfill model incorporates this anisotropic behaviour. Reported behaviour has shown that the transverse modulus of deformation (Et) is consistently larger than the vertical modulus of deformation (Ev) with a registered ratio (Et/Ev) that ranges from 1 to 8 depending upon the characteristics of the rockfill [5]. The rockfill constitutive model applied by INGETEC follows a hyperbolic stress-strain curve which incorporates this anisotropic behaviour.

The rockfill constitutive model parameters were derived from published laboratory data of similar rockfill [3,10] and from a systematic iterative procedure to match the observed contours of dam displacements after full impounding. The INGETEC model suggests an average vertical deformation modulus of 40 MPa in the upstream fill, and 30 MPa in the

downstream side, which is consistent with the estimated modulus obtained from the dam instrumentation.

The ratio between transverse and vertical deformation modulus in the rockfill was found to be the key-element controlling the level of stresses in the concrete face after impounding. For a modulus ratio ranging from 3 to 6, the maximum horizontal compressive stresses increased from 12 MPa to 16 MPa, and the stresses along the face slabs increased more dramatically, from 10 MPa to values greater than 20 MPa. This suggested the onset of cracking at the bottom part of the concrete face. Thus, a modulus ratio of 4.0 was adopted to describe the level of stresses observed in the concrete face.

Considering the size of the model, the existing interfaces within the model, that crack propagation was outside the scope of this exercise, and that the primary purpose was to estimate the initial stress concentration of the face, a linear elastic approach was adopted to model the concrete face behaviour.

Comparison of numerical results

The summary of measurements and results provided by the participants is presented herein. The following abbreviations have been adopted: Coyne Et Bellier (COB), Civil engineering school of Skopje, Republic of Macedonia (UKIM), TNO DIANA (DIANA4) and INGETEC.

Fill settlements

- Fill settlements during construction

Figure 3 shows the location of settlement cells within the dam body. The two sets of measurements available during construction (Steps 6 and 13) are presented in Figure 4. The measurements are compared with the fill settlements estimated by COB and INGETEC. The other participants did not provide these results.

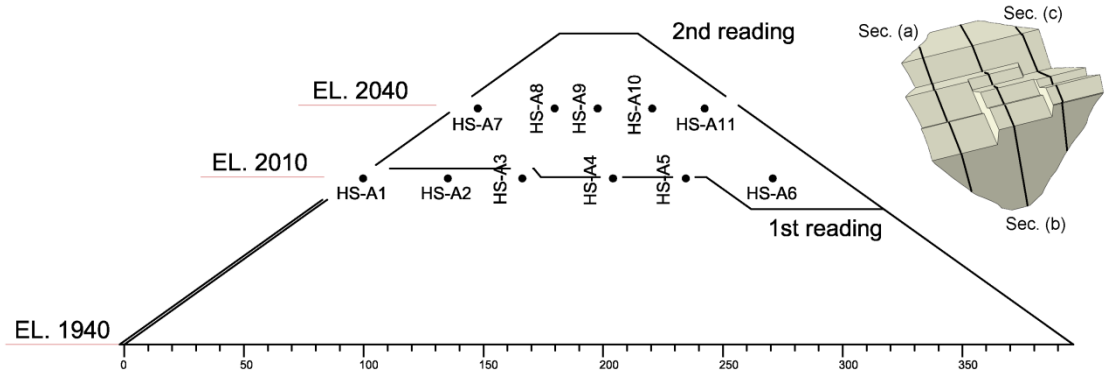

(a)

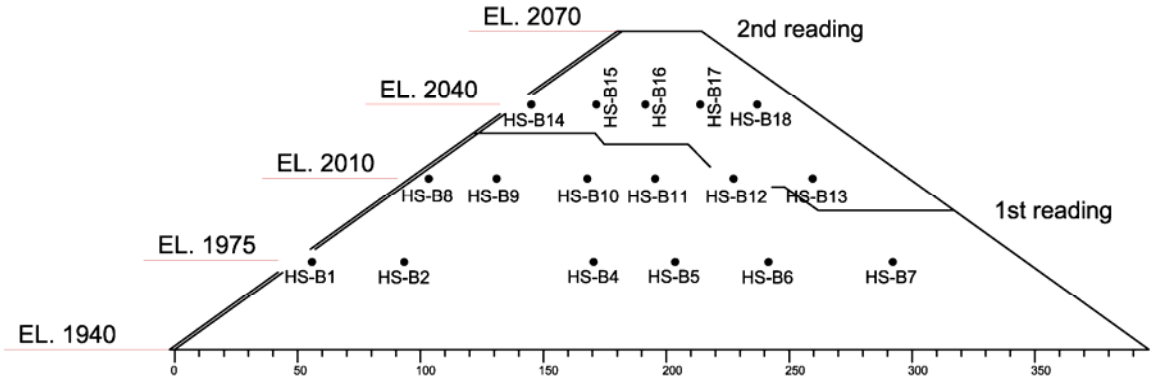

(b)

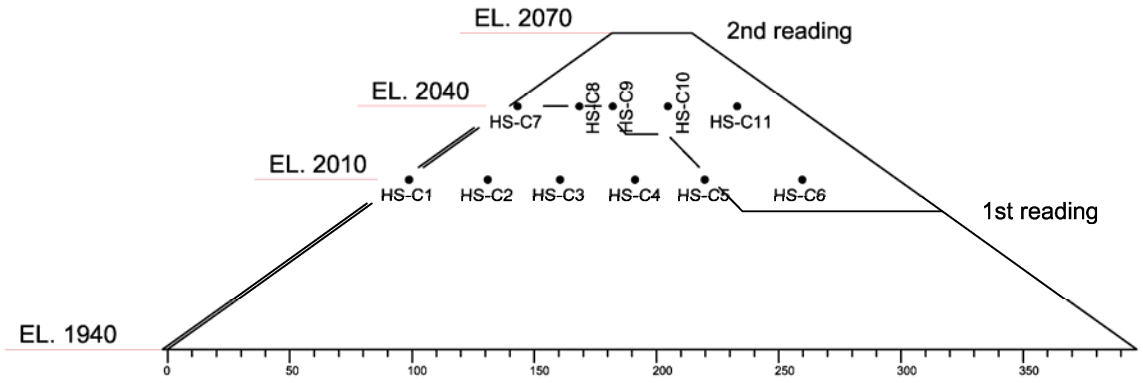

(c)

Figure 3: Location of settlement cells. (a) Left abutment, (b) Central section, (c) Right abutment.

Figure 4 shows settlements along the central section (see Figure 3b) in settlement cells located at different elevations within the dam body (EL.1975, EL.2010, and EL.2040). The observed settlement behaviour indicates that during construction smaller deformations occurred upstream compared to the downstream sector and the peak values were located around the central section. This comparison between upstream and downstream settlements suggests that the upstream rockfill is stiffer than the downstream one. This agrees with the fact that the placement and gradation requirements are more rigorous in the upstream side in order to control face slab deformation.

In general, the numerical results tend to slightly underestimate the measured settlements in all cases. However, both models follow the general trend of the measurements. It is worth mentioning that the predicted values are expected to be highly sensitive to uncertainties in the location of the settlement cells and details about the construction sequence but for a practical point of view the predictions seems reasonable.

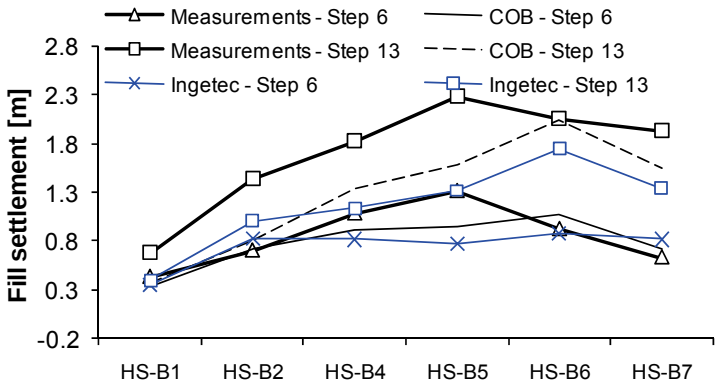

(a)

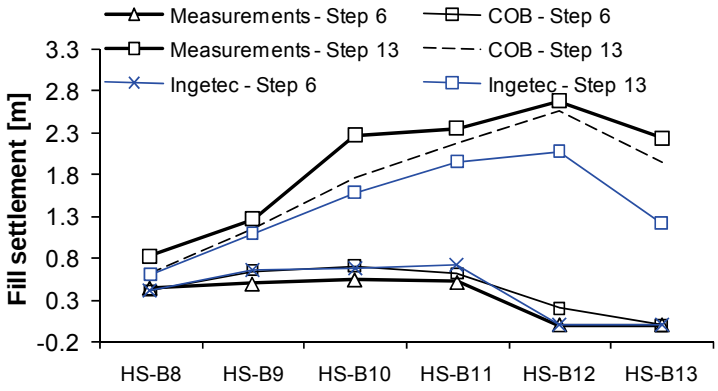

(b)

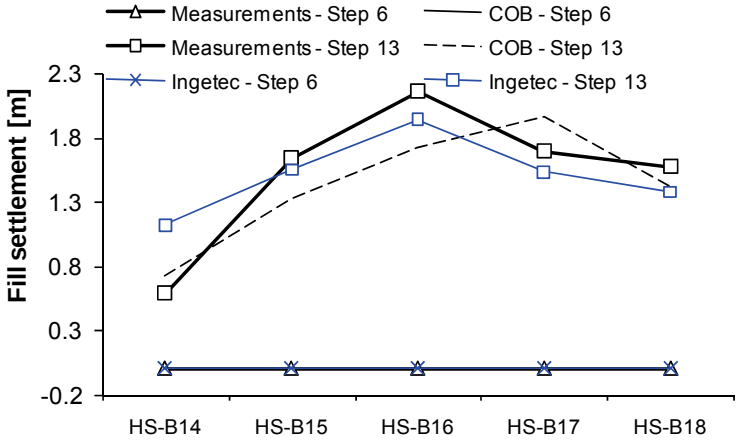

(c)

Figure 4: Measured and estimated rockfill settlements during construction (Steps 6 and 13). (a) Settlement cells HS-B1 to HS-B7 at EL.1975, (b) Settlement cells HS-B8 to HS-B13 at EL.2010, (c) Settlement cells HS-B14 to HS-B18 at EL.2040

Fill stresses

The location of load cells within the dam body is shown in Figure 5. Stresses induced in the rockfill by the reservoir when it reaches El.2078 are presented in Figure 6.

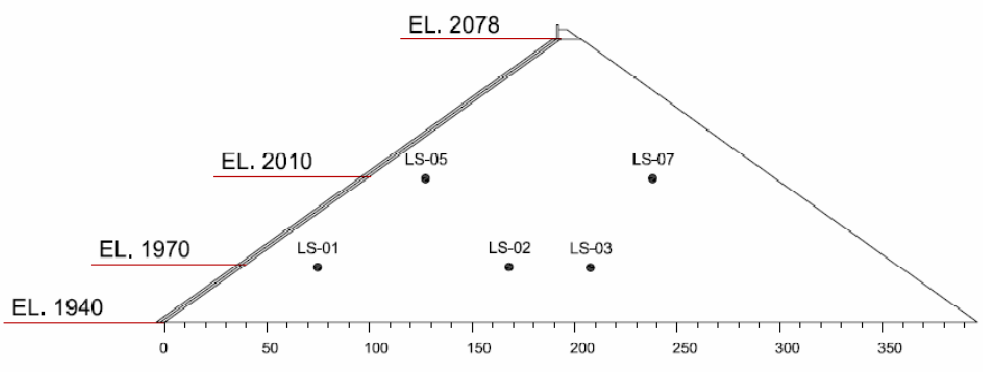

Figure 5: Location of load cells at maximum cross section

In general terms, the predicted behaviour of some of the participants follows the general trend of the measurements, which can be considered an appropriate estimate. Nevertheless, the predicted behaviour of UKIM is in clear discrepancy with the observed behaviour. This team predicted higher stresses in the downstream sector, which is further away from the reservoir loading, and is not consistent with the registered behaviour, that shows, as anticipated, higher stresses in load cells closer to the upstream face. A key-element that may have affected the results is the construction sequence implemented by this particular team, which clearly influences the distribution of settlements within the dam. However, no discussion was provided by this team on their predicted behaviour of settlements during construction.

The DIANA4, COB and INGETEC models predicted vertical stresses decreasing from upstream to downstream which agree with the instrumentation data (See LS01 to LS03 and LS05 to LS07 in Figure 6). However, the predicted values are particularly high in the COB and DIANA4 models for LS01 and LS05 cells (load cells located closer to the upstream face), overestimating the stresses induced by the reservoir.

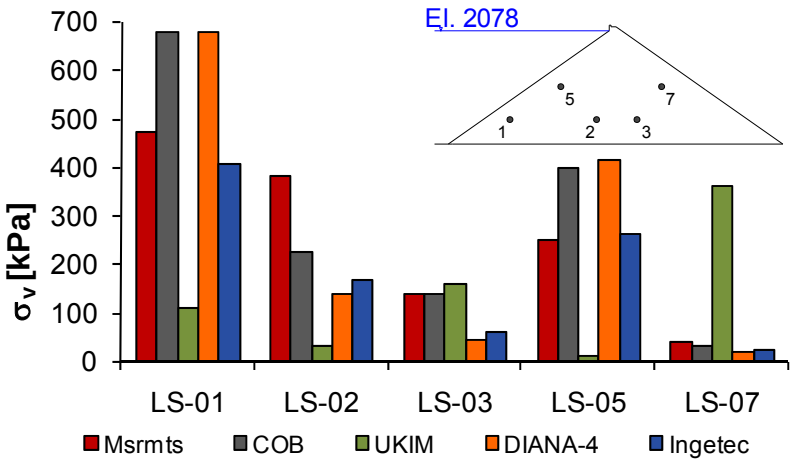

Figure 6: Stresses induced only by reservoir impoundment and predicted rockfill stresses. Reservoir level at EL.2078.

Concrete face stresses

The location of strain gauges along slabs 18 and 21, inter-slab joint meters and perimeter joint meters in the concrete face are shown in Figure 7. The recordings at these locations started at the beginning of impoundment (end of 2002).

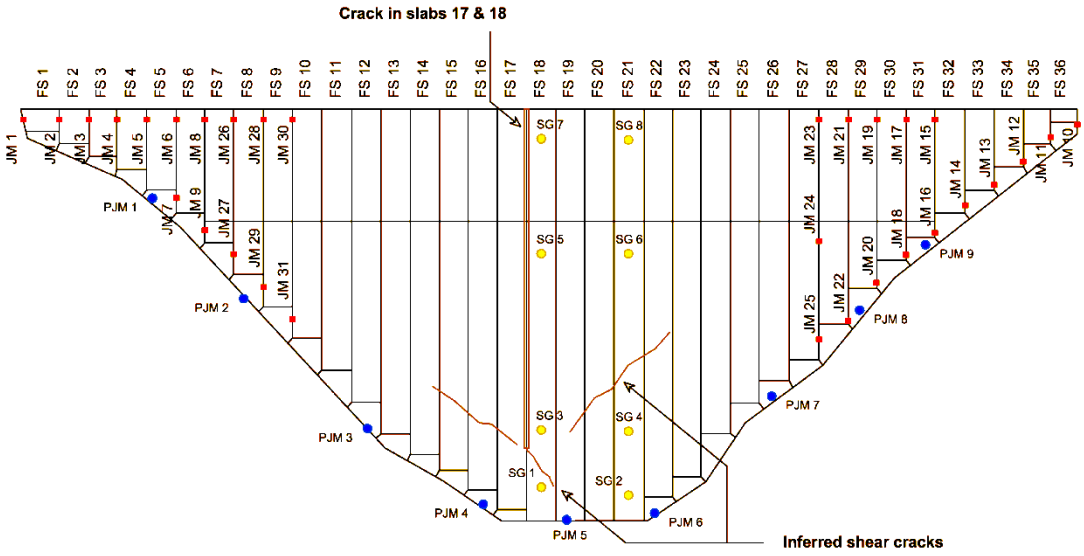

Figure 7: Location of strain gauges, inter-slab, perimeter joint meters and crack pattern [2]

Figure 8 and Figure 9 present the comparison between derived horizontal stresses and stresses estimated from the numerical models when the reservoir reached El.2060 and El.2078. It should be noted, that the so called registered stresses, are based on strain measurements.

To calculate the stresses in the face slabs from strain measurements and due to lack of detailed information some simplifications were performed. Under the assumption of plane stress conditions and linear elastic behaviour, the following expressions were used to estimate horizontal and vertical stresses:

$$\sigma_v = \frac{E}{1-\upsilon^2}(\varepsilon_v + \upsilon\varepsilon_h)$$

$$\sigma_h = \frac{E}{1-\upsilon^2}(\varepsilon_h + \upsilon\varepsilon_v)$$

The Poisson's ratio and the elastic modulus were adopted as 0.25 and 25 GPa, respectively [1]. Due to the lack of vertical strains along face slab 18, only stresses in face slab 21 are available for comparison. The simplifications generate some imprecision to the calculations. Nevertheless, a tendency can be observed and some conclusions drawn.

The measurements presented in Figure 8 indicate horizontal compressive stresses for reservoir level at EL.2060, which consistently increase from 3 MPa at the bottom of the face slabs (SG02) to 13.3 MPa at crest level (SG08).

In contrast, DIANA4 and COB models suggest that the level of stress decreases towards the dam crest. Hence, both models overestimate the measurements at SG02; and underestimate the measurements at SG06 and SG08. INGETEC predicts stress concentration in the central part of the face slabs, and underestimates the stresses in SG06 and SG08. The UKIM model gives compressive stresses below 2 MPa along the face slab.

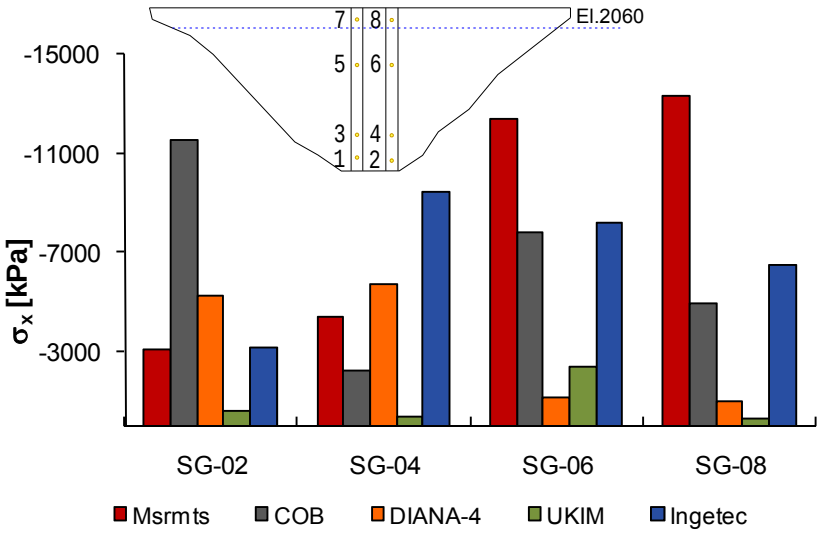

Figure 8: Horizontal stresses for reservoir level at EL.2060. Strain gauges along face slab 21

Figure 9 shows the horizontal stresses when the reservoir level reached EL. 2078 masl. The measurements prior to failure indicate a maximum compressive stress of near 16 MPa in the upper part of slab 21 (SG08).

The level of stress predicted by the DIANA and UKIM models increased due to the rise in reservoir level but the DIANA model still shows decreasing stress levels towards the crest and the UKIM model show small values of compressive stress in comparison with measured values. Their results did not exhibit stress reduction as a result of slab cracking although these two teams included a plasticity based constitutive model for the concrete face.

As the INGETEC model adopted a linear-elastic model, the level of stress increased reaching almost 14 MPa. The COB team did not report results because of convergence problems with their analysis.

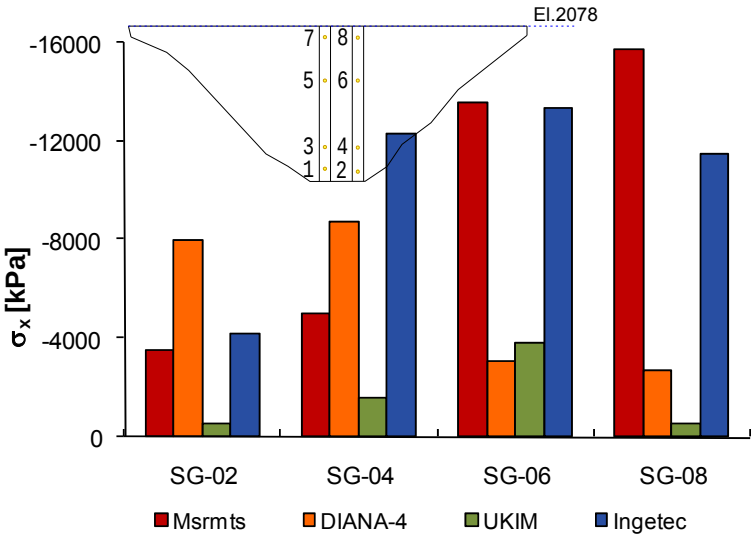

Figure 9: Horizontal stresses for reservoir level at EL.2078. Strain gauges along face slab 21

Figure 10 summarizes the registered stresses along the face slab 21 and the predicted stresses when the reservoir reaches El.2060 masl and El.2078 masl. The recorded stresses for reservoir level at El.2060 masl show compressive stresses of 8.3 MPa in the lower part of the slab (SG02) increasing up to 19.3 MPa in the upper part (SG06). When the reservoir reached El.2078 masl and prior to slab cracking, the stresses in the concrete slabs slightly increased, peaking at 20.1 MPa.

The maximum compressive stresses predicted by UKIM and DIANA4 models are less than 3 MPa along the face slab when the reservoir is at El.2060 masl, underestimating considerably the observed values. Importantly, tension stresses of around 0.5 MPa are predicted at SG06 by the UKIM model. The stress levels increase for both models in compression as well as in tension stresses, suggesting values that still underestimate the observations.

For the stage when the reservoir reaches El. 2060 masl, the COB model suggests that the lower part of the face slab is under considerable tension, compressive stresses only appear at the top of the face slab, which does not conform to the observations. For reservoir level at El. 2078 masl, COB did not report results due to convergence problems as mentioned before. The INGETEC model predicts compressive stresses for both reservoir levels (El. 2060 masl and 2078 masl) which agree with the observed trend, but predicting that the maximum compressive stresses occur at SG04 whilst the strain measurements suggests that the maximum values occurred SG06. Owing to the use of linear elasticity, both models did not predict any stress reduction.

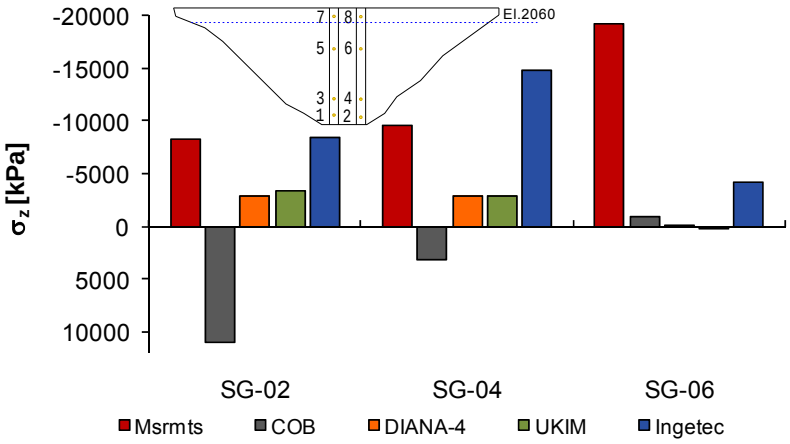

(a)

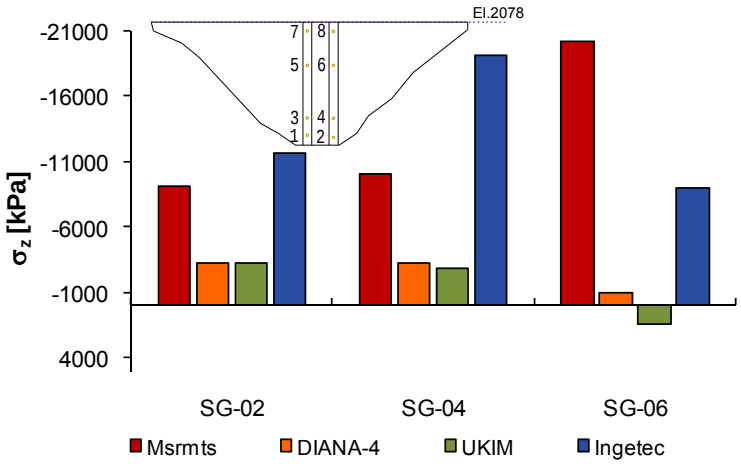

(b)

Figure 10: Vertical stresses obtained from strain gauges along face slab 21. (a) Reservoir level at EL.2060, (b) Reservoir level at EL.2078

Figure 11 shows the contour stresses presented by the participants. The format of presentation was different for all participants; however, some comments can be drawn from the results:

Contour of stresses on the concrete face are presented in Figure 11. The INGETEC model predicts compressive stresses higher than 20 MPa in the lower part of the concrete face, which correspond to the location of mayor slab cracking. The UKIM model shows high compressive stresses on the right abutment reaching 9.8 MPa.

Finally, the submitted document by DIANA4 mentioned a maximum compressive stress of 18 MPa located in the lower half of the slab. However, this high value seems to represent a local value near the bottom of the face slab, rather than a maximum compressive stress within an area of stress concentration. It is worth noting that the slab cracking pattern shown in Figure 11d does not predict the failure of the central slab. However, it shows cracks around the concrete beam located at EL.2040 masl, which agrees well with the observations; however was not the main focus of the exercise.

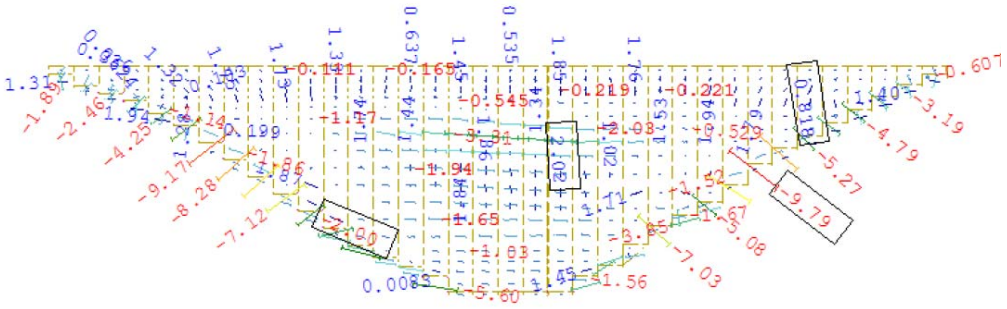

(a)

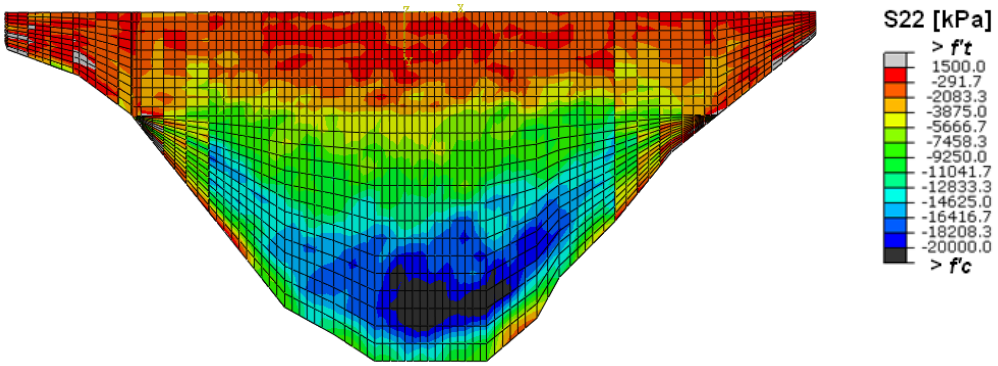

(b)

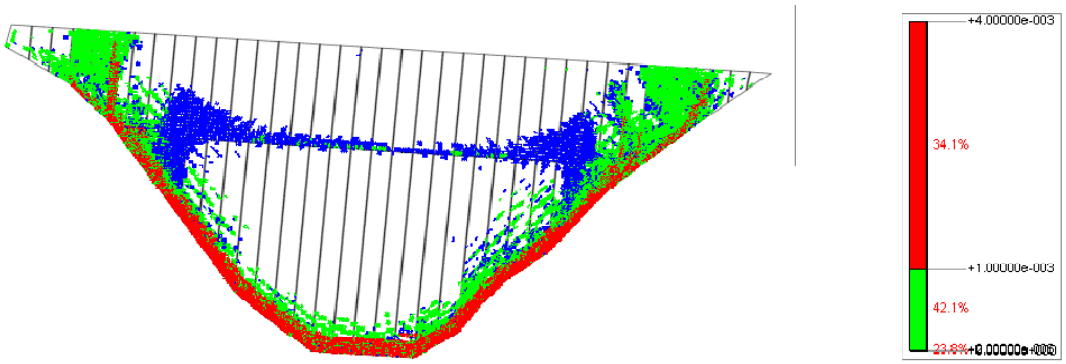

(c)

Figure 11: Contour of maximum stresses acting upon concrete face. (a) UKIM, (b) INGETEC, (c) DIANA4

Joint openings

- *Tension Joints*

The location of joint meters is presented in Figure 7. Figure 12 summarizes the observations and predictions for all four models. Openings in the upper part of the left abutment (JM1 to JM30) follow a bell-shaped behaviour starting from zero opening in JM1 and increasing up to 26 mm in the middle (JM5). The predicted opening by the INGETEC and UKIM models follow a similar trend, but the INGETEC model highly overestimates the opening in JM1, reaching 35 mm. On the other hand, the COB and DIANA4 models predict very small openings, reaching negative values in the COB model, which are not realistic.

Observations along the bottom part of the face slabs in the left abutment indicated an opening of 25 mm in JM7 that increased up to 43 mm in JM27 and then decreased up to 10 mm in JM31. The observed trend is better described by the UKIM model, but the openings are slightly overestimated. The INGETEC model estimates relatively well the joint opening in JM 29 and 31, however, underestimates the deformation for the remaining three locations. The COB and DIANA models do not conform to the observed trend and underestimate the observations. However, all predicted displacements consistently show positive joint movements, which agrees with the fact that these slabs are subjected to tensile stresses in the horizontal direction.

On the right abutment, the measurements indicate small openings at both ends (JM10 and JM22) and values between 20 and 30 mm in the intermediate tension joints. Even though, almost all models predicted positive joint movements, the magnitude of these openings underestimates the observations. However, the UKIM model overestimates significantly the opening at JM22 and shows an increasing trend towards the bottom of the concrete face, overestimating the size of the tension zone in the concrete face. The INGETEC model largely overestimates the movement of the last joint against the

abutment (JM10) but estimates relative well the maximum opening on the tension joints of this abutment.

The DIANA4 and COB models are rather insensitive to the location of the tension joints, indicating very small openings remaining almost constant regardless of the location of the jointmeters. The information provided on the characteristics of the interface elements adopted by DIANA4 is limited. On the other hand, the INGETEC model predicts values that vary depending upon the location of the face slabs and in some cases reproduces accurately the observed trends. However, important overestimations are observed at both ends along the crest level. Finally, the UKIM model reproduces more consistently the observed values, suggesting that the assumption of hinges along the interslab joints describes more adequately the observed values. This assumption implies that interslab movements take place in the upper surface of the concrete slabs with zero relative displacements in the bottom.

- *Perimeter Joint*

As the main function of the perimeter joint is to maintain a watertight seal against full reservoir load, while allowing for movements between the plinth and face slabs; it is important to rationally estimate the expected openings, so that proper measurements are taken to reduce leakage during dam operation. In order to assess the modelling capabilities for predictions of perimeter joint openings, Figure 13 compares the observations (red continuous line) with the numerical results from COB and INGETEC.

The INGETEC model agrees well with the observations, suggesting bigger openings along the abutments that decrease towards the riverbed. On the other hand, the COB model predicts openings that increase downhill reaching peak values in the riverbed (78 mm).

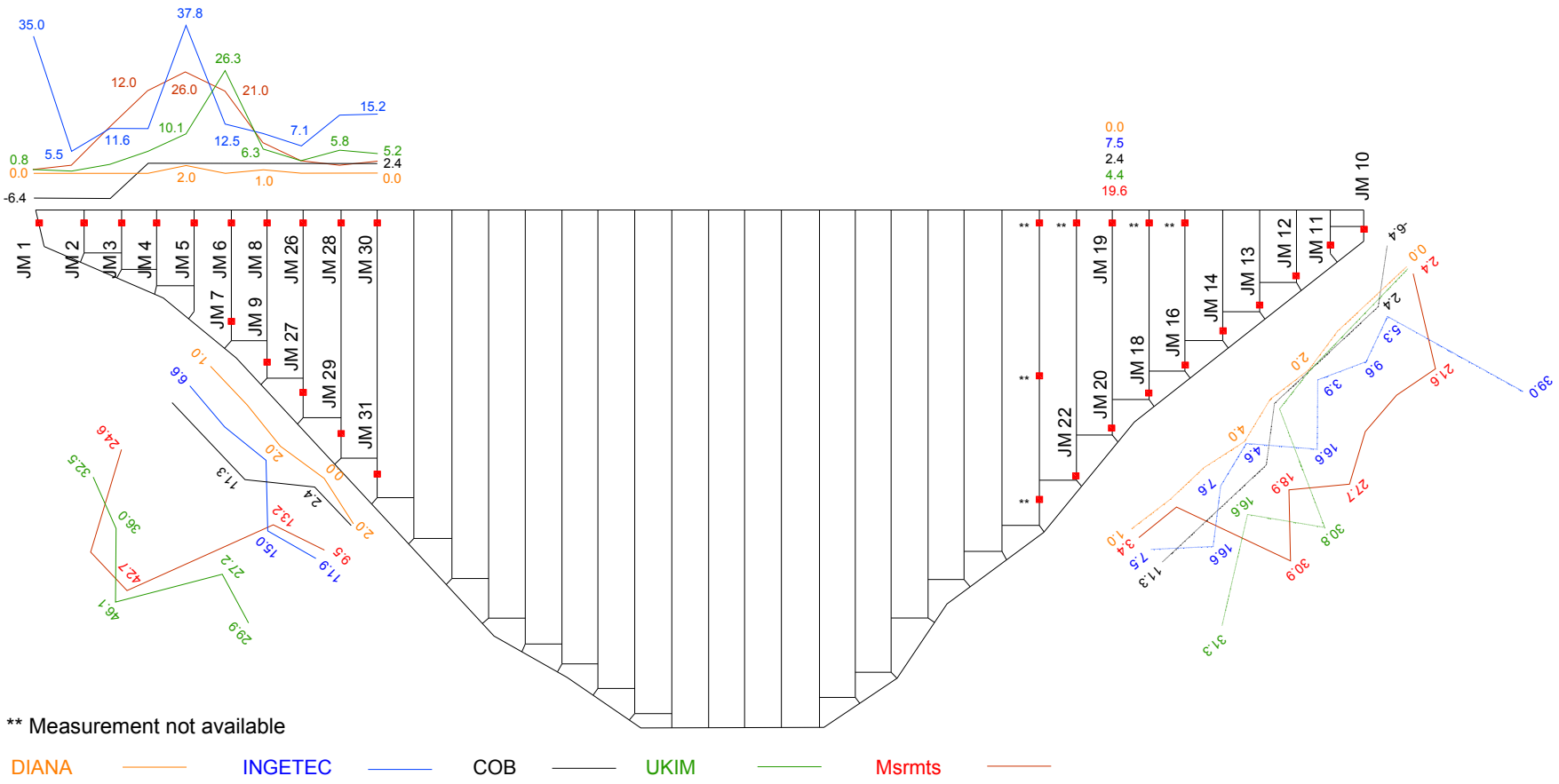

Figure 12: Inter-slab joint openings after full impoundment.

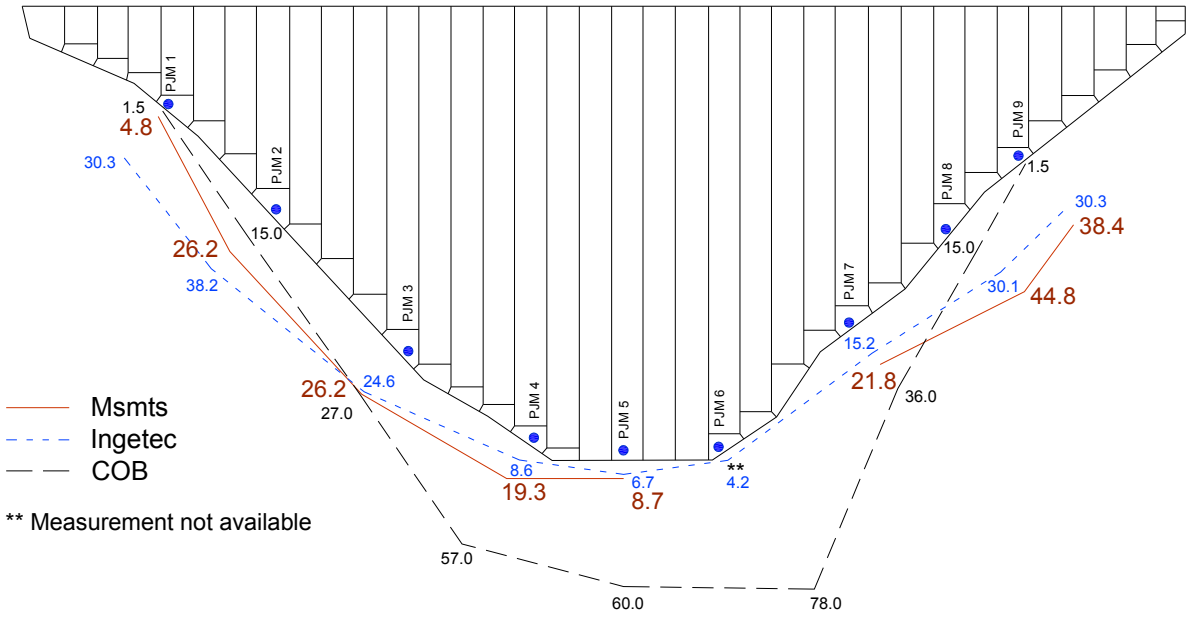

Figure 13: Perimeter joint openings for reservoir level at EL.2078 [mm]

Concluding remarks

Based on the observed behaviour, it can be concluded that the main problem in Mohale dam was the characteristics of the rockfill, which confirmed that a strong rockfill does not depend on having hard fill particles but gradation is the key element to obtain a less deformable rockfill. This issue was well recognized several decades ago [3], however, it seems like because of the pressure to further reduce costs and time for this already economical dam, this fundamental knowledge on rockfill behaviour was somehow overlooked. The adequate processing of a rockfill, including gradation, sluicing and compaction are essential to obtain an adequate behaviour of a rockfill dam.

Numerical analyses are now a common tool to predict dam behaviour, including the behaviour of the concrete face. However, the physical mechanisms involved in the interaction of the different structural components of a CFRD dam are a very complex problem to model. The results presented for this theme further confirmed the complexity of including the key physical mechanisms that should be included in a numerical analysis to adequately predict the behaviour of a CFRD.

With regard to the fill behaviour predictions, two teams (COB and INGETEC) predicted reasonably well the deformation pattern of the dam fill. INGETEC identified the issue of including anisotropic behaviour within the rockfill constitutive model as an essential topic. With respect to fill stresses; measurements of stresses induced in the rockfill by reservoir impoundment indicate, as expected, higher stress levels in the upstream zone. Although, most results follow this trend, the UKIM model shows large discrepancies in spite of the fact that their rockfill model follows a hyperbolic stress-strain relationship, which was also adopted for other participants. However, no information was available on their calibration process.

Among the participants, only DIANA and UKIM included the interaction between the dam and the foundation. However, none of those two teams provided settlements estimates during construction to compare with the measurements available. The other participants, based on the grounds that the foundation is much stiffer than the rockfill, assumed that the dam foundation is fully constrained. Additionally, the INGETEC team elaborated on the effects of the inclination of the abutments, concluding that this assumption is valid for the Mohale dam. Based on the agreement observed between measurements and the estimated settlements by the INGETEC and COB models, it may be concluded that the assumption of no interaction between dam and foundation is appropriate for this particular case.

In general terms, it can be concluded that predicting rockfill behaviour relatively well is possible with the available numerical models. The main difficulty when modelling the CFRD behaviour is the interaction between the rockfill and the structural elements (i.e., face, plinth, joints, curb). With regard to the constitutive model selected to predict the behaviour of the concrete face, two teams (COB and INGETEC) selected a linear elastic approach, based on the premise that the main objective of the exercise was to predict the stage when cracking initiated and that up to that point the concrete behaviour can be predicted fairly well with such an assumption. The COB team did not reported results because of convergence problems with their analysis.

INGETEC was the only team that predicted stresses higher than the strength of the concrete within a considerable area in the central portion of the face, which is consistent with the zone where the major cracking was registered in the Mohale dam. Nonetheless, published analysis of the Mohale instrumentation [1] suggested that the location where cracking initiated based on strain gauges measurements was at a higher elevation.

Two other teams (UKIM and DIANA) selected a plasticity based model to predict the behaviour of the concrete and to better capture the cracking; nevertheless, their prediction did not show satisfactory results in terms of the observed vertical cracking in the central zone of the concrete face. However, it is worthy of note, that the DIANA model was able to describe the horizontal crack pattern observed at level EL.2040 masl.

Further investigation should be performed to evaluate the influences of having a more sophisticated plasticity based model for the concrete; however, it should be clear that a premise for a CFRD design is that the concrete of the face should behave widely within the elastic range

In terms of the modelling of concrete face joints, the inter-slab model approach proposed by UKIM, in which the bottom part of the interslab joints is modelled with hinges, so that the upper part opens freely; showed good agreement with the observations; however, is does not agree with the real behaviour of a joint of this type of dam. In terms of the openings along the perimeter joint, the model proposed by INGETEC, in which the interface between the plinth wall and the face slabs transmits only compressive stresses, was able to describe the observed openings.

Through the development of the numerical model and based on the experience of INGETEC in similar projects, the effect of two design issues was evaluated: the

variations in the vertical deformation modulus in the rockfill, and the benefits of including compression joints in the central part of the concrete face. The results suggested that an average vertical modulus in the upstream rockfill of 80 MPa, would have reduced the compressive stresses approximately in 40%. Additionally, if three compression joints, located in the central part of the concrete face, would have been included, the compression could have been further reduced by 30%.

Based on the presented results, large variations on the predicted behaviour were observed. Due to the lack of detailed information provided on each model, was not possible to clearly identify the sources of such variations. This indicates that detail guidelines should be developed to help practitioners to better predict the behaviour of a CFRD

The analysis presented in this workshop show from a general perspective the capabilities currently available to be used in the design stages to evaluate the stress-strain behavior of a CFRD dam and assess the influence of certain parameters such as canyon geometry and rockfill modulus. The analyses are also quite useful to evaluate the effectiveness of different mitigation measures to alleviate stresses in the concrete face. It should be noted that the results of such a numerical analysis cannot be taken as absolute and precise values. The analysis will point up tendencies and estimates of stress- strain behavior of the different components of the dam, so that engineers with good judgment can make further decisions.

It should be emphasized that the three recent incidents, including the Mohale dam, show the need to carefully evaluate and analyze every aspect of a project when extrapolating from precedent. This should be based on good engineering judgment and complemented with detailed analysis tools. This applies not only to CFRDs but to any engineering structure. Nevertheless, this type of dam continues to be an attractive engineering solution for many project sites, which can be adequately designed and constructed with excellent quality.

References

[1] Johannesson P. (2007). Lessons learned from the cracking of Mohale CFRD slab. International WaterPower and Dams Construction, August, 2007.

[2] Johannesson P. (2007). Slab performance on a few CFRDS and suggested improvements in slab design. Workshop on High Dam Know-how, May 22-24, 2007, Yichang, China.

[3] Marsal, R.J. Mechanical Properties of Rockfill. In Embankment Dam Engineering. Casagrande Volume (eds R.C. Hirschfel & S.J. Poulos), John Wiley & Sons, New Cork, pp. 109-200. 1973.

[4] Marulanda, C. (2009). Analysis of a concrete face rockfill dam including concrete face loading and deformation. Theme B. International Commission on Large Dams. Committee on Computational Aspects of Analysis and Design of Dams

[5] Pinto, N. L., Marques, P. L., “Estimating the Maximum Face Deflection in CFRDs”, Hydropower and Dams, Issue 6, 1998, p. 28.

[6] Pinto N.L.S., (2007) – “A Challenge of very high CFRD dams: Very high concrete face compressive stresses” 5th Int. Conf. on Dam Eng., Lisbon, Portugal

[7] Sobrinho J.A., Xavier L.V., Albertoni C., Correa C., Fernandes R. (2007) – “Performance and concrete repair at Campos Novos” Hydropower and dams. Issue two.

[8] W. Riemer. Personal communication. Construction schedule, settlement readings and pictures during construction.

[9] W. Riemer. Personal communication. Construction sequence, settlement readings and deformation of face slabs during construction.

[10] Duncan, J.M., Byrne, P., Wong, K.S., Mabry, Phillip. Strength, stress-strain and bulk modulus parameters for finite element analyses of stresses and movements in soil masses. University of California. Berkeley, California. August, 1980.